Open University Geological Society Journal
Symposium Edition 2007
Our Dynamic Planet
Lancaster University
17-19 August 2007

Contents

Is there a unifying theory for Phanerozoic glaciation? 1
Dr Howard A Armstrong, Durham University

Neoproterozoic glaciation in the Earth System: a progress report 10
Prof Ian J. Fairchild, University of Birmingham

Carbon in the Atmosphere and the Human Volcano 14
Dr Fred Broadhurst, University of Manchester

The Great Plume Debate 16
Prof. Gillian Foulger, Durham University

Does Acid Rain Reduce Methane Emission? 22
Prof. Nancy Dise, Manchester Metropolitan University

Volcanoes in the Laboratory 24
Dr Stephen Lane & Steven Corder, Lancaster University

Dynamic Planets Elsewhere 30
Dr Dave Rothery, The Open University

****

The Geology of the Canary Islands: a Review 37
Duncan Woodcock

Geological observations in the Precambrian and Cambrian rocks of the St. David's Peninsula 43
John Downes

At last, the Ruapehu Crater Lake Lahar 48
Philip Clark

Siberian Winter © Duncan Woodcock 50

Book reviews 8, 9, 13, 29, 36

It is the responsibility of authors to obtain the necessary permission to reproduce any copyright material they wish to use in their article. The views expressed in this Journal are those of the individual author and do not represent those of the Open University Geological Society. In the opinion of the author the description of venues are accurate at the time of going to press; the Open University Geological Society does not accept responsibility for access, safety considerations or adverse conditions encountered by those visiting the sites.

ISSN 0143-9472

© Copyright reserved

Editor: Jane Clarke

email: journal@ougs.org

OUGS Journal 28(2)
Symposium Edition 2007

Cover illustration: Thin sections of several different habits of barite. Photographs: Jane Clarke.

Botryoidal barite Mag 538; ppl.	Acicular barite Mag 549; xpl.	Poikilotopic barite Mag 530; xpl.
Bladed barite (white) Mag 580; ppl.	Botryoidal barite Mag 538; xpl	Spherulitic barite Mag 584; xpl.
Fasicular-optic barite Mag 549; xpl.	Banded barite Mag 538; xpl.	Banded barite Mag 538; ppl.

Committee of the Open University Geological Society 2007

Executive Committee Members

President: Dr Sandy Smith, Department of Earth Sciences, The Open University, Milton Keynes MK7 6AA
Chairman: Joe Jennings
Secretary: Polly Rhodes
Treasurer: Bob Morley
Membership Secretary: Stuart Bull
Newsletter Editor: David Jones
Information: Linda McArdell
Events Officer: Glynis Sanderson
Sales Manager: Lesley Laws

Non-voting postholders

Gift Aid: Ann Goundry
Journal Editor: Jane Clarke
Archivist/Review Officer: Jane Michael
Minutes Secretary: Mike Jones
OUSA Representative: Alasdair Farquharson
OUSA Deputy Representative: Karen Scott

Branch Organisers

East Anglia: Andrew Fleming
East Midlands: Don Cameron
East Scotland: Anne Burgess
Gogledd Cymru: Rachel Atherton
Ireland: Phyllis Turkington
London: Sue Vernon
Mainland Europe: Annette Kimmich
Northumbria: Annie Hedley
North West: Jane Schollick
Oxford: Sally Munnings
Severnside: Janet Hiscott
South East: Roger Baker
South West: Gordon Neighbour
Walton Hall: Michael Friday
Wessex: Sheila Alderman
West Midlands: Linda Tonkin
West Scotland: Jacqueline Wiles
Yorkshire: Amy Thomson

Past Presidents of the OUGS

1973-4	Prof Ian Gass	1985-6	Dr Peter Skelton	1997-8	Dr Dee Edwards
1975-6	Dr Chris Wilson	1987-8	Mr Eric Skipsey	1999-0	Dr Peter Sheldon
1977-8	Mr John Wright	1989-90	Dr Sandy Smith	2001-2	Prof Bob Spicer
1979-80	Dr Richard Thorpe	1991-2	Dr David Williams	2003- 4	Prof Chris Wilson
1981-2	Dr Dennis Jackson	1993-4	Dr Dave Rothery	2005 - 6	Dr Angela Coe
1983-4	Prof Geoff Brown	1995-6	Dr Nigel Harris	2007 -	Dr Sandy Smith

Vice Presidents of the OUGS

Dr Evelyn Brown
Dr Michael Gagan
Norma Rothwell

Is there a unifying theory for Phanerozoic glaciation?

Howard A. Armstrong, Durham University, Department of Earth Sciences, Palaeozoic Environments Group, South Road, Durham DH1 3LE, U.K.

Abstract

Climate proxy records show that a common pattern of environmental change occurred in the sequence of events leading to the Cenozoic and Ordovician glaciations. Both glaciations were set against a backdrop of long-term declining Atmospheric carbon dioxide (pCO_2) likely initiated by changes in plate configuration that resulted in increased weathering and nutrient cycling into the oceans. It is postulated that rapid expansion of ice volume was triggered by the re-direction of warm, circum-equatorial currents into high latitudes to provide a source of warm moist air and high levels of snowfall. A synthetic orbital model for the Ordovician indicates that the coldest austral summers (minimal solar insolation during the austral summer) occurred when eccentricity was high, obliquity low and aphelion occurred during austral summer. This configuration promoted the survival of snow through successive precession and obliquity maxima. Once ice sheets were large enough eccentricity pacing of ice margin processes (entrained by obliquity) and the monsoonal climate system (entrained by precession) largely controlled their size. This leads to a unifying view of the causes of Phanerozoic glaciation.

Introduction

For much of geological time the Earth has experienced a mild greenhouse climate, punctuated by severe glaciations. Glaciations have a profound effect on landscape evolution, the biosphere and the Earth's ocean-atmosphere system. Were all glaciations caused by the same mechanisms?

In this essay I will attempt to answer this question by comparing the patterns and processes of climate change leading to the Ordovician and Cenozoic glaciations. Evidence is largely drawn from the literature and has recently been reviewed in more detail (Armstrong 2007).

Cenozoic glaciation and key hypotheses for understanding the Ordovician

A sequence of stepped changes in Cenozoic climate proxy records can be identified and interpreted in terms of deteriorating climate during the developing glaciation (Figure 1).

Onset of Antarctic glaciation (Oi-1 glaciation)

Mechanisms for the sudden and widespread increase in ice volume in Antarctica and the associated shift toward colder temperatures near the Eocene-Oligocene boundary (~34Ma) have centred largely on the opening of Southern Ocean gateways, the initiation of the Antarctic Circumpolar Current and the thermal isolation of the continent (Kennett 1977). Unfortunately, general circulation models (GCM) developed to simulate an open and closed Drake Passage, show only a modest role for gateway opening in the formation of the Antarctic ice sheet and, suggest warmer (rather than cooler) high latitude sea surface tempera-

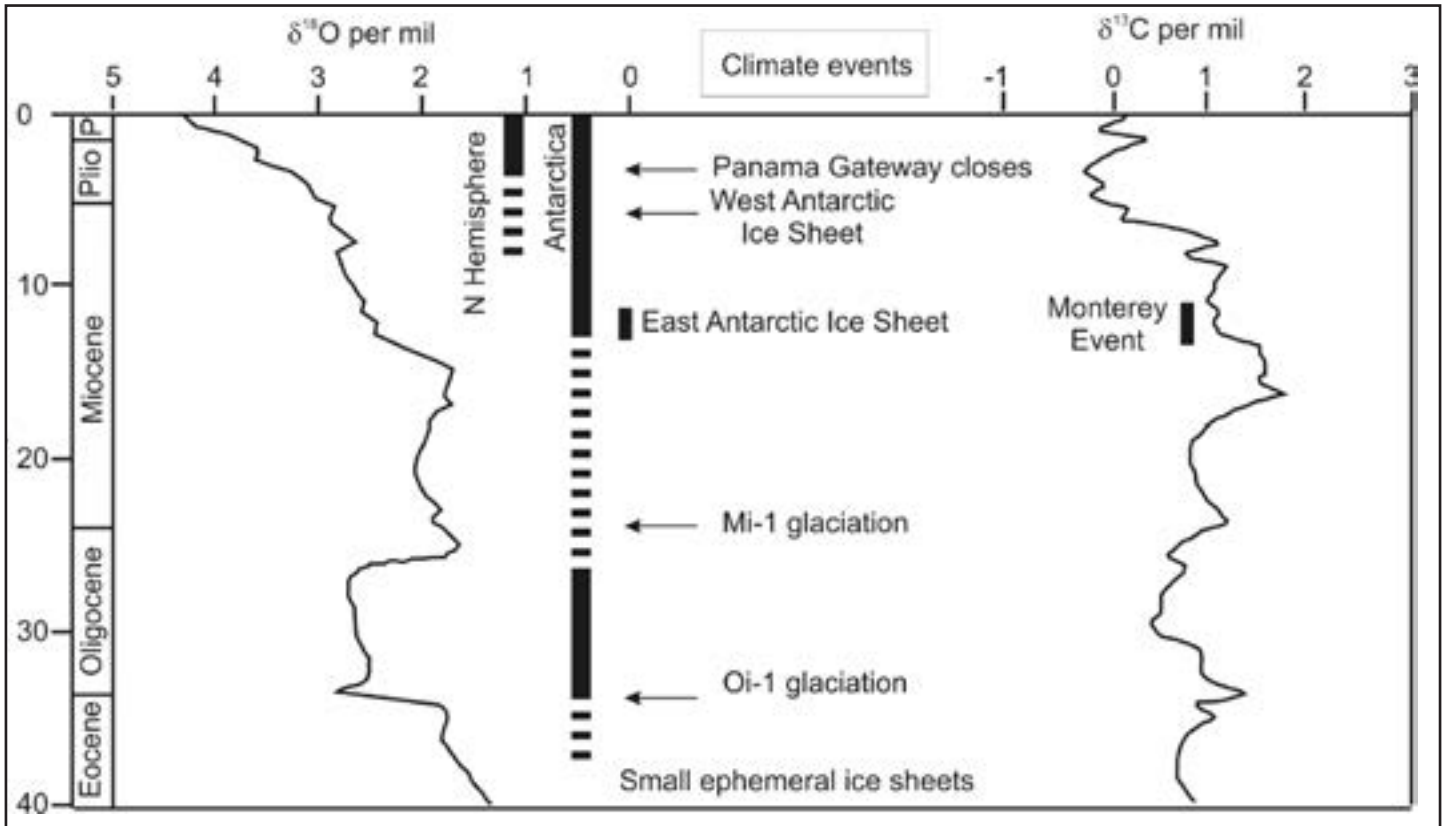

Figure 1. Global deep-sea oxygen and carbon isotope records based on data compiled from over 40 ODP and DSDP cores. Key events during the development of the Cenozoic glaciation are marked. The thick vertical bars provide a rough estimate of ice volume, relative to the Last Glacial Maximum, dashed bars represent minimal ice coverage (<50%) whilst the full bars represent close to the maximum ice coverage (>50%). (Redrawn from Zachos *et al.* (2001)).

tures (SSTs) were necessary to increase snowfall in the continental interior; the pre-condition for ice sheet growth (Oglesby 1989, Prentice & Mathews 1991). Problems of constraining the relative timing of the opening of the gateways between the Eocene and Miocene also confound this hypothesis.

Instead, it has been shown that declining Cenozoic pCO_2 played the dominant role in causing the glaciation (DeConto & Pollard 2003). Estimates of early Cenozoic pCO_2 are between 2 and 5 x present atmospheric levels (PAL), declining to near modern values in the early Neogene (Pearson & Palmer 2000). The DeConto & Pollard model shows the progressive enlargement of the East Antarctic Ice Sheet (EAIS) from small, isolated ice caps on the highest Antarctic plateaus. As pCO_2 declined and the Earth cooled, these isolated ice caps eventually merged into permanent ice sheets. The model also shows that the orbital configuration of the Earth was an important factor in pacing ice sheet growth. At pCO_2 levels between ~3x and 2x PAL, a configuration of high eccentricity, low obliquity and aphelion during austral summer is required to produce the cold austral summers necessary for winter snows to survive year on year. The DeConto & Pollard model predicts that within a single 40ky obliquity cycle East Antarctic ice reached sea level around most of the continental margin, significantly enhancing thermohaline circulation (THC).

Two, largely unanswered, questions arise from this model: what were the causes of declining pCO_2 during the Cenozoic and, what sequence of events led to increased snowfall at high southerly latitudes necessary to trigger ice sheet growth?

Mid-Miocene cooling and expansion of the EAIS

The mid-Miocene Monterey positive carbon isotope excursion which defines the Monterey Event coincides with a major expansion of the EAIS but its cause remains controversial. The base of the excursion coincides with a positive shift in $^{87}Sr/^{86}Sr$ isotope values, correlated with the rise of the Himalaya (particularly Tibet) to present day elevation (Raymo & Ruddiman 1992). The most likely explanation of the Monterey Event is that the increased supply of nutrients to the oceans from the Himalaya forced a carbon cycle response leading to drawdown of CO_2 into the oceans that produced a negative greenhouse effect and cooling. But, global cooling, recorded in the marine $\delta^{18}O$ record started ~ 2Ma after the start of the Monterey carbon isotope excursion (Pagani *et al.* 1999) and it has been suggested that volcanic CO_2 from the erupting Colorado River plateau basalts retarded cooling.

Onset of Northern Hemisphere glaciation.

Models for the initiation of the Northern Hemisphere glaciation (~3.5Ma to present) provide insight into the question of increasing supply of moisture to high latitudes and increased precipitation. This is encapsulated in the "snow gun hypothesis" (originally proposed for the Pacific by Billups 2005). Two current hypotheses attempt to explain this phenomenon:

1) The closure of the Central Atlantic Seaway at the Isthmus of Panama isolated the North Atlantic circulation from the Pacific. This was shortly followed by a shift equatorially in the mean latitude of the Atlantic Inter-tropical Convergence Zone (ITCZ; Billups *et al.* 1999; Peterson & Haug 2006). This shift diverted warm water into the subtropics via the North Brazil Coastal Current. Pole-ward oceanic transport of warm salty surface water (via the Gulf Stream) increased inducing increased snow fall at high northern latitudes (the "snow gun hypothesis" Haug & Tiedemann 1998; Billups *et al.* 1999; Haug *et al.* 2005) and an increased rate of North Atlantic deep-water formation increasing the THC (Billups *et al.* 1999).

2) Down-wind changes in Sub-Arctic Pacific Ocean stratification resulting from increasing seasonal temperature contrast (Haug *et al.* 2005). Warmer summer SSTs result in a warmer atmosphere that can hold more moisture and this is blown onto continental North America, to fall as snow.

The Mid Pleistocene Transition

The Laurentide ice sheet reached a critical size in the mid-Pleistocene (~1Ma) when ice volume became sensitive to orbital forcing. Eccentricity modulation of ice margin processes (entrained by obliquity), the monsoon climate system and responses from the boreal wetlands (entrained by precession) forced changes in pCO_2 at a 100-kyr timescale. These feedbacks drove the system deeper into glaciation, and initiated the glacial-to-interglacial cycles, quasi-persistent until today (Ruddiman 2003).

The Ordovician glaciation

The Ordovician world was significantly different from that in the Cenozoic: the land was largely devoid of vegetation, atmospheric oxygen levels were ~50% PAL (Berner 2001). Ordovician sea levels were the highest in the Phanerozoic (Frakes *et al.* 1992) and large areas of the continents were submerged. Greenhouse climate conditions were maintained by higher (8 to 18x PAL) pCO_2 levels (Berner 1992; Berner & Kothavala 2001), though there is some doubt over the very high pCO_2 estimates (Boucot & Gray 2001). Virtually all work on trying to understand the causes of Ordovician glaciation has focussed on the Hirnantian Glacial Maximum. Two general explanatory hypotheses have emerged.

1) A "Monterey mechanism" of increased primary marine productivity and organic carbon burial, stimulated by newly available nutrients from the developing Caledonian Mountains or brought to the surface by upwelling (Berry & Wilde 1978; Wilde 1991). A chert-phosphate association is found in shelfal settings along the southern margin of Laurentia, from the Caradoc and has been cited as evidence for the existence of vigorous THC at this time (Pope & Steffen 2003) but this interpretation is inconsistent with the widespread ventilation of the oceans in the Ashgill. As an alternative, the chert-phosphate deposits could have formed beneath shallow, coastal upwelling systems, driven by offshore winds, rather than a vigorous THC, and would have had little impact on the deep sea. Climate modelling indicates much of southern Laurentia lay beneath the zone of north-easterly trade winds during the Upper Ordovician, and offshore winds would have predominated (Parrish 1982; Herrmann *et al.* 2004, 2005).

The "Monterey hypothesis" requires large-scale carbon burial to drive a fall in pCO_2 (Vincent & Berger 1985). During the Ashgill there is no evidence, at least to bathyal depths, of widespread deposition of organic carbon, only short periods of black shale deposition and ocean anoxia (e.g. Armstrong & Coe 1997). Surprisingly, $\delta^{13}C$ values from central Nevada suggest rising pCO_2 during the Hirnantian glacial maximum (Kump *et al.* 1995, 1999).

2) The "silicate weathering hypothesis" was proposed to counter these problems (Kump *et al.* 1999). In this hypothesis the rate of silicate weathering is the dominant control on atmospheric CO_2 levels. In this explanation growing ice sheets cover areas previously undergoing silicate weathering. Global silicate weathering

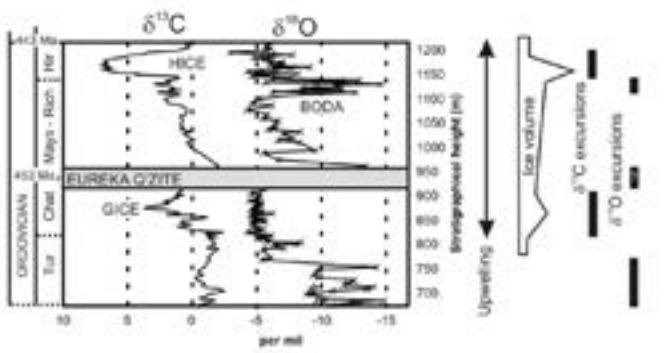

Figure 2. Middle to Upper Ordovician low latitude stable carbon and oxygen isotope curves from central Nevada (data from (Saltzman & Young 2005). These show a positive shift in $\delta^{13}C$ in the Chatfieldian (GICE excursion) and a negative shift in $\delta^{18}O$ (equivalent to the Boda Event) that precedes the Hirnantian glacial maximum. Radiometric ages for stage boundaries taken from (Webby *et al.* 2004). Abbreviations: C is cold, T transitional and W warm. Saltzman & Young (2005) and Tobin *et al.* (2005) have argued the case for the fidelity of their data as a primary seawater record. Anomalously low stable oxygen isotope values for the Early Palaeozoic have been interpreted to be indicative of diagenetic alteration (Land 1995), high seawater temperatures Karhu & Epstein 1986), salinity stratification (Railsback *et al.* 1990), high seawater pH (Wenzel *et al.* 2000), low seawater $\delta^{18}O$ (Veizer *et al.* 1986) or a combination of high tropical temperatures and low $\delta^{18}O$ seawater (Shields *et al.* 2003). Depleted $\delta^{18}O$ values are a common feature of the Early Palaeozoic. Values in excess of -10 ‰ are also recorded from the Upper Cambrian - Lower Ordovician and the Upper Silurian (Wenlock-Ludlow) in the Nevada section. "Megacycles" of highly depleted (> -10 ‰) to more positive (-5 ‰) $\delta^{18}O$ values, occur through the Nevada record with a frequency ~ 30 Ma. Carboniferous $\delta^{18}O$ values, for the period affected by glacial and interglacial climate episodes are also highly depleted and fall within the range -10 ‰ to -1 ‰ (Bruckschen *et al*. 1999). Tropical values fall as low as -16 ‰ (Tucker *et al.* 2003). The most depleted $\delta^{18}O_{Calcite}$ values are interpreted to occur during Namurian and Visean greenhouse climate phases (Bruckschen *et al.* 1999). Carboniferous $\delta^{13}C_{Calcite}$ values rise from 1 to 5 ‰ between interglacial and glacial periods, similar to those from the Ordovician. Highly depleted $\delta^{18}O$ values are also reported at the present day in low tropical and subtropical latitudes (34°N to 34°S) where fluvial discharge is high. $\delta^{18}O$ values of -8 to -12.8 ‰ are recorded in surface ocean waters during winter months (October to April) close to the Ganges-Bramaputra and the Indus river discharges and at the mouth of the Orinoco River. During southern hemisphere summer months, similar, highly depleted waters occurs along the western seaboard of South America
(http://www.giss.nasa.gov/data/o18data).
Highly depleted stable isotopic values in the Nevada records is therefore regarded as a primary oceanographic signal.

rates decline and pCO_2 rises, providing the positive feedback that moderated climate and finally brought the glaciation to an end. This hypothesis provides an explanation for rising atmospheric pCO_2 levels during the glacial maximum, but this phenomenon could be equally well explained by increased exposure and hydrolysis of low latitude carbonate platforms during the glacial lowstand. In an absence of a calcifying plankton, the mechanism by which CO_2 is adsorbed into the oceans at the present day, carbonate compensation, would not have been operating. The net result would have been an increase in ocean and atmosphere CO_2. At the present day only hydrolysis affects atmospheric CO_2 balance and this would have been much reduced by the low temperatures during the Ashgill. A further criticism has been raised, that this hypothesis is based only on evidence of rising atmospheric pCO_2 levels from a single section and such records tend to be dominanted by regional effects (Sheehan 2001).

Both the proposed hypotheses for late Ordovician glaciation therefore remain plausible but flawed and no glacial scenario has yet been developed for the entire Ordovician glaciation.

Evidence of climate change during the Caradoc and Ashgill

Geological proxy data provides the opportunity to recognise a similar sequence of events leading to the Ordovician glaciation (Figure 2).

The onset of glaciation and Guttenburg Isotope Excursion as an equivalent to the Monterey Event

Direct evidence of glaciation from high palaeolatitudes is poorly documented and the early record is largely incomplete. Glaciogenic deposits are known from the late Caradoc in Bolivia, Peru, Argentina, Morocco and the Sahara. The Guttenburg Positive Carbon Isotope Excursion (GICE) during the Chatfieldian (mid-Caradoc; Table 1, Figure 2) has been proposed as the start of the Ordovician glaciation approximately 10Ma before the Hirnantian glacial maximum (Saltzman *et al.* 2003; Saltzman & Young 2005; Tobin *et al.* 2005). In Britain, pre-Ashgill deep-sea fan deposits (such as at Dob's Linn, Scotland and in the Welsh Basin) were dominated by anoxic black shales. In contrast, Ashgill deposits comprise predominantly grey mudstones, indicating ventilation of the oceans, at least to bathyal water depths (Armstrong & Coe 1997). The THC associated with the developing glaciation has been invoked as the primary mechanism leading to oxic oceans at this time, though the deepest parts of the oceans may have remained anoxic (Brenchley *et al.* 1994; Armstrong & Coe 1997).

Table 1. Upper Ordovician chronostratigraphy showing the correlation of schemes for Britain, North America and Balto-Scandinavia. Time slices and radiometric timescale are as defined in Webby *et al*. (2004).

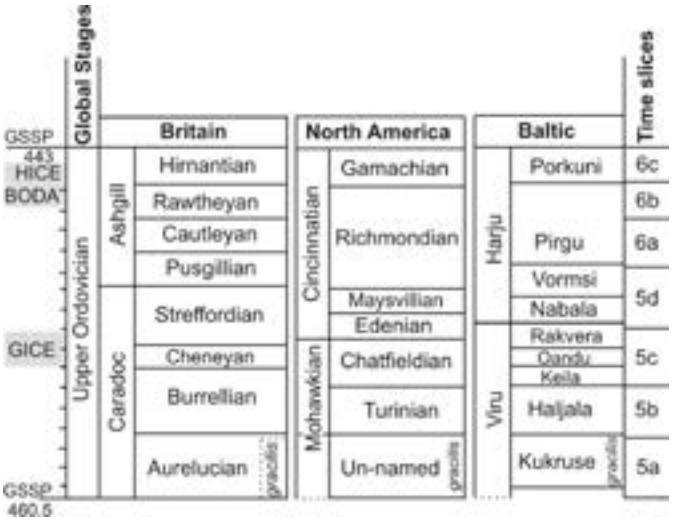

The ocean general circulation model for the Caradoc and Ashgill indicates that polar temperatures would have been low enough to sustain ice sheets once pCO_2 levels fell to 8 x PAL and that falling sea level reinforced this possibility (Herrmann *et al.* 2005). GICE coincides with the onset of low latitude coastal upwelling (Pope & Steffen 2003) and an increase in frequency of glacial deposits (Frakes *et al.* 1992). $^{87}Sr/^{86}Sr$ values also show an intriguing switch to a positive trend in the mid-Caradoc that is sustained into the Silurian. In most areas of the world GICE appears to correlate with regressive or lowstand deposits (Saltzman & Young 2005, Tobin *et al*. 2005) and the appearance of cold oceanic water in the epeiric sea of Laurentia (Kolata *et al.* 2001). These coincidences indicate GICE represents a major perturbation in the carbon cycle and a pCO_2 threshold was crossed at GICE that allowed the formation of a polar ice sheet. The short-lived nature of GICE is comparable to that of the Monterey Event.

The prominent HICE carbon isotopic excursion is regarded as coincident with the glacial maximum within the *persculptus* Biozone (Brenchley *et al.* 1994, Underwood *et al.* 1997; Figure 2). In many parts of the world a major unconformity occurs in shallow marine settings, coincident with the Hirnantian Glacial Maximum (Brenchley *et al.* 1994). Sea levels are thought to have fallen between 85 and 120 m, on a similar scale to that during the Last Glacial Maximum.

Defining the end of the Ordovician glaciation also proves difficult. The onset of post-glacial sea level rise and a return of anoxic black shale deposition occur within the mid-*persculptus* Biozone. However, glacial deposits are known into the Silurian (Frakes *et al*. 1992; Grahn & Caputo 1992) and periodic positive carbon isotope excursions within the lower Silurian have been attributed to renewed glacial conditions (Loydell 2007). Biotic cycles in the early Silurian also correlate broadly with postulated sea-level changes, and have been explained by a model that involves episodic changes from cool to warm oceanic state (Aldridge *et al.* 1993). The cold cycles have an approximate periodicity of 2.5Ma that likely correlates with orbitally-forced ice re-advances at high latitudes, suggesting the glaciation continued to the Wenlock (Page *et al.* 2007).

The BODA Event: a record of ocean gateway closure and changing ocean circulation

Closure of ocean gateways and concomitant changes in ocean circulation are an essential precursor of the snow gun hypothesis. During the Middle Ordovician Gondwana drifted southward, towards the South Pole. In high southern latitudes the Rheic Ocean opened with the continued drift northwards of Avalonia. The Iapetus Ocean and Proto-Tethys were connected though a seaway, north of Baltica and currents may have flowed between them (Wilde 1991; Figure 3A).

During the Ashgill, Gondwana continued to move southward with South America, Africa, Australasia and parts of the Antarctic in high southern latitudes astride the South Pole. The Tornquist Sea closed, linking Avalonia and Baltica. The Iapetus Ocean narrowed with a seaway at the equator separating Laurentia-Siberia from Avalonia-Baltica. The Rheic Ocean widened, which acted as the major water communication between the widening south Palaeo-Pacific and Proto-Tethys (Figure 3B).

There is general agreement between several generations of OGCM modelled circulation patterns (Poussart *et al.* 1999, Wilde 1991; Herrmann *et al.* 2004, 2005; Figure 3). The ocean circulation in the northern hemisphere was predominantly zonal due to an absence of large land masses. During the Caradoc, the north equatorial counter-current flowed westward, relatively uninterrupted from the west coast of Laurentia to Siberia. The south equatorial counter current was blocked in the west by the Australian-Antarctic region of Gondwana and was re-directed into the pole-ward flowing "West Gondwana Current" to join with the South Gondwana Current at the south Panthalassic convergence. Southward movement of Gondwana in the Ashgill caused a reduction in the strength of the South Gondwana Current and at low sea levels, this current disappeared. The northward movement of Avalonia in the Ashgill narrowed the Iapetus Ocean, which in turn, narrowed and increased the strength of the Iapetus Current (Figure 3B).

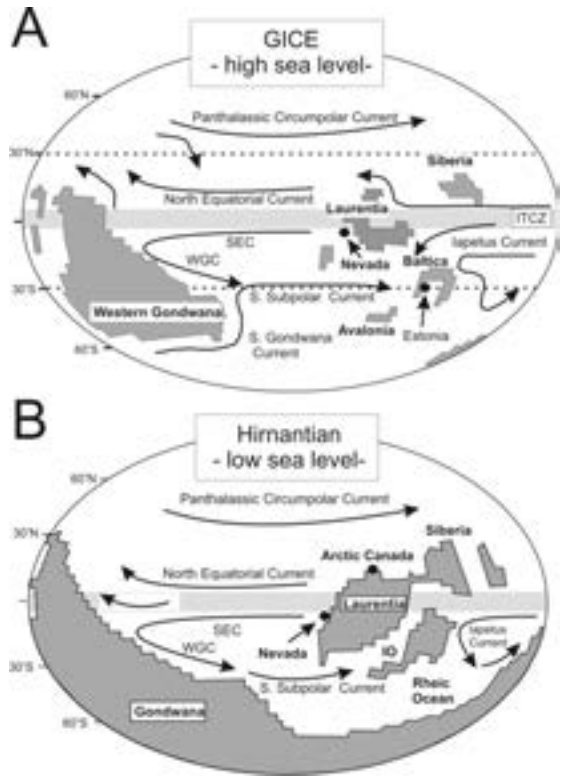

Figure 3. Palaeogeographical reconstructions and surface ocean circulation patterns for the Early and Late Ordovician (simplified from Herrmann *et al.* 2005). Sketch maps show palaeogeography, palaeooceanography and ITCZ position during the early part of the Late Ordovician (3A, Caradoc; 3B Ashgill). Maps are simplified from OGCM model outputs from Herrmann *et al.* 2005). Current patterns are generalized to bold arrows centred on currents with velocities > 5 cm sec^{-1}, the dotted zone is the ITCZ. Abbreviations: SEC, South Equatorial Current; WGC, West Gondwana Current (new name proposed to avoid confusion with Antarctica which did not come into existence until the Cretaceous); IC, Iapetus Current; IO, Iapetus Ocean.

Figure 4 shows stable oxygen isotope ratios of bulk micrites values from Arctic Canada (~20°N), Nevada (~6°S) and Estonia (~23°S) plotted onto temperature-salinity-isotope diagrams. These show a coherent pattern of shifting tropical and subtropical water masses between peak Boda and HICE (Armstrong *et al.* in review). Tropical water beneath the Inter-tropical Convergence Zone (ITCZ; $\delta^{18}O$ = -10 to -15 ‰) was isotopically light reflecting high SST and potentially reduced sea surface salinity (SSS). Subtropical

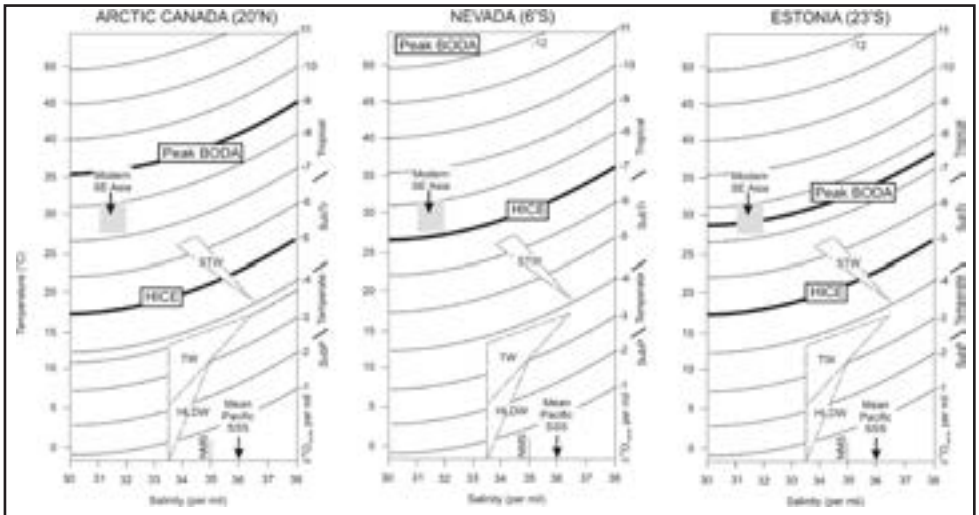

Figure 4. Temperature-salinity-$\delta^{18}O$ plot based on that first published by (Wilde & Berry 1984) and modified by (Tobin *et al.* 2005). Published data are from Nevada (Saltzman & Young 2005), Arctic Canada (Melchin *et al.* 2003) and Estonia (Kaljo *et al.* 2004, 2007); $\delta^{18}O_{calcite}$ values shown by dotted lines; dashed lines define tropical through polar notation (James 1997). Modelled seawater fields HLDW (high latitude deep, low salinity water); TW (transitional water); STW (subtropical) are after Wilde & Berry (1984); NMS, "normal marine salinity." Modern SE Asia and Pacific values are taken from Wilson & Vecsei (2005).

water in both the northern and southern hemispheres was characterized by $\delta^{18}O$ values from -4 to -7 ‰ indicating a SST in the range of ~15 to 20°C. Temperate water masses were cooler than 15°C.

The ITCZ was positioned at the equator during the Boda Event and, compared to the Pliocene, resulted in a symmetrical distribution of sea surface currents about the equator (Figure 5). This led to a net increase in heat flow towards the poles and lower latitudinal temperature gradients; potentially, explains the migration of warm water faunas to higher latitudes at this time. During the Hirnantian glaciation the ITCZ was north of the equator, resulting in a reduced poleward heat transport. The position of the ITCZ appears to have tracked the pattern of climate change during the Late Ordovician.

Orbital forcing during the Hirnantian glacial maximum

Growing ice sheets reach a critical size when they become sensitive to orbital forcing (Ruddiman 2003). It has been proposed, using analogy with the Pleistocene, that the Hirnantian Glacial Maximum represents two eccentricity paced glacial – interglacial cycles (Sutcliffe *et al.* 2000; Armstrong *et al.* 2005) and that biotic extinction occurred at these timescales (Armstrong 1995). But no evidence has yet been provided to support this hypothesis.

A model of synthetic orbital variations has been constructed to calculate January solar insolation values for the top of the atmosphere

A

	Peak BODA	HICE
Arctic Canada	**40** (35 - 45) **Tropical**	**22** (17 - 27) **STW**
Nevada	**>50** **ITCZ**	**31** (26 - 36) **Tropical**
Estonia	**34** (29 - 38) **Tropical**	**24** (18 - 29) **STW**

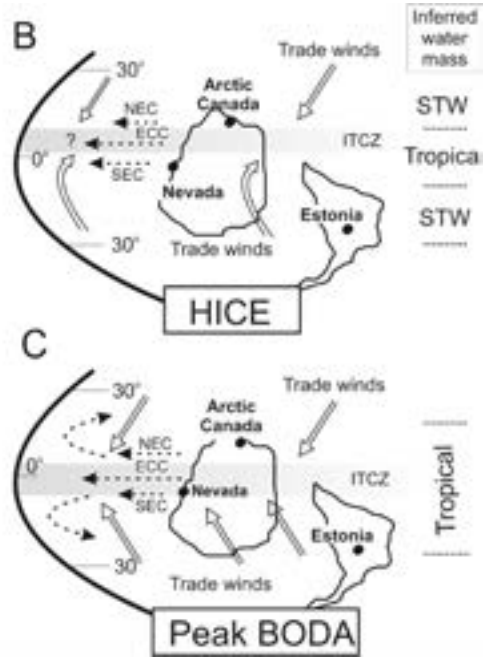

Figure 5. Conceptual model of water mass characterisation, sea surface temperature (5A, based on Figure 4) and shifting pattern of climate belts between the peak Boda Event and HICE (5B, 5C). This illustrates the northwards shift of the ITCZ during the Late Ordovician, concomitant with the development of the Hirnantain ice sheet. Water mass classification: TW, temperate water; STW, sub-tropical water and tropical water masses are as defined in the text and confirm the model predictions of Wilde and Berry (1984). The position of trade winds are extrapolated from the present day and the computer simulations (e.g. Herrmann *et al.* 2005). As the trade winds cross the equator during peak Boda Event the Coriolis effect turns the winds towards the east. Abbreviations: NEC, North Equatorial Current; ECC, Equatorial Counter Current; SEC, South Equatorial Current (redrawn from Armstrong *et al.* in review).

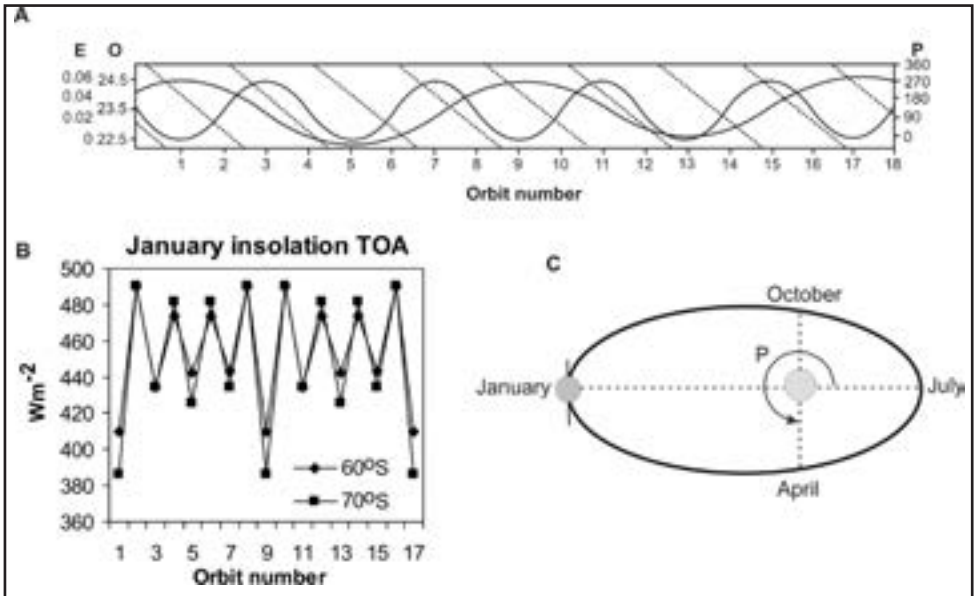

Figure 6. Synthetic orbital variation used in the GCM-ice sheet model for Antarctic glaciation (DeConto & Pollard 2003). A. Synthetic orbital sequence. Numbers 1-18 correspond to orbit time steps of 10ka, orbit 1 corresponds to the diagram in (A). With maximum eccentricity (0.05), minimum obliquity (22.5°) and P=270°. Precession, obliquity and eccentricity have sinusoidal periodicities of 20, 40, 80ka respectively, so that eccentricity completes half a cycle during an obliquity cycle. B. Austral summer (January) insolation at the top of the atmosphere in watts per square metre for orbital steps 1 to 17. Values are for 60° and 70° south. C. Schematic representation of the orbital configuration at the beginning of each 40ka sequence, yielding the coldest possible austral summers (Orbit 1 in other figures). P, is the prograde angle between the perihelion and the Northern Hemisphere vernal equinox and is related to the precession cycle. This determines the month when the Earth is at aphelion.

at 60° and 70°S (Figure 6). The model spans two eccentricity cycles consistent with the proposed duration of the Hirnantian glacial maximum. Pleistocene values for the amplitude of precession and obliquity have been used in the model.

The coldest austral summers (minimal solar insolation during the austral summer) occur when eccentricity is high, obliquity low and aphelion occurs during austral summer (Figure 6). Assuming summer temperature (ablation) is the most important limitation on ice sheet size, major ice advances will occur during the coldest possible austral summers with an eccentricity period (equivalent to glacial – interglacial cycles). Smaller scale ice advances will occur during intermediate insolation conditions (stadial and interstadials). Ice retreats would occur during the warmest austral summers and have an obliquity period.

If the size of Hirnantian ice sheet was orbitally paced then glaciogenic sections at high latitudes should show a pattern of major (equivalent to glacials) and intermediate ice advances (equivalent to stadials), distinguished on the degree of ice incision. The Hirnantian section in southern Jordan records two ice-related, unconformity bounded palaeovalley sequences, with up to 150m of erosion at each unconformity. The upper sequence contains a glacially striated pavement with two cross cutting striation directions (Turner *et al.* 2005). This record has been interpreted to indicate two major ice advances that can be correlated to Saudi Arabia (Miller & Mansour 2007, Vaslet 1990) and Libya (Turner *et al.* 2005). Minor and intermediate ice advances appear to have a more regional extent (Turner *et al.* 2005). From the field evidence it would appear that the Hirnantian glacial maximum spanned two eccentricity cycles and included stadial-interstadial changes.

Termination of the Hirnantian glacial maximum

The rapid termination of glacial conditions in the late Hirnantian remains problematic. This may have been the result of a coincidence of rising atmospheric CO_2 levels, sourced from the weathering of exposed low latitude carbonate platforms and warm austral summers. If the melting Hirnantian ice sheet remained at a size to be sensitive to orbital effects; postulated further small-scale ice advances, during the Early Silurian, might then be explained in terms of Milankovich forcing.

Conclusions

This review demonstrates a common pattern in the sequence of events leading to the Cenozoic and Ordovician glaciations and supports a "reductionist" and uniformitarian hypothesis in which both glaciations had the same cause. Though pCO_2 levels were different during the two time periods both glaciations were set against a backdrop of long-term declining pCO_2, likely initiated by changes in plate configuration that resulted in increased silicate weathering and nutrient cycling into the oceans. Rapid expansion of ice volume was triggered by the re-direction of warm, circum-equatorial currents into high latitudes to provide a source of warm moist air and high levels of snowfall. Once ice sheets were large enough to survive successive precession and obliquity maxima, eccentricity pacing of processes embedded in obliquity and precession largely controlled their size.

This unified theory for Phanerozoic glaciation integrates plate tectonics, changing ocean circulation and orbital/insolation effects.

Acknowledgements

This contribution has benefited from discussions with colleagues particularly Dr A. W. Owen, Dr P. Brenchley (University of Liverpool), Dr M. Williams (University of Leicester) and Prof. T. Meidla (University of Tartu) plus members of IGCP Project 503. Some of the ideas were developed during the tenure of NERC grant (NER/B/2000/000068).

References

Aldridge, R. J., Jeppsson, L. & Dorning, K. J. 1993. Early Silurian oceanic episodes and events *Journal of the Geological Society* **150**, 501-513.

Armstrong, H. A. 1995. High-resolution biostratigraphy (conodonts and graptolites) of the Upper Ordovician and Lower Silurian- a chronometric framework in which to evaluate the causes of the mass extinction. *Modern Geology* **20,** 1-28.

Armstrong, H. A. 2007. On the cause of the Ordovician glaciation. In: *Deep time perspectives on climate change* (edited by Williams, M., Haywood, A. & Gregory, J.) Special Publication of the Geological Society of London. The Micropalaeontological Society, 101-121.

Armstrong, H. A., Baldini, J., Challands, T. J., Grocke, D. & Owen, A. W. in review. Links between the ITCZ and Ordovician glaciation. *Palaeogeography Palaeoclimatology Palaeoecology.*

Armstrong, H. A. & Coe, A. L. 1997. Deep sea sediments record the geophysiology of the end Ordovician glaciation. *Journal of the Geological Society* **154**, 929-934.

Armstrong, H. A., Turner, B. R., Makhlouf, I. A., Williams, M., Al Smadi, A. & Abu Salah, A. 2005. Origin, sequence stratigraphy and depositional environment of an Upper Ordovician (Hirnantian), peri-glacial black shale, Jordan. *Palaeogeography Palaeoclimatology Palaeoecology* **220**, 273-289.

Berner, R. A. 1992. Palaeo-CO_2 and climate. *Nature* **358**, 114.

Berner, R. A. 2001. Modelling atmospheric O_2 over Phanerozoic time. *Geochimica et Cosmochimica Acta* **65**, 685-694.

Berner, R. A. & Kothavala, Z. 2001. Geocard III; a revised model of atmospheric CO_2 over Phanerozoic time. *American Journal of Science* **301**(182-204).

Berry, W. B. N. & Wilde, P. 1978. Progressive ventilation of the oceans-an explanation for the distribution of the Lower Paleozoic black shales. *American Journal of Science* **278**, 27-75.

Billups, K. 2005. Snow maker for the ice ages. *Nature* **433,** 809-810.

Billups, K., Ravelo, A. C., Zachos, J. C. & Norris, R. D. 1999. Link between oceanic heat transport, thermohaline circulation, and the Intertropical Convergence Zone in the early Pliocene Atlantic. *Geology* **27**, 319-322.

Boucot, A. J. & Gray, J. 2001. A critique of Phanerozoic climatic models involving changes in the CO_2 content of the atmosphere. *Earth Science Reviews* **56**, 1-159.

Brenchley, P. J., Marshall, J. D., Carden, G. A. F., Robertson, D. B. R., Long, D. G., Meidla, T., Hints, L. & Anderson, T. F. 1994. Bathymetric and isotopic evidence for a short lived Late Ordovician glaciation in a greenhouse period. *Geology* **22**, 295-298.

Bruckschen, P., Oesmann, S. & Veizer, J. 1999. Isotope stratigraphy of the European Carboniferous: proxy signals for ocean chemistry, climate and tectonics. *Chemical Geology* **161**, 127-163.

DeConto, R. M. & Pollard, D. 2003. A coupled climate-ice sheet modelling approach to the Early Cenozoic history of the Antarctic ice sheet. *Palaeogeography Palaeoclimatology Palaeoecology* **198,** 39-52.

Frakes, L. A., Francis, J. E. & Sykes, J. I. 1992. *Climate Modes of the Phanerozoic.* Cambridge University Press, Cambridge.

Grahn, Y. & Caputo, M. V. 1992. Early Silurian glaciations in Brazil. *Palaeogeography Palaeoclimatology Palaeoecology* **51**, 9-15.

Haug, G. H., Ganopolski, A., Sigman, D. M., Rosell-Mele, A., Swann, G. E. A., Tiedemann, R., Jaccard, S. L., Bollmann, J., Maslin, M. A., Leng, M. J. & Eglington, G. 2005. North Pacific seasonality and the glaciation of North America 2.7 million years ago. *Nature* **433**, 821-825.

Haug, G. H. & Tiedemann, R. 1998. Effect of the formation of the Isthmus of Panama on Atlantic Ocean thermohaline circulation. *Nature* **393**, 673–676.

Herrmann, A. D., Haupt, B. J., Patzkowsky, M. E., Seidov, D. & Slingerland, R. L. 2005. Response of Late Ordovician paleoceanography to changes in sea level, continental drift, and atmospheric pCO_2: potential causes for long-term cooling and glaciation. *Palaeogeography Palaeoclimatology Palaeoecology* **210,** 385-401.

Herrmann, A. D., Patzkowsky, M. E. & Pollard, D. 2003. Obliquity forcing with 8-12 times preindustrial levels of atmospheric pCO_2 during the Late Ordovician glaciation. *Geology* **31**, 485-488.

Herrmann, A. D., Patzkowsky, M. E. & Pollard, D. 2004. The impact of paleogeography, pCO_2, poleward ocean heat transport and sea level change on global cooling during the Late Ordovician. *Palaeogeography, Palaeoclimatology, Palaeoecology* **206,** 59-74.

James, N. P. 1997. The cool-water carbonate depositional realm. *Special Publication, SEPM*, 1-20.

Kaljo, D. L., Hints, L., Martma, T., Nolvak, J. & Oraspold, A. 2004. Late Ordovician carbon isotope trend in Estonia, its significance in stratigraphy and environmental analysis. *Palaeogeography Palaeoclimatology Palaeoecology* **210,** 165-185.

Kaljo, D. L., Martma, T. & Saadre, T. 2007. Post-Hunnebergian Ordovician carbon isotope trend in Baltoscandia, its environmental implications and some similarities with that of Nevada. *Palaeogeography Palaeoclimatology Palaeoecology* **245,** 138-155.

Karhu, J. & Epstein, S. 1986. The implication of the oxygen isotope records in coexisting cherts and phosphates. *Geochimica et Cosmochimica Acta* **50,** 1745-1756.

Kennett, J. P. 1977. Cenozoic evolution of Antarctic glaciation, the circum-Antarctic oceans and their impact on global paleooceanography. *Journal of Geophysical Research* **82,** 3843-3859.

Kolata, D. R., Huff, W. D. & Bergström, S. M. 2001. The Ordovician Sebree Trough: An oceanic passage to the Midcontinent United States. *Geological Society of America, Bulletin* **113**, 1067-1078.

Kump, L. R., Arthur, M. A., Patzkowsky, M. E., Gibbs, M. T., Pinkus, D. S. & Sheehan, P. M. 1999. A weathering hypothesis for glaciation at high atmospheric pCO_2 during the Late Ordovician. *Palaeogeography Palaeoclimatology Palaeoecology* **152**, 173-187.

Kump, L. R., Gibbs, M. T., Arthur, M. A., Patzkowsky, M. E. & Sheehan, P. M. 1995. Hirnantian glaciation and the carbon cycle. In: *Ordovician Odyssey: Short papers for the 7th Int. Symp. Ordovician System. Pacific section.* (edited by Cooper, J. D. e. a.). Society for Sedimentary Geology, Fullerton, 299-302.

Land, L. S. 1995. Oxygen and carbon isotopic composition of Ordovician brachiopods: Implications for co-eval seawater: Discussion. *Geochemica et Cosmochim Acta* **59,** 2843-2844.

Loydell, D. K. 2007. Early Silurian positive $\delta^{13}C$ excursions and their relationship to glaciations, sea-level changes and extinction events. *Geological Journal* **42**, 531-546.

Melchin, M. J., Holmden, C. & Williams, S. H. 2003. Correlation of graptolite biozones, chitinozoan biozones and carbon isotope curves through the Hirnantian. In: *Ordovician from the Andes* (edited by Albanesi, G. L., Beresi, M. S. & Peralta, S. H.) 17. INSUGEO, Serie Correlacion Geologica, 101-104.

Miller, M. A. & Mansour, H. A.-R. 2007. Preliminary palynological investigation of Saudi Arabian Upper Ordovician glacial sediments. *Revue de Micropaleontologie* **50**, 17-26.

Oglesby, R. J. 1989. A GCM study of Antarctic Glaciation. *Climate Dynamics* **3,** 135-156.

Pagani, M., Arthur, M. A. & Freeman, K. H. 1999. Miocene evolution of atmospheric carbon dioxide. *Paleoceanography* **14**, 273-292.

Page, A. A., Zalasiewicz, J. A., Williams, M. & Popov, L. E. 2007. Were transgressive black shales a negative feedback modulating glacioeustacy in the Early Palaeozoic icehouse? In: *Deep-Time perspectives on Climate Change: Marrying the Signal from Computer Models and Biological Proxies* (edited by Williams, M., Haywood, A., Gregory, F. J. & Schnmidt, D. N.) Special Publication of the Geological Society of London. The Micropalaeontological Society, 123-156.

Parrish, J. T. 1982. Upwelling and petroleum source beds, with reference to Palaeozoic. *AAPG Bulletin* **66**, 750-774.

Pearson, P. N. & Palmer, M. R. 2000. Atmospheric carbon dioxide over the past 60 million years. *Nature* **406**, 695-699.

Peterson, L. C. & Haug, G. H. 2006. Variability in the mean latitude of the Atlantic Intertropical Convergence Zone as recorded by riverine input of sediments to the Cariaco Basin (Venezuela). *Palaeogeography Palaeoclimatology Palaeoecology* **234**, 97-113.

Pope, M. C. & Steffen, J. B. 2003. Widespread, prolonged late Middle to Late Ordovician upwelling in North America: A proxy record of glaciation? *Geology* **31**, 63-66.

Poussart, F., Weaver, A. J. & Barnes, C. R. 1999. Late Ordovician glaciation under high atmospheric CO_2: A coupled model analysis. *Paleooceanography* **14,** 542-558.

Prentice, M. L. & Mathews, R. K. 1991. Tertiary ice sheet dynamics: The snow gun hypothesis. *Journal of Geophysical Reseach* **96**, 6811-6827.

Railsback, L. B., Ackerly, S. C., Anderson, T. F. & Cisne, J. L. 1990. Palaeontological and isotope evidence for warm saline deep waters in Ordovician oceans. *Nature* **343**, 156-159.

Raymo, M. E. & Ruddiman, W. F. 1992. Tectonic forcing of late Cenozoic climate. *Nature* **359**, 117-122.

Ruddiman, W. F. 2003. Orbital insolation, ice volume, and greenhouse gases. *Quaternary Science Reviews* **22**, 1597-1629.

Saltzman, M. R., Bergström, S. M., Huff, W. D. & Kolata, D. R. 2003. Conodont and graptolite biostratigraphy and the ordovician (Early Chatfieldian, Middle Caradocian) $\delta^{13}C$ excursion in North America and Baltoscandia: implications for the interpretation of the relations between the Millbrig and Kinnekulle K-bentonites. *Serie Correlation Geologica-INSUGEO* **17,** 137-142.

Saltzman, M. R. & Young, S. A. 2005. Long-lived glaciation in the Late Ordovician? Isotopic and sequence-stratigraphic evidence from western Laurentia. *Geology* **33**, 109-112.

Shields, G. A., Carden, G. A. F., Veizer, J., Meidla, T., Rong, J.-Y. & Rong, Y.-L. 2003. Sr, C, and oxygen isotope geochemistry of Ordovician brachiopods: a major isotopic event around the Middle -Late Ordovician transition. *Geochemica et Cosmochimica Acta* **67**, 2005-2025.

Sutcliffe, O. E., Dowdeswell, J. A., Whittington, R. J., Theron, J. N. & Craig, J. 2000. Calibrating the Late Ordovician glaciation and mass extinction by the eccentricity of Earth's orbit. *Geology* **28**, 967-970.

Tobin, K. J., Bergström, S. M. & De La Garza, P. 2005. A mid-Caradocian (453 Ma) drawdown in atmospheric pCO_2 without ice sheet development? *Palaeogeography Palaeoclimatology Palaeoecology* **226**, 187-204.

Tucker, M. E., Gallagher, J., Lemon, K. & Leng, M. J. 2003. The Yoredale Cycles of Northumbria: High-frequency clastic-carbonate sequences of the mid-Carboniferous icehouse world. Open University *Geological Society Journal* **24**, 1-6.

Turner, B. R., Makhlouf, I. M. & Armstrong, H. A. 2005. Late Ordovician (Ashgillian) glacial deposits in southern Jordan. *Sedimentary Geology* **181**, 73-91.

Underwood, C. J., Crowley, S. F., Marshall, J. D. & Brenchley, P. J. 1997. High resolution carbon isotope stratigraphy of the basal Silurian stratotype (Dob's Lin, Scotland) and it's global correlation. *Journal of the Geological Society, London* **154**, 709-718.

Vaslet, D. 1990. Upper Ordovician glacial deposits in Saudi Arabia. *Episodes* **13**, 147-161.

Veizer, J., Fritz, P. & Jones, B. 1986. Geochemistry of brachiopods: oxygen and carbon isotopic records of Paleozoic oceans. *Geochemica et Cosmochimica Acta* **50,** 1679-1696.

Vincent, E. & Berger, W. H. 1985. Carbon dioxide and polar cooling in the Miocene: the Monterey hypothesis. In: *The Carbon Cycle and Atmospheric CO_2: Natural variations Archean to Present* (edited by Broecker, W. S. & Sundquist, E. T.) 32. AGU Geophysical Monograph, 455-468.

Webby, B. D., Paris, F., Droser, M. L. & Percival, I. G. 2004. *The Great Ordovician Biodiversification Event.* Columbia University Press, New York.

Wenzel, B., Lécuyer, C. & Joachimski, M. M. 2000. Comparing oxygen isotope records of Silurian calcite and phosphate-$\delta^{18}O$ compositions of brachiopods and conodonts. *Geochemica et Cosmochim Acta* **64**, 1859-1872.

Wilde, P. 1991. Oceanography in the Ordovician. *In: Advances in Ordovician geology* (edited by Barnes, C. R. & Williams, S. H.) Paper 90-9. Geological Survey of Canada, 283-298.

Wilde, P. & Berry, W. B. N. 1984. Destabilization of the oceanic density structure and its significance to marine "extinction" events. *Palaeogeography Palaeoclimatology Palaeoecology* **48,** 143-162.

Wilson, M. E. J. & Vecsei, A. 2005. The apparent paradox of abundant foramol facies in low latitudes: their environmental significance and effect on platform development. *Earth Science Reviews* **69,** 133-168.

Zachos, J. C., Pagani, M., Sloan, L. & Thomas, E. 2001. Trends, rhythms, and aberrations in global climate 65 Ma to present. *Science* **292**, 686-693.

Estuaries: Monitoring and Modeling the Physical System. Jack Hardisty. 2007. Blackwell Publishing. 157 pp. £34.99 hardback. ISBN–13: 978-1-4051-4642-5 ISBN-10: 1-4051-4642-7

Jack Hardisty is Professor of Environmental Physics at the University of Hull and has also been involved with NERC's Land Ocean Interaction Study (LOIS) programme. This book is both a research monograph incorporating the author's vision of combining research data with operational forecasts from within and without LOIS to produce operational information systems, and also a graduate and professional reference book; it is "in many ways" the book of the University of Hull's graduate smodule on Estuaries. Each new section, on the evolution and monitoring of estuaries, and on their bathymetry, tides, currents, temperature and salinity, and suspended particulate matter, is followed by a section on modelling these six parameters. On-line resources are an integral part of the approach: logging on to http://www.blackwellpublishing.com/hardisty/ brings up links to models appropriate to these parameters, and to "estuarine toolboxes" which are pages from an Excel workbook containing implementations of equations and formulae. There are supposed to be sixteen of these toolboxes, but only one was on the website when I accessed it; similarly the links to the twenty-seven "dynamic internet references" listed in the book were "coming soon".

How useful is this book as a supplement to S330? I should say that it is so only if you want to go much deeper into estuarine modelling; the main sections are clearly laid out, but not more so than in our own course. However the internet references provide a lot of extra data which can supplement one's understanding, whether of Milankovitch cycles, acoustic current meters, salinometers, or data from Hardisty's backyard in the Humber Estuary. So many of our rocks must have been laid down in estuaries; anything that aids our appreciation of these dynamic and complicated systems is welcome.

Philip Clark, BSc Hons (Open)

Practical and Theoretical Geoarchaeology by Paul Goldberg and Richard I Macphail, 2006, Blackwell Publishing (Oxford), xii + 456pp, £34.99 (paperback), ISBN 0632060441.

Practical and Theoretical Geoarchaeology (like Caesar's Gaul) is divided into three parts: Part I is "Regional scale geoarchaeology". It covers 1 Sediments, 2 Stratigraphy, 3 Soils, 4 Hydrological systems I: slopes and slope deposits, 5 Hydrological systems II: rivers and lake, 6 Aolian settings and geoarchaeological environments, 7 Coasts, and 8 Caves and rockshelters.

Part II is "Nontraditional geoarchaological approaches". It covers 9 Human impact on the landscape, 10 Occupation deposits I: concepts and aspects of cultural deposits, 11 Occupation deposits II: examples, 12 Experimental geoarchaeology, 13 Human materials, and 14 Applications of geoarchaeology to forensic science.

Part III is "Field and laboratory methods, data, and reporting. It covers 15 Field-based methods, 16 Laboratory techniques, 17 Reporting and publishing, and 18 Concluding remarks and the geoarchaeological future.

There are two appendixes, one each to chapters 15 and 16, with practical notes and tables, especially on the laboratory techniques. The thorough bibliography runs to 38pp. There are three indexes: general subject (10pp), Sites and Place Names (2pp), and Archaeological, Geological, Chronological and Cultural Periods (1p).

The text is liberally accompanied by black and white photographs of adequate print quality, and by line drawings, diagrams and charts. Those in Part I will be especially familiar to geologists (some are even from our OU texts!). An 8-page colour plate section has 14 photographs, numbered by the book's chapters, in the middle of the book — obviously making for economical printing, but also necessitating finger place-keeping as one reads the book.

Part I is virtually a textbook in sedimentary, soft rock geology, made relevant to archaeology with special boxed sections of archaeological examples world-wide, but mostly of Palaeolithic and Palaeoindian date.

The curious use of 'Nontraditional' for Part II, to me, seems unnecessary. The techniques and principles are basically the same as a geologist would use — thus, the preceding Part I. The difference is that these approaches are applied to archaeological contexts, which necessarily means that they are applied to periods of human occupation on the Earth, effectively Pleistocene and Holocene. The emphasis is on the application of methods and techniques, in a comparatively 'micro-scale' (mostly) to proto-historic and historic sites (anything from Palaeolithic occupations, to Near Eastern tells, to New World Palaeoindian sites). The emphasis is on the human impact on the environment, and on natural processes that, in turn, affect human activities. Several chapters apply to human remains and burials, including forensic science techniques.

Part III is self-explanatory. It is the 'how to do' bit.

Should Part III have come first? Possibly, but its 'drier' text — being a basic manual — would have the potential effect of putting the reader off! Parts I and II are much more exciting and readable.

This book gives an excellent and thorough coverage of the subject. Its world-wide coverage is down to the two highly qualified authors: PG from the Department of Archaeology, Boston University; PIM from University College London. It will be an extremely valuable manual for students, as it gathers so much geological and archaeological information together and shows where and how the two fields can apply to and help each other. The result is, as it should be, greater understanding of the environment and of archaeological site-creation processes and how both the roles of natural processes and human activities create and affect the landscape.

Naturally, I have a few quibbles. Pleased to see the inclusion of a section devoted to the "Harris Matrix" on archaeological stratigraphy, I was disappointed to see that the authors seem to miss a fundamental difference between geological stratigraphy and archaeological stratigraphy, and therefore one reason for the creation of the Harris Matrix. Archaeological stratigraphy comprises not just layers. The cut line of a pit (for example) is as important as the fill of the pit, because there could be a period of time between when the pit was dug and when it was filled. This potential time lapse has implications for the chronological sequence (and therefore interpretation) of events on the site. Other events, not physically connected to the pit's cut line, could occur, and lay down deposits. The chronological relationships between these deposit events and the open pit, and between the deposits that eventually fill the pit, all need to be sorted into their correct order of occurrence. Therefore the pit's cut line must be numbered and placed in the Harris Matrix as a stratigraphic event, just as a layer of pit fill or soil layer elsewhere on the site must be numbered and put in the matrix. The authors do not seem to recognise this possibility in their diagrammatic example of a Harris Matrix, which is too simple and does not recognise a feature that looks very much like a pit cutting. This is a pity, as this fundamental difference between the way archaeologists use and interpret 'stratigraphy' is extremely important in interpreting human activities on archaeological sites.

A second quibble is with the choice of examples. They are world-wide and cover a wide range of archaeological cultures. I was disappointed, therefore, to see that the New World examples are Palaeoindian. I searched the index in vain for a superb example of geoarchaeology, namely, the mass sacrificial burial at the Huaca de la Luna at Moche (an ancient Andean Area coastal civilization). My disappointment in the exclusion has less to do with my own speciality in the ancient civilizations of the New World, than with the fact that this is an extremely illuminating example. The corpses were thrown from the huaca platform into soft, muddy silt and subsequently covered in a layer of fine flood-borne silt. The geoarchaeological evidence shows that these silts were caused by the weather patterns of an El Niño event year. This in turn supports the interpretation that the sacrifices were performed in reaction to the weather, and consequent poor crop production, believed by the executioners to be caused by angry gods — they were imploring and appealing to their gods, and hoping to induce them to treat humans more kindly. Surely this is a big part of the reason for geoarchaeology: to study natural and human impacts on environment and to support cultural interpretation and understanding.

David M Jones BA (Hons) Anthropology, MA & PhD Archaeology, BSc (Hons) (Open) Earth Sceinces

De beers Geological Journeys: a traveller's guide to South Africa's rocks and landforms by Nick Nroman and Gavin Whitfield,2006, Struik Publishers, Cape Town, pp320, SA Rand 174 (paperback) ISBN 1770070621.

I celebrated finishing S260 last autumn with a holiday in South Africa and, alas, only during the second week did this delightful book appear in the shops. The authors are professional geologists who have written a lucid, beautifully illustrated guidebook for the interested traveller.

It covers the whole of South Africa and is divided into eighteen sections each covering either a city ("Greater Johannesburg and environs") or a road route (N2; Cape Town to Port Elizabeth"). Each chapter has clear maps, cross sections, descriptions of field expeditions and excellent photographs - all in colour - as well as informative essays on subjects that include mining, norphology, palaeontology and neolithic art.

At around £15 this is the bargain of the year.

Tony Drummond BA Hons (Open), MB., ChB (Manc)

Neoproterozoic glaciation in the Earth System: a progress report

Professor Ian J. Fairchild, School of Geography, Earth and Environmental Sciences, University of Birmingham, Edgbaston, Birmingham B15 2TT, UK

Introduction

The occurrence of glaciation in Earth history is sporadic and apparently unpredictable from any underlying physical principles: there were perhaps three episodes around 2.5-3Ga, three in the later part of the Neoproterozoic (say 0.75 to 0.58Ga), the short-lived Ordovician event(s), Permo-Carboniferous and Cenozoic. Those in the Neoproterozoic are not associated with continental collision and positive carbon isotope anomalies as in the Phanerozoic and so, to explain them, we need to go back to the basic building blocks of climate control, rather than using Phanerozoic analogues.

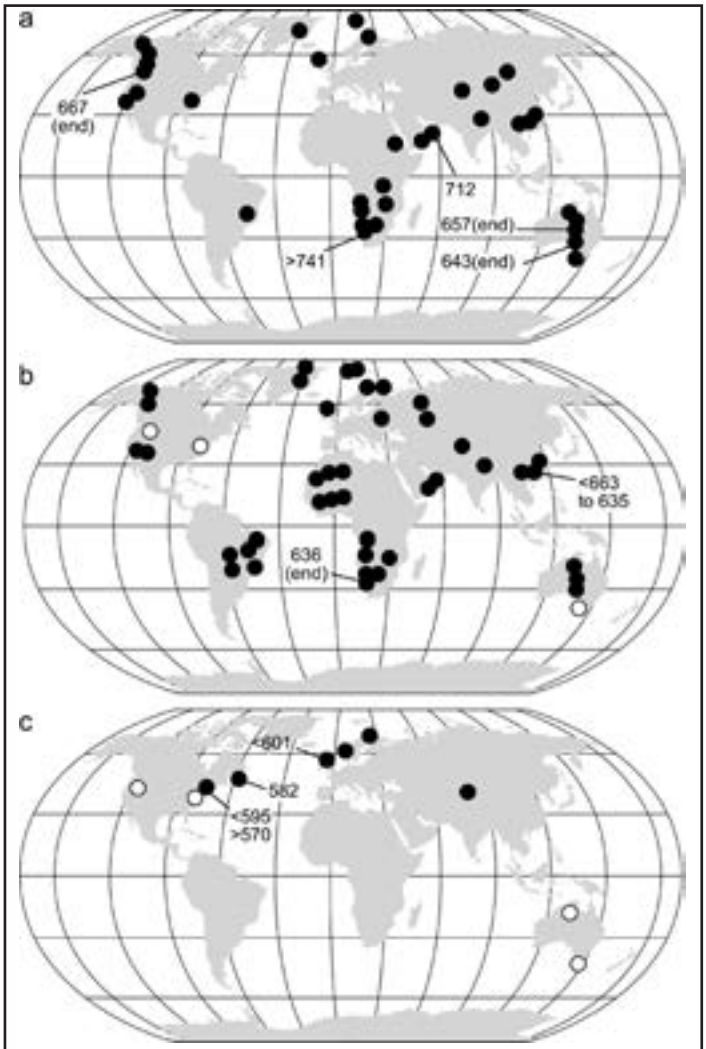

Figure 1. Geographic distribution of Neoproterozoic alleged glacial deposits grouped by age (modified from Halverson 2006) with critical age constraints. In most cases, the assignment to a given interval is based on stratigraphic or loose geochronological constraints and/or the occurrence of a cap carbonate with distinctive characteristics. Some uncertain assignments are shown as open circles. (a) period 740-660Ma ("Sturtian"). More and less certain assignments are not distinguished. (b) period <660 to 635Ma ("Marinoan"). (c) Ediacaran glacial ("Gaskiers"), e.g. 580Ma. For a fuller explanation see Fairchild and Kennedy (2007). Reproduced with permission of the Geological Society London.

Fundamentally the climate of a planet depends on the amount of incident solar radiation, but since this has steadily increased during the life of the Earth, it cannot explain the distribution of glaciations. A second basic control is the reflectivity of its surface (the albedo). Current concerns about the loss of sea ice in the Arctic ocean are linked to the strong positive feedback between the loss of reflective snow and ice and the amount of heat retained and hence global temperature. The Snowball Earth hypothesis, most vigorously advocated by Paul Hoffmann (Hoffman *et al.* 1998; Hoffman & Schrag 2002) advocates that there were at least two runaway glaciations in the Neoproterozoic caused by this effect which were probably the most severe in the history of the planet. A third fundamental control is the amount of radiant heat retained by absorption by greenhouse gases in the atmosphere. In order for the Earth not to have progressively warmed through its history, it follows that the total greenhouse gas forcing must have reduced over time.

Other factors control the distribution of energy within the Earth and could also influence the strength of the second and third of the above controls. Cyclic variations in the Earth's orbit (precession, tilt and eccentricity, the Milankovich parameters) are very important in pacing Cenozoic glaciation. The precise patterns of atmospheric and ocean circulation control the extent to which heat is transferred poleward and hence influence the possibility of polar glacial inception. However, plate tectonic conditions can influence atmospheric physical circulation (distribution of mountains) and ocean circulation and in the Phanerozoic, the closing of oceanic gateways is known to be important in glacial inception.

Geological Evidence

Neoproterozoic glacial deposits are known worldwide (Figure 1), but typically represent only a small proportion of the thickness of geological sections and it can be inferred that at any one location, glacial conditions prevailed for say 5-20% of the time. It is common to find two discrete glacigenic intervals and in some locations such as Scotland (Figure 2) or Oman a number of discrete levels with coarse glacially-derived debris occur. An extraordinary feature is the common presence of tropical carbonate platform sediments immediately underlying glacials: these were still mineralogically unstable when eroded and incorporated in glacial sediments (Fig-

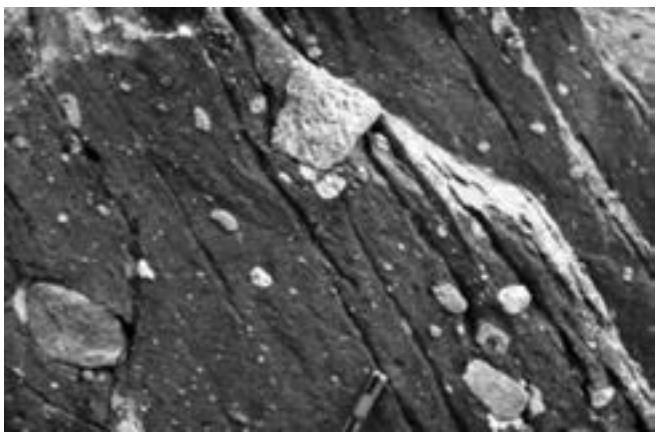

Figure 2. Diamictite with granite clasts in cleaved matrix, Port Askaig Tillite (Garvellachs, Scotland).

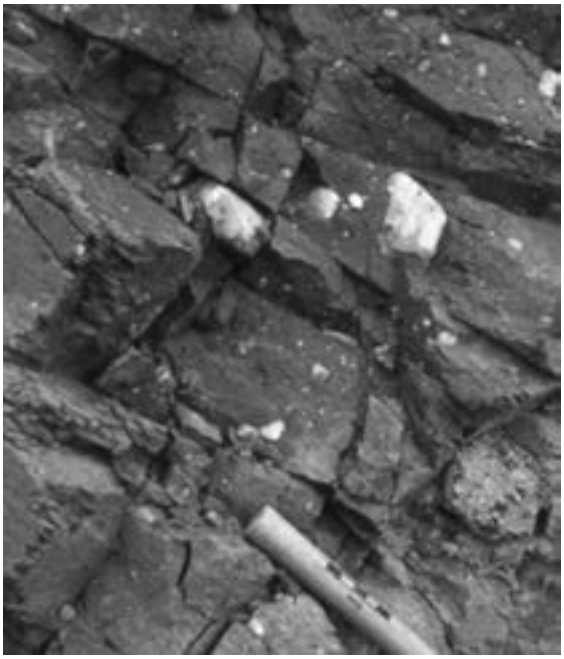

Figure 3. Diamictite with abundant clasts and matrix of dolomite eroded from the underlying carbonate platform (Petrovbreen members, NE Svalbard, see Fairchild, 1993).

ure 3). The implication is that glaciation reached tropical latitudes, a conclusion reinforced by palaeomagnetic evidence of low palaeolatitudes at several locations. Glacial deposits are often overlain by a "cap carbonate", the basal part of a major transgressive systems tract. Recent palaeomagnetic work has shown repeated palaeomagnetic reversals at low palaeomagnetic latitudes in several modern southern hemisphere sites (e.g. Trindade *et al.* 2003), consistent with slow deposition on sediment-starved post-glacial shelves (Kennedy 1996). Initial claims by Hoffman *et al.* (1998) of a negative carbon isotope anomaly that pre-dated and persisted through glaciation is clearly not generally present (Fairchild et al., 2000; Kennedy et al., 2001a). Instead the negative anomaly is particularly characteristic either of deep-water stratified basins (Fairchild *et al*. 2000) or of cap-carbonates and Kennedy *et al.* 2001b and Jiang *et al.* (2003) have found isotopic (as well as structural) evidence for catastrophic methane release in caps where they have been protected from dolomitization.

Neoproterozoic successions are perhaps the worst-dated in the entire geological column because of a relative paucity of igneous rocks for precise determinations. Figure 1 shows a handful of reliable precise dates amongst hundreds of published attempts and these have been achieved by U-Pb dating of zircons in tuffs, and in one case by Re-Os dating of shale. One can conclude that there must have been at least three separate glacial episodes, but the extent of diachroneity is poorly constrained. Palaeogeographically, only reconstructions around 800-750Ma have any solid foundation because of this paucity of dates. It is known that Laurentia, Australia, and possibly several other cratons were equatorial and it is a reasonable proposition that a supercontinent, Rodinia, fragmented in this interval of time and was associated with Sturtian glaciation.

Biostratigraphic correlation is not possible with any precision, but there are several major negative carbon isotope excursions. However, contrary to what was believed up until recently, only some of these have any relationship to glaciation. Because carbon isotope excursions are multiple, and some of them have local significance, they should not be used for global correlation. Sr isotope signatures in well-preserved carbonate rocks however do appear to show a progressive increase over time from values below 0.707 at 750Ma to over 0.709 by the last of the glacial events. In the Phanerozoic such a trend would be linked to increased silicate weathering related to continental collision, but the tectonic condition was quite different in the middle Neoproterozoic. Instead, it is becoming increasingly clear that a primitive land biota of lichens and algae was emerging that amongst other things increased the efficiency of silicate weathering.

Conceptual models of glaciation

Four conceptual models for the icehouse conditions are contrasted in Figure 4. High-tilt Earth posits that the Earth had a high tilt of its spin axis leading to preferential low-latitude glaciation. Zipper-Rift Earth refers to diachronous glaciation related to continental rift margins. Snowball Earth as mentioned above relates to extreme glaciation caused by a runaway ice-albedo feedback. The glaciation would have been terminated eventually by build-up of greenhouse gases in the atmosphere from volcanic emissions. Finally Slushball Earth allows for coexistence of unfrozen oceans and sea-level glaciers in the tropics: it represents a more pragmatic synthesis.

High-tilt Earth (Williams 2000), which leads to extremely strong seasons, is the simplest explanation for the development of periglacial structures in Australian deposits associated with glaciation. However, the Earth's tilt has been stabilized by the Earth-Moon system since the early Precambrian and there is also no other sedimentological evidence of exceptional seasonality. Instead the periglacial structures must relate to diurnal rather than annual temperature change in the tropics, or the incidence of seasonal extreme weather systems (Pierrehumbert, 2005).

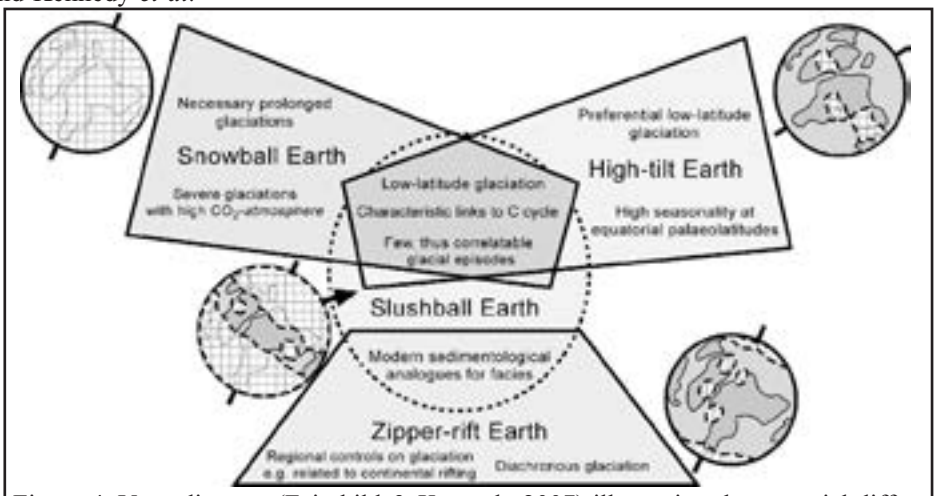

Figure 4. Venn diagram (Fairchild & Kennedy 2007) illustrating the essential differences in interpretation used to support contrasting views of Neoproterozoic glaciation. For example, the Snowball and High-tilt models are quite distinct, although accept some evidence in common, as illustrated. Distribution of ice on cartoons shown by cross-hatched ornament. Reproduced with permission of the Geological Society London.

Zipper-rift Earth readily explains the association of glaciation focused on rift-shoulders of a fragmenting supercontinent (Eyles & Januszczak 2004), is not comfortable with evidence of equatorial glaciation at sea level and also has no explanation for cap carbonates which are distinctive feature of these glacials as distinct from Phanerozoic ones. It is true that many alleged glacigenic successions show considerable evidence of slope-related resedimentation, but there is enough evidence of contemporary glaciation at sea-level in most examples to suggest that Zipper-Rift is insufficient as an explanation.

Snowball Earth has attracted enormous attention to this part of Earth history. It has stimulated a great deal of work by modellers who have demonstrated that even with a mean planetary temperature of -45°C, a significant hydrological cycle persists and could build up significant ice sheets. There would also be the development of equatorward-flowing sea-glaciers, not known in modern times, by a combination of freezing of seawater and accumulation of snow. These insights could be interesting when studying other planetary bodies. Snowball Earth requires globally synchronous glaciation and has had value as a hypothesis against which to measure radiometric age determinations. It has also been instrumental in stimulating other new geological observations, but currently it is a bandwagon still rolling despite falsification of the many of the original ideas used to support it. So, the carbon isotope evidence, as shown above, does not support a mass shutdown of organic productivity leading to a negative carbon isotope anomaly (that is, a carbon isotope signature of carbonates close to that of the bulk Earth rather than segregated between heavy carbonate and light organic carbon). The occurrence of repeated glacial episodes with intervening open water deposition in some successions, is incompatible with the Snowball model. The presence of palaeomagnetic reversals in cap carbonates does not sit easily with a model of rapid carbonate deposition during a hothouse phase following glaciation. New modelling also does not find deglaciation of a Snowball Earth to be possible at plausible CO_2 concentrations of the atmosphere (Pierrehumbert 2005).

Rather, by default we are left with some kind of Slushball Earth as the preferred model. Although not having such a strong, simple theoretical underpinning, such a model is a more realistic way to view the various biogeochemical cycling processes that go on and which so strongly define the state of the Earth system as discussed in the next section.

The Neoproterozoic glacial era

Figure 5 illustrates the timing of Neoproterozoic glaciation in relation to the latter part of Earth history. Although greenhouse gas forcing was continually reducing on the long-term, glaciations only occurred sporadically. The occurrence of individual glacial events would be associated with transient reductions in greenhouse forcing; to a greater or lesser extent tectonic factors influencing for example ocean circulation, would also have had a role.

The timing of glaciation relates to two sets of feedback cycles: one associated with carbon dioxide creation and consumption, and one associated with redox reactions (Catling & Claire 2005; Hayes & Waldbauer 2006). Some reactions are in common with each. Some persuasive geological and modelling evidence has been produced arguing that the Neoproterozoic was a time when the Earth was susceptible to relatively rapid CO_2-drawdown leading to widespread glaciation. One is the modelling of Donnadieu *et al.* (2004)

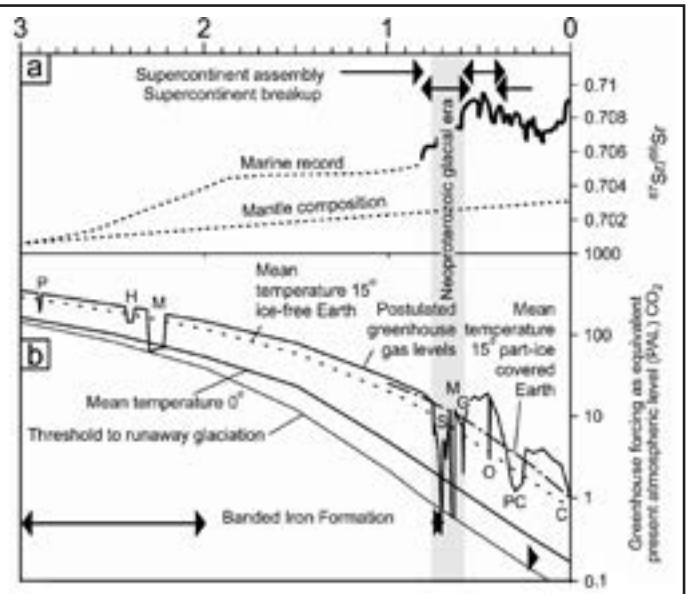

Figure 5. The Neoproterozoic glacial era in the context of long-term evolution of a. tectonics and Sr isotope marine chemistry and b. greenhouse gas forcing (Fairchild & Kennedy 2007). Timescale in billions of years. In b., thresholds for climatic states at different temperatures from energy balance models of Tajika (2004), combined with Phanerozoic PCO2 curve of Berner (1994) supplemented in the Ordovician and Precambrian by inferred variations in greenhouse forcing consistent with the glacial record. Glacial periods are: Pongola (P), Huronian (H), Makganyene (M), Sturtian (S), Marinoan (M), Gaskiers (G), Ordovician (O), Permo-Carboniferous (PC) and Cenozoic (C). Note the Neoproterozoic Glacial Era also probably coincides with a tendency for increased oxidation of surface environments. Reproduced with permission of the Geological Society London.

who show that break-up of an equatorial supercontinent allows high rainfall conditions and associated strong CO_2-drawdown by weathering of continents (and in particular rift-related volcanics) to persist even whilst ice sheets advanced from the poles. Ridgwell and Kennedy (2004) also point out that in the absence of planktonic calcifiers such as forams and coccoliths, marine calcification would have been inefficient at times of low sea-level (glaciation) which would have reduced the rate of re-supply of CO_2 to the atmosphere during the precipitation of carbonate minerals in the ocean. Another is the role of the primitive land biota which not only increased the rate of CO_2-consumption by silicate weathering, but also increased rates of P weathering, leading to higher marine C deposition (Lenton & Watson 2004), and increased rates of clay formation. The clay led to more efficient binding and preservation of organic carbon in marine environments (Kennedy *et al.* 2006). The latter processes also increased the rate of oxygen supply to the atmosphere. To the extent to which they speeded the reduction in the methane content in the atmosphere and seawater, such processes both reduced greenhouse gas forcing and set the scene for the replacement of methane by CO_2 as the most critical greenhouse gas (although their relative abundances during the Neoproterozoic are only loosely constrained).

So, biogeochemical models highlight the lack of CO_2-buffering in the Neoproterozoic and the likely transition from a methane- to a CO_2- dominated climate system. Relevant processes include trop-

ical weathering of volcanic provinces, and new land biotas stimulating both clay mineral formation and P delivery to the oceans, facilitating organic C burial. Hence a step change in the Earth System was probably both facilitated by organisms and responsible for moderating Phanerozoic climate. The precise relationship between drivers and passengers in terms of oxygenation, greenhouse gas evolution and organic evolution (e.g. Canfield *et al.* 2006) remains a major topic of current research.

References

BERNER, R.A. 1994. Geocarb II: A revised model of atmospheric CO_2 over Phanerozoic time. *American Journal of Science,* **294**, 56-91.

CANFIELD, D.E., POULTON, S.W. & NARBONNE, G.M. 2006. Late Neoproterozoic deep-ocean oxygenation and the rise of animal life. *Science*, **10**.1126/science.1135013.

CATLING, D.C. & CLAIRE, M.W. 2005. How Earth's atmosphere evolved to an oxic state: A status report. *Earth and Planetary Science Letters,* **237**, 1-20.

DONNADIEU, Y., GODDÉRIS, Y., RAMSTEIN, G., NÉDÉLEC, A. & MEERT, J. 2004. A 'snowball Earth' triggered by continental breakup through changes in runoff. *Nature,* **428,** 303-306.

ETIENNE, J.L., ALLEN, P.A., RIEU, R. & LE GUERROUÉ, E. 2007. Neoproterozoic glaciated basins: a critical review of the Snowball Earth hypothesis by comparison with Phanerozoic glaciations. IN: HAMBREY, M.J., CHRISTOFFERSEN, P., GLASSER, N.F. & HUBBARD, B. (eds.) *Glacial Processes and Products*. Special Publication of the International Association of Sedimentologists, (in press).

EYLES, N. & JANUSZCZAK, N. 2004. 'Zipper-rift': a tectonic model for Neoproterozoic glaciations during the breakup of Rodinia after 750 Ma. *Earth-Science Reviews*, **65,** 1-73.

FAIRCHILD, I.J. 1993. Balmy shores and icy wastes: the paradox of carbonates associated with glacial deposits in Neoproterozoic times. IN WRIGHT, V.P. (ed.) *Sedimentology Review*, **1**, 1-16.

FAIRCHILD, I.J. AND KENNEDY, M.J. 2007 Neoproterozoic glaciation in the Earth System. *Journal of the Geological Society*, *London,* **164,** 895-921

FAIRCHILD, I.J., SPIRO, B., HERRINGTON, P.M. & SONG, T. 2000. Controls on Sr and C isotope compositions of Neoproterozoic Sr-rich limestones of E Greenland and N China, IN: GROTZINGER, J.P. & JAMES, N.P. (eds.) *Carbonate Sedimentation and Diagenesis in the Evolving Precambrian World SEPM Special Publication* **67,** 297-313.

HALVERSON, G.P. 2006. A Neoproterozoic Chronology IN: Xiao, S. & Kaufman, A.J. (Eds.) *Neoproterozoic Geobiology and Paleobiology*, Springer, New York, 231-271.

HAYES, J.M. & WALDBAUER, J.R. 2006. The carbon cycle and associated redox processes through time. *Philosophical Transactions of the Royal Society,* **361B**, 931-950.

HOFFMAN, P.F. & SCHRAG, D.P. 2002 The snowball Earth hypothesis: testing the limits of global change. *Terra Nova*, **14,** 129-155.

HOFFMAN, P.F., KAUFMAN, A.J., HALVERSON, G.P. & SCHRAG, D.P. 1998. A Neoproterozoic Snowball Earth. *Science*, **281,** 1342-1346.

JIANG, G., KENNEDY, M.J. & CHRISTIE-BLICK, N. 2003. Stable isotopic evidence for methane seeps in Neoproterozoic postglacial cap carbonates. *Nature*, **426**, 822-826.

KENNEDY, M.J. 1996. Stratigraphy, sedimentology, and isotopic geochemistry of Australian Neoproterozoic cap dolostones: deglaciation, d13C excursions, and carbonate precipitation. *Journal of Sedimentary Research*, **66,** 1050-1064.

KENNEDY, M.J., CHRISTIE-BLICK, N. & PRAVE, A.R. 2001a. Carbon isotopic composition of Neoproterozoic glacial carbonates as a test of paleoceanographic models for snowball Earth phenomena. *Geology,* **29,** 1135-1138.

KENNEDY, M.J., CHRISTIE-BLICK, N. & SOHL, L.E. 2001b. Are Proterozoic cap carbonates and isotopic excursions a record of gas hydrate destabilization following Earth's coldest intervals. *Geology,* **29,** 443-446.

KENNEDY, M., DROSER, M., MAYER, L.M. PEVEAR, D. & MROFKA, D. 2006. Late Precambrian oxygenation; Inception of the clay mineral factory. *Science,* **311**, 1446-1449.

LENTON, T.M. & WATSON, A.J. 2004. Biotic enhancement of weathering, atmospheric oxygen and carbon dioxide in the Neoproterozoic. *Geophysical Research Letters,* **31**, L05202, doi:10.1029/2003GL018802.

PIERREHUMBERT, R.T. 2005. Climate dynamics of a hard snowball Earth. *Journal of Geophysical Research,* **110**, D01111, doi:1029/2004JD005162.

RIDGWELL, A. & KENNEDY, M. 2004. Secular changes in the importance of neritic carbonate deposition as a control on the magnitude and stability of Neoproterozoic ice ages. IN: JENKINS, G.S., MCMENAMIN, M., SOHL, L.E. & MCKAY, C.P. (eds.) *The Extreme Proterozoic: Geology, Geochemistry and Climate*, American Geophysical Union Monograph, 146, 55-72.

TAJIKA, E. 2004. Analysis of carbon cycle system during the Neoproterozoic: Implication for Snowball Earth events. IN: JENKINS, G.S., MCMENAMIN, M., SOHL, L.E. & MCKAY, C.P. (eds.) The *Extreme Proterozoic: Geology, Geochemistry and Climate,* American Geophysical Union Monograph, 146, 45-54.

TRINDADE, R.I.F., FONT, E., D'AGRELLA-FILHO, A.S., NOGUEIRA, A.C.R. & RICCOMINI, C. 2003. Low-latitude and multiple geomagnetic reversals in the Neoproterozoic Puga cap carbonate, Amazon craton. *Terra Nova*, **15**, 441-446.

WILLIAMS, G.E. 2000. Geological constraints on the Precambrian history of Earth's rotation and the Moon's orbit. *Reviews of Geophysics,* **38,** 37-59.

Please e-mail: i.j.fairchild@bham.ac.uk if you would like an electronic (pdf) copy of the Fairchild and Kennedy article, or earlier publications.

Groundwater in the Environment, An Introduction by Paul L.Younger, 2007, Blackwell Publishing, 318pp, £27.99 (paperback) ISBN 1405121432.

This is a very well written introduction to the subject of groundwater research and management. It is very much aimed at those with solid geological knowledge but not necessarily any real knowledge of hydrology and therefore its suitable as course material for anyone studying groundwater systems as part of a course in environmental sciences or earth sciences. The glossary makes it relatively easy to check up on any terms that the reader may not be immediately familiar with and I found it to be a good read and a book that was difficult to put down once started. The text does cover the subject of groundwater in a very comprehensive manner without too much emphasis on mathematical data and statistics. It therefore serves the purpose of introducing the reader to the subject matter without too many intimidating symbols familiar to those with strong statistical backgrounds. A recommended read for anyone contemplating entry into the field of hydrology. Well illustrated with ample tables and figures and sufficient references to enable the reader to use as an initial research tool into the field of hydrology.

Alasdair Farquharson, Dip Geosciences (Open)

Carbon in the Atmosphere and the Human Volcano

Fred Broadhurst, University of Manchester

The talk given at the Symposium in Lancaster, 2007, and this summary, are dedicated to the memory of Tony Browne, an active supporter of the OUGS, who died shortly before the 2007 meeting.

The carbon in the atmosphere occurs mainly as carbon dioxide (CO_2) and methane (CH_4). The concentrations of these two gases are low. That of carbon dioxide is rather more than 385 parts per million (ppm), methane rather more than 1.6ppm, but the amounts of both gases are currently increasing. As both carbon dioxide and methane are greenhouse gases, their increasing abundance is of great interest to climatologists and is of general concern. Atmospheric carbon is dominated by the isotope carbon-12 (^{12}C), comprising about 99%, the remaining 1% being mostly carbon-13 (^{13}C). These two isotopes are stable, but there are also traces of the radioactive carbon-14 (^{14}C) generated by the action of cosmic rays on nitrogen in the upper atmosphere. Carbon-12 is preferentially taken up during photosynthesis, so a higher proportion of this isotope is characteristic of organic matter, the methane generated by it and the carbon dioxide produced by its oxidation (as in the burning of fossil fuels). The relationship between carbon in the atmosphere and environmental factors such as volcanicity, temperature change, solar cycles, cloudiness, etc is complex. Geological history provides an imperfect record of the response of atmospheric carbon to past geological events, particularly volcanic episodes and the processes of plate tectonics. An outline of significant events in the geological history of atmospheric carbon follows.

The stromatolites of the Precambrian make a good starting point. These fossils, dating from over 3,000Ma, have been recognised as closely related to modern Cyanobacteria. These organisms practise photosynthesis so take in carbon dioxide and water from their surroundings and through the energy of sunlight produce organic matter with release of free oxygen (O_2). Stromatolites are found in many geological formations indicating that drawdown of carbon dioxide and generation of free oxygen has been going on for a long time. In the fossil record, the stromatolites were followed by marine organisms including plants (algae) and animals (trilobites, brachiopods, etc) and creatures of uncertain affinity such as Ediacarans. The earliest substantial terrestrial organisms date only from the late Silurian/early Devonian, some 400Ma ago and the reason for their late appearance may well relate to bacterial photosynthesis and the rate at which oxygen was released into the environment. Until the concentration of this oxygen reached critical levels there was inadequate production of ozone (O_3) to protect terrestrial life from UV radiation.

The best-preserved of the early terrestrial plants (and associated fauna) come from the Rhynie Chert of Aberdeenshire. The enclosing silica rock indicates deposition from hot springs associated with volcanism and the plants are preserved as silica petrifactions. These early plants have only rudimentary or no leaves. However, by the end of the Devonian and into the Carboniferous, some 40Ma later, leaves had appeared. Leaves are equipped with openings (stomata) to facilitate gaseous exchange. Comparison of specific plant types in herbariums from the mid 1700s with their present-day representatives shows that the number of stomata per unit area has decreased significantly over a 250-year period of rising carbon dioxide levels. The implication is that leaf stomata serve an important function in collecting carbon dioxide and that the appearance of leaves at the close of the Devonian was linked to a fall in the carbon dioxide content of the Devonian atmosphere. Stomata also facilitate water loss from plants, so leaves in arid regions today are restricted in development. However the settings of both early and late Devonian plants were rich in water, so the appearance of leaves cannot be assigned to a change from dry to wet conditions.

Figure 1. Upright trees over the Bottom Yard Seam, Lancashire Coalfield. Carboniferous carbon sequestration.

During the Carboniferous abundant carbon sequestration took place both on land, in the form of peat/coal formation (Figure 1), and in the seas as limestones (by burial of carbonate shells and skeletons). The very name Carboniferous relates to the richness of carbon in its deposits. Such carbon sequestration was not, apparently, balanced by enough volcanism to replace the carbon dioxide, leading to an 'icehouse world' and the development of an extensive ice cap in the southern hemisphere of the period. At the same time the free oxygen released by photosynthesis can explain the observed gigantism observed in Carboniferous insects (dragonflies with a wing span of 0.75m, millipedes 2m in length (Figure 2)) and plants (horsetails to 12m) and other organisms.

The icehouse conditions of the Carboniferous persisted into the Permian, as is clear from the glacial sediments of high Permian latitudes. But at the close of the Permian there came the most exten-

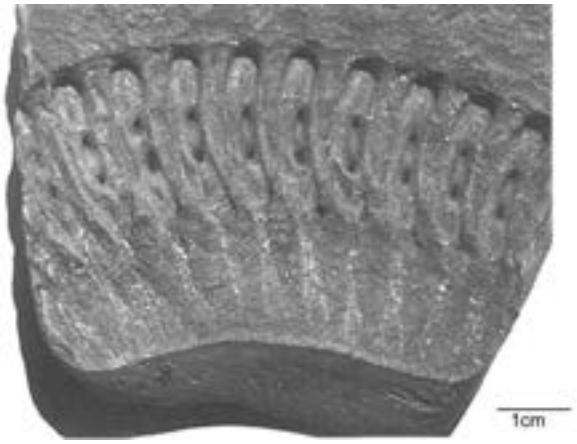

Figure 2. The millipede *Myriacantherpestes,* from the Carboniferous of Illinois. A case of gigantism.

sive mass extinction event to be seen in geological history. Some 90% of marine species and 30% of terrestrial forms were lost. The extinction event occurred during the eruption of the massive Siberian Traps. Not only was volcanogenic carbon dioxide pumped into the atmosphere but at the time of the extinction event carbon dioxide of organic origin, (distinguished by its high carbon-12 content) was also added. Methane hydrates, methane molecules encased by a net of water molecules, 'frozen' under high pressure at low temperature) are under suspicion. These are commonly developed today in marine sediments. The stability of these deposits can be broken by rising temperatures or by physical disturbance. Elevated temperatures caused by the carbon dioxide of the Siberian Traps would explain the eruption of methane. Oxidisation of this methane would deplete the supply of oxygen and so account for the anoxia of which there is evidence in the fossil record at the extinction boundary. An alternative explanation for the end-Permian extinction is that the Siberian Traps released ozone-destroying gases. The extinction event at the end of the succeeding Triassic period is also accompanied by extensive volcanism – the late Triassic Central Atlantic Magmatic Province. There is also a 'spike' of high ^{12}C and the faunas show evidence consistent with anoxia.

The Jurassic faunas indicate a rapid recovery from the anoxic conditions of the end-Triassic. In the Cretaceous there is, again, extensive formation of coal and marine limestones (such as the Chalk) indicating active carbon sequestration and suggesting comparison with the Carboniferous. However the Cretaceous rocks, unlike those of the Carboniferous, reveal evidence of immense volcanic eruptions, particularly on the ocean floors. The occurrence of coals, abundant plant fossils, and dinosaurs at high latitudes in both hemispheres are evidence of a 'greenhouse world' without polar ice caps. The evidence for this greenhouse world is well seen in New Zealand, Alaska and Svalbard. The end of the Cretaceous is marked by another, major, extinction event well known because of its association with the end of the dinosaurs and of the ammonites. The discovery of an asteroid impact site, dated as end-Cretaceous, at the Chicxulub site off the Yucatan Peninsula, Mexico, appeared to confirm the suggestion that an extra-terrestrial impact was the cause of the extinction. However, the end-Cretaceous extinction event took place during the eruption of the Deccan Traps when large volumes of volcanogenic carbon dioxide must have contributed its greenhouse warmth to an already warm globe. At the extinction level there is yet another carbon-12 spike, indicating an organic source of carbon dioxide, leading to the conclusion that methane hydrates and their subsequent oxidation produced the anoxic conditions of the end-Cretaceous extinction. The coincidence of the date of extinction and the arrival date of the asteroid suggest very strongly that the impact played a role in the disturbance and emission of the methane hydrates.

The high temperatures of the Cretaceous world continued into the Cenozoic, on the evidence of oxygen-18/oxygen-16 ratios in marine fossils. These temperatures reached a peak towards the close of the Palaeocene (the Palaeocene-Eocene Thermal Maximum), in association with the volcanism of the North Atlantic Volcanic Province, so well known to us in the form of the Hebridean volcanic rocks of Northern Ireland and the Western Isles of Scotland. This volcanism is linked to another carbon-12 spike and to yet another extinction event (Palaeocene/Eocene).

The oxygen isotope record from the Eocene onwards indicates a general fall in temperatures towards the Pleistocene. By reference to the oxygen isotope ratios of appropriate fossils the temperatures of ocean floors and those of near surface waters can be estimated and variations between the two can be used to indicate times of glaciation. Search for the causes of falling temperatures is focussed on the collision between India and Asia, commencing sometime in the Eocene. The consequent uplift of Tibet and the Himalayan mountain system provided a major region of chemical weathering involving the drawdown of carbon dioxide and the eventual formation of limestone on the sea floor. The result is a reduction in the greenhouse effect. The opening of the North Atlantic Ocean and the closing of the Panama isthmus must also have played a part in the global cooling of the Cenozoic in that they facilitated the flow of tropical waters northwards into high latitudes (via the Gulf Stream).

By the Pleistocene carbon dioxide and methane levels were low and comparable to those of the present day (by the late Pleistocene they could be determined directly by analysis of gas bubbles in borehole ice cores). The relationships between carbon dioxide, methane and temperature suggest that temperature changes preceded those of both carbon dioxide and methane. Variations in the concentrations of these gases together with temperature data relate to Milankovich cycles.

During the Holocene (Recent) the rapid increase in atmospheric carbon dioxide and methane (both with high carbon-12 content) and temperature rise is associated with industrialisation and particularly with the combustion of the fossil fuels coal, oil and natural gas. These fossil fuels have, in effect, replaced volcanoes as a source of carbon dioxide. As a geological agent mankind is acting as a proxy for volcanism. Rising temperatures, unabated, may threaten the stability of methane hydrates, of which there is an abundance. The oxidation of this methane and consequent oxygen depletion, raises the danger of anoxia – which has caused devastation in the past.

In Summary

Geological history shows the importance of the Cyanobacteria and plant life in generating and maintaining the oxygen of the atmosphere. It also indicates the role of major volcanic eruptions in generating carbon dioxide and therefore influencing temperature by the greenhouse effect. High temperatures may be responsible, in part, for the release of methane hydrates and their oxidation to produce conditions of anoxia, threatening life systems. Over the last 250 years mankind appears to have taken over the role of the volcanoes.

Whereas the progress of science has led to ever-increasing degrees of specialism, the current interest in the climate and its future is demonstrating the value of generalist approaches.

Reading

Much of the information in the account above is available through Open University texts. However there is a new book of great interest, emphasizing the generalist approach:

Beerling D, 2007, *The Emerald Planet. How Plants changed Earth's History.* Oxford University Press ISBN 978-0-19-280602-4.

The Great Plume Debate

Gillian R. Foulger, Dept. Earth Sciences, University of Durham, Durham, U.K.

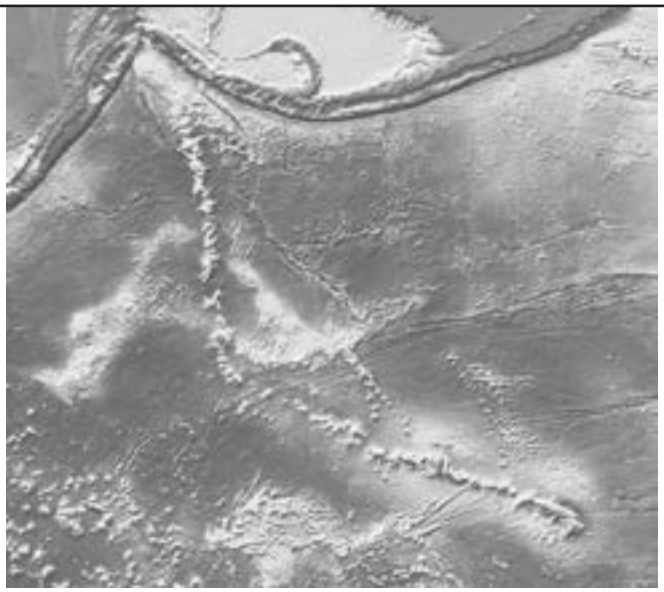

Figure 1. Bathymetry and topography of the Hawaiian-Emperor chain region (from Smith & Sandwell 1997).

Introduction

Hawaii and its associated island chain and archipelago has long been recognised to be a unique volcanic feature on Earth's surface (Figure 1). It is highly productive – Mauna Loa on "the big island" is the largest volcano in the world, rising ~ 8 km above the level of the surrounding sea floor. It has been known for centuries, even to the original Polynesian pioneers who settled Hawaii, that the islands become progressively older to the northwest. Modern radiometric dating spectacularly confirmed this time progression. It was at Hawaii that the term "hot spot" was originally coined. It was used in 1963 by J. Tuzo Wilson, who suggested that the time-progressive island/seamount chain could be explained by motion of the Pacific sea floor over a hot region in the mantle beneath (Wilson 1963).

The development of plate tectonics in the years that immediately followed rapidly offered plausible and elegant explanations for much of Earth's volcanism. Along spreading plate boundaries, the volcanism was understood to be a consequence of upwelling and partial melting of mantle in response to progressive separation of the plates. The volcanism behind subduction zones was understood to result from slab heating, dehydration and partial melting of the overlying mantle.

The spectacular ability of plate tectonics to explain most of the planet's volcanism brought into even sharper focus the exceptions to the general rules, and the glaring exception was Hawaii. This melting anomaly is hugely productive, it lies almost in the centre of the great Pacific plate, several thousand kilometres from any plate boundary, and the islands and seamounts along the Hawaiian and Emperor chains are regularly time-progressive. Hawaii was an elephant in the plate tectonic living room. It clearly did not, by any stretch of the imagination, comprise either a spreading-plate-boundary or a subduction-zone volcano.

The plume hypothesis

In 1971 a new theory was proposed, separate and independent of plate tectonics, to explain Hawaii and other features thought to be

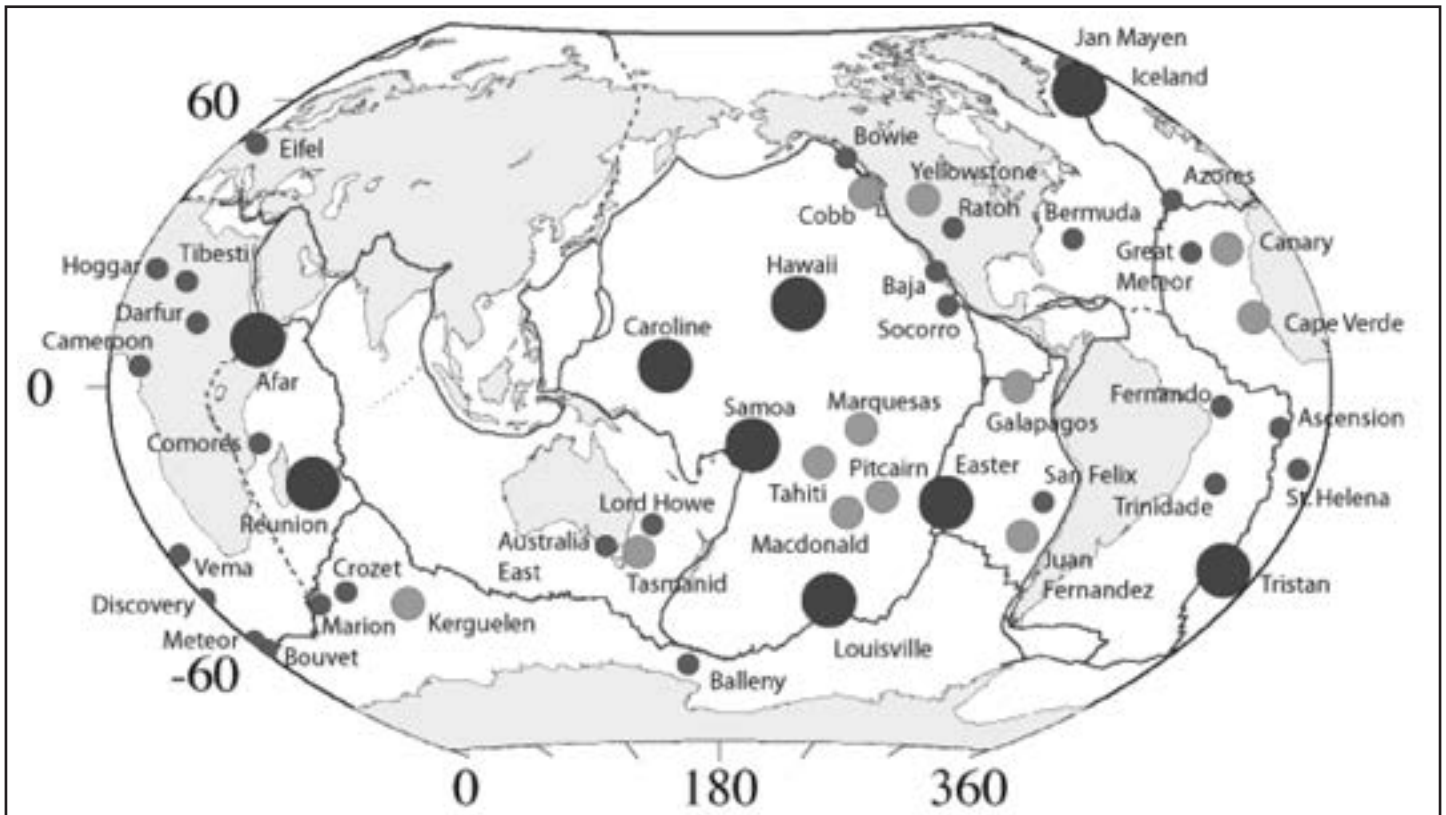

Figure 2. The 49 "hot spots" listed by Courtillot *et al.* (2003).

volcanic exceptions. Morgan (1971) proposed that Wilson's suggested hot region beneath Hawaii was continually re-fuelled by an upward flowing thermal of hot mantle material from the deep mantle. Morgan (1971) extended his theory beyond Hawaii. He postulated that there were "about 20" such plumes in Earth's mantle and that they were fixed relative to one another. He proposed that they currently underlie Hawaii, the Macdonald seamount, Easter island, the Galapagos islands, Bowie, Yellowstone, Iceland, the Azores, the Canary islands, Ascension island, Tristan da Cuhna, the Bouvet triple junction, Marion-Prince Edward island, Réunion, Kerguelen and Afar. There has subsequently been vigorous discussion of exactly how many plumes are thought to exist in Earth (e.g., Figure 2), a problem that was ironically foreshadowed in Morgan's seminal paper where he states that there are "about 20 deep mantle plumes", but plots only 16 on his accompanying figure.

Morgan's plume model was eminently scientific. It made predictions, which scientists immediately went out to test. Its most fundamental predictions are:

1. Precursory domal uplift: The arrival of a bulbous "plume head" at the base of the lithosphere results in domal surface uplift of 500-1000 m a few Ma before flood basalt volcanism starts. The amplitude of the uplift depends on the temperature of the plume, and the area over which uplift is significant has a diameter of about 1,000 km (Figure 3).
2. Flood basalt eruption (the plume head): The arriving plume head flattens to a disk at the base of the lithosphere, causing extension, and flood basalt eruptions rapidly cover an area 2000-2500 km in diameter. The diameter of the region over which flood basalt eruption occurs is dependent on the temperature difference between the plume and the surrounding mantle. If the plume head rises beneath continental lithosphere it may cause continental breakup and form a volcanic margin.
3. A narrow conduit to the core-mantle boundary (the plume tail): Following flood basalt eruption, plume material continues to flow upward from the core-mantle boundary through a tail-like conduit 100-200 km in diameter.
4. A time-progressive volcanic chain: As the tectonic plate above moves on Earth's surface, continued volcanism from the relatively fixed plume tail forms a trail of volcanism. The youngest volcanism occurs above the present-day location of the plume tail and older volcanism occurs progressively further along the trail;
5. High temperatures: The lavas associated with both the plume head and the plume tail melted at unusually high temperatures. Excess temperatures of 300 ± 100˚C occur at the centre of the plume head, above the tail, reducing to ~100˚C away from the centre. Because of the high temperatures, picritic (high-MgO) melts dominate early on and close to the centre of the plume head.

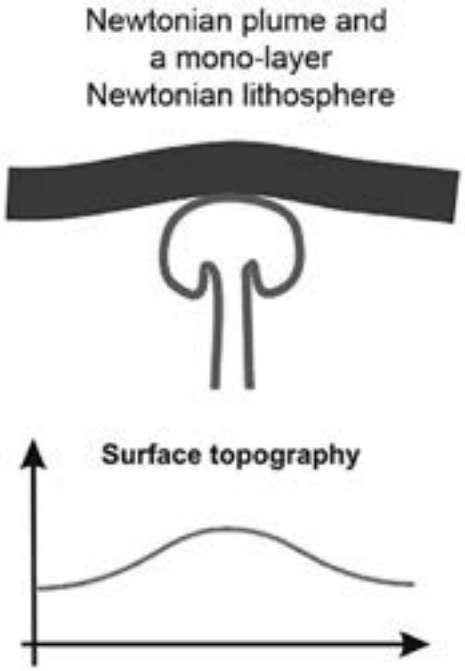

Figure 3. Pattern of uplift predicted for impingement of a plume beneath the lithosphere (courtesy of E. Burov).

Many instances have been cited where these predictions of the plume hypothesis are upheld. The eruption of a flood basalt, and widespread uplift are perhaps nowhere better illustrated than in the north Atlantic. That ocean began to open at ~54 Ma, at which time vast volcanic margins were built along the edges of the new ocean. The volume of this huge province has been estimated to be ~ 6 x 10^6 km^3 (Eldholm & Grue 1994). Uplift was at the kilometre level and widespread. The postulated plume is suggested to have impacted beneath central Greenland, but uplift occurred as far south as Britain.

Many seismic tomography images of the mantle have been calculated that have been interpreted as showing continuous high-temperature bodies that traverse the mantle from top to bottom, e.g., at Tahiti. At Hawaii, the best petrological evidence for high temperature in the mantle has been reported (Clague *et al.* 1991). Picrite glass sand grains dredged from the submarine Puna ridge southeast of Hawaii, have been interpreted as olivine controlled crystalisation, pointing to a mantle potential temperature of some 150- 270˚C hotter than normal (Herzberg *et al.* 2007).

Why then, is the plume hypothesis presently under such intense criticism and scrutiny? The reason is well-illustrated by the very examples quoted above – at not one single hypothesised plume locality are all five predictions fulfilled. At the majority (Figure 2) few are fulfilled, and at many none. In the north Atlantic, for example, there is no time-progressive volcanic chain and no seismically imaged structure traversing the mantle that could plausibly be interpreted as a plume tail. At Tahiti there is no uplift, flood basalt or evidence of high temperature and a time-progressive volcanic chain is only weakly, if at all, developed.

At Hawaii there is no initial flood basalt or uplift and a mantle-traversing seismic anomaly has yet to be found. Nowhere other than at Hawaii have modern picrite glasses, that might indicate high mantle temperature, been found. It is for this reason that the term "melting anomalies" is used in this article, rather than "hot spots". The latter term pre-supposes a source characteristic that is almost nowhere confirmed. The former, on the other hand, is based on an observation that is incontrovertible, unless one wishes to take issue with what is "anomalous" and what is "normal". This issue is a valid one, but it will not be discussed in this article.

Simply put, the plume hypothesis is very poor at predicting the observations at melting anomalies. If the health outcomes of a drug or medical procedure were so poorly predicted it is unlikely that it would be considered reliable enough to use!

The rise of the plate hypothesis

In recent years, many scientists have felt that the failure of the plume hypothesis (Fgure 4) to explain observations has reached a level that cannot be ignored. As a result, and since the turn of the century, there has been renewed effort to develop alternative theories to explain the magmatism that seems to be unusual in the context of plate tectonics. The theories developed can basically be divided into two groups – the secondary effects of plate tectonics, and bolide impacts. These theories raise the source of melting anomalies from the core-mantle boundary to the shallow mantle, and to space. Bolide impacts are mentioned for completeness, but will not be discussed further here.

The theory that relates melting anomalies to plate tectonics postulates that lithospheric extension permits volcanic material to rise passively from beneath. This theory is in keeping with the observation that approximately a third of all melting anomalies on typical lists (e.g., Figure 2) lie on or close to a spreading ridge. Others, such as Yellowstone, the Basin and Range province (western USA), and several postulated to lie in east Africa and in European and Asian rift valleys, lie in continental extensional zones. The plate hypothesis suggests that the volume of magma produced is dependent on the fusibility of the source. Where the source rocks have a relatively low solidus temperature, relatively large volumes of melt are produced. Where they are refractory, with a high-temperature solidus, the volumes erupted and intruded will be relatively small. The mantle may be relatively fusible where subducted crust and mantle lithosphere are recycled into the shallow mantle. Another source of fusible material is continental mantle lithosphere, which may delaminate where it becomes thickened and eclogitised e.g., in collision zones, and be recycled in the shallow mantle. Fluxing by water or carbon dioxide, which may have been introduced into the mantle by subducting slabs, also lowers the melting point of the mantle (Foulger 2007).

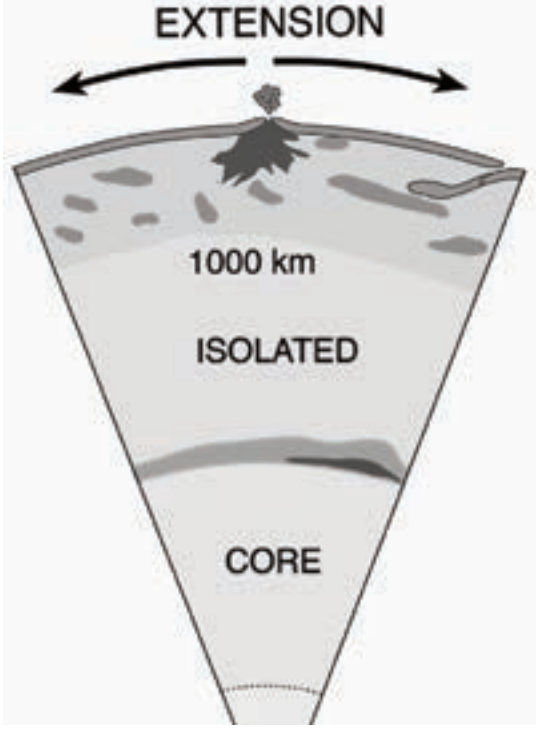

Figure 4. The plate hypothesis: Melting anomalies arise from permissive volcanism in extending regions (adapted from Anderson 2005).

Iceland

Efforts have been made to apply the plate theory to a number of melting anomalies (see www.mantleplumes.org), but there is only space herein to mention a couple. Iceland has been intensely studied because it can be. It comprises a large island, some 450 x 300km in extent, where ~ 20 spreading segments and even more active and extinct, deeply eroded volcanoes lie above sea level. Rock exposure is excellent over much of this windswept, vegetation-poor island, making mapping and sampling relatively easy. The island is broad enough that large-scale seismic experiments may be conducted – a vital detail since the depth to which seismic tomography images attain good resolution is approximately equal to the aperture of the seismometer network deployed. Thus, using networks deployed in Iceland, the structure of the mantle beneath may be probed in detail down to the top of the mantle transition zone at ~ 410km depth. Ideally one would wish to image deeper – through the ~ 660km-deep base of the transition zone and into the lower mantle, but this is not possible without deploying additional seismic stations at sea around Iceland. This would be a difficult and expensive enterprise, and it has not yet been undertaken. Nevertheless, Iceland is still one of the best localities in the world for seismic imaging of a proposed plume.

How do the plume and plate hypotheses match against one another in the case of the north Atlantic igneous province and Iceland? The

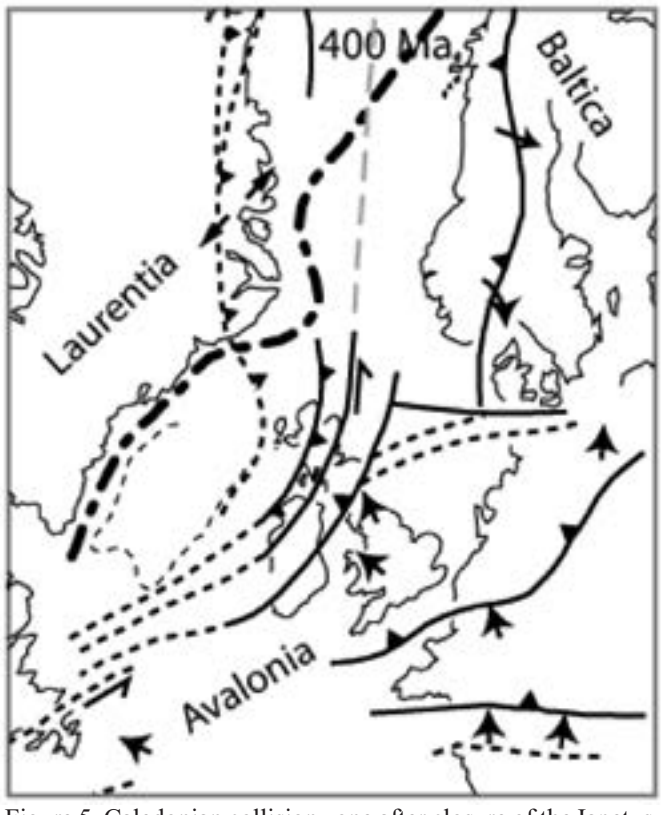

Figure 5. Caledonian collision zone after closure of the Iapetus ocean at 400Ma. Thick lines - faults and orogenic fronts, grey dashed line - inferred position of the Caledonian suture. Slabs were subducted beneath Greenland, Baltica, and Britain. Bold dashed line indicates position of future mid-Atlantic ridge that formed at ~54Ma. The Greenland-Iceland-Faeroes ridge, and Iceland itself, later formed at the locality where the mid-Atlantic ridge crossed the western frontal thrust of the suture.

widespread volcanism in the region that is popularly attributed to a plume started at ~ 62Ma. It formed a northwest-trending linear zone stretching from Britain through east and west Greenland. Some local uplifts occurred at this time, but not the widespread regional uplift that later raised the Britain area and much of the volcanic margins. That later uplift was synchronous with – it did not predate – the massive outpourings that built the northeasterly trending volcanic margins at ~ 54Ma. These margins accompanied breakup of the Laurasian supercontinent (Figure 5). The plume hypothesis views the volcanism as occurring independent of, or even causing, continental breakup.

Subsequent to breakup, and volcanic margin building, the magmatic rate subsided everywhere except at the latitude of Iceland. There, a mirror image pair of ridges of thickened crust developed on either side of the spreading ridge, as the ocean widened (Figure 6). Like Hawaii, the top part of this thickened crust started life subaerially, and gradually subsided and sank beneath sea level as it cooled. The locus of melt production in the region has always been centred on the mid-Atlantic ridge, and thus no classical time-progressive volcanic trail was built. The Greenland-Iceland and Iceland-Faeroes ridges differ from normal sea floor only in their crustal thickness, not in the chronology of volcanism on them.

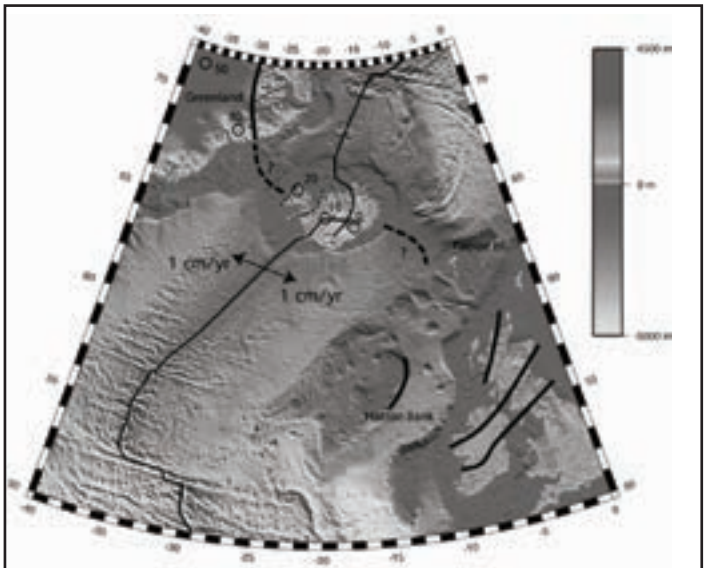

Figure 6. Bathymetry and altitude of the Iceland region. The Greenland-Iceland and Iceland-Faeroe ridges are underlain by unusually thick crust. Circles and numbers (Ma) indicate locations at various times of postulated plume. Thin line indicates present mid-Atlantic ridge, thick lines indicate Caledonian suture faults and dashed line indicates projection of western Caledonian frontal thrust between Greenland and Britain (from Foulger 2002).

A suite of seismic experiments have all revealed a strong low-wave-speed region beneath Iceland with a strength of ~ 2% in Vp and 5% in Vs (e.g., Figure 7; Foulger *et al.* 2000). However, they all agree that it is confined to the upper mantle and extends no deeper than ~ 600 km. The anomaly essentially represents a thickening of the seismic "low-velocity zone" that is widespread beneath mid-ocean ridges but typically extends no deeper than ~ 200km. The highest-resolution seismic studies find that its lower part is elongated north-south, mirroring the shape of the mid-Atlantic ridge above. What does this anomaly represent? It is commonly assumed that all mantle tomographic anomalies are due to temperature, but it is an incontrovertible fact that their interpretation is ambiguous. The phase of the mantle, composition and temperature may all cause low wave speeds with phase having the strongest effect and temperature the weakest. A very small trace of partial melt – much less than 1% – could account for the anomaly. It has been suggested that trace melting as a result of the presence of CO_2 could account for both the common low-velocity zone and the anomaly beneath Iceland. Such a model would be consistent with the results of other seismic experiments, petrology, heat flow and modelling vertical motions that suggest that there is no, or only a very modest temperature anomaly in the mantle beneath Iceland (Foulger *et al.* 2005).

What of the plate model? Obviously the requirement for extension is easily met at Iceland. It is erupting from a 500km-long portion of the mid-Atlantic ridge, including the insular shelf. The spreading rate is ~ 2cm/a. The other ingredient required by the model is fertility. The crust currently being built at Iceland is ~ 30km thick, which is approximately three times thicker than crust being built further south on the Reykjanes ridge. A mantle source rock is required that is fertile enough to produce this amount of melt at much the same temperature as "normal" mantle produces 7-10km.

The source of this fertility could be recycled slabs of oceanic crust and mantle lithosphere that were the last-subducted remnants of the floor of the Iapetus ocean that closed at ~ 400Ma to assemble the Laurasian supercontinent. The continents that collided when the Iapetus closed were 100-200km thick. This length of latest-subducting slab would have been trapped in the resulting Caledonian suture, which was reopened when the new Atlantic ocean formed. Petrology suggests that the source of Icelandic lavas contains recycled oceanic lithosphere (Fitton *et al.* 1997). Many Icelandic lavas are of the ocean-island-basalt type, i.e., characterised by relative enrichment in incompatible elements such as U and Th, and in light rare earth elements relative to heavy ones. These geochemical characteristics are widely accepted as resulting from recycled subducted slabs. Recent estimates of the percentage of recycled crust vary from 100% to 10% (Foulger *et al.* 2005; Sobolev *et al.* 2007). The question of how much is required to produce the large volume produced at Iceland remains to be quantitatively addressed, as does the question of exactly what these volumes actually are. Although the seismically determined crustal thickness at Iceland is ~ 30km, Iceland does not have a correspondingly high topographic elevation. This means that the lower "crust" must be much denser than "normal" gabbroic lower crust, and might well contain a component of mantle material. In that case, the amount of melt needing to be explained would be less than 30km.

The new mid-Atlantic ridge that opened at ~ 54Ma ran largely along the old Caledonian suture, but at the future latitude of Iceland

Figure 7. Whole-mantle tomography image through Iceland (from Ritsema *et al.* 1999).

it departed from this. Instead, it formed a pristine fracture that ran through cratonic south Greenland and carved off the Rockall block. As a result, the thick zone of crust that formed the Greenland-Iceland-Faeroes ridge, and Iceland itself, has formed at the position where the Caledonian suture runs offshore, to continue on land again in Britain. This strange correlation is a coincidence in the plume hypothesis. In the plate hypothesis it is not clear why it should coincide with a zone of exceptional fertility, but future work may cast light on this intriguing observation.

Yellowstone

Yellowstone is often considered to be the type example of a continental mantle plume and is thus a location of interest for comparing the two hypotheses. The plume hypothesis views the nearby Columbia River Basalt flood basalts as the initial "plume head" (Figure 8). The eastern Snake River Plain comprises a 450km-long volcanic zone that contains both large basaltic lava flows and a time-progressive chain of silicic calderas, of which the presently active Yellowstone is the youngest.

The question of whether formation of the Columbia River Basalts was preceded by uplift is currently a contentious issue, with arguments presented for both uplift and subsidence (Hales *et al.* 2005; Hooper *et al.* 2007). The centre of eruption of these basalts also lies ~350km north of the oldest end of the eastern Snake River Plain volcanic track, and no migrating volcanism connects the two (Figure 8) . There is no evidence for unusually high mantle temperatures. The time-progressive volcanism is silicic in nature and thus evolved and of crustal provenance. The basaltic volcanism in the eastern Snake River Plain is not time progressive, but has occurred all along the zone recently.

Seismic tomography experiments image a low-wave-speed zone beneath Yellowstone. In some experiments this anomaly is imaged to dip to the northwest and to extend weakly to ~400km depth. Other experiments suggest that the weak, deep extension is an artifact due to smearing along the seismic ray paths and that the anomaly instead bottoms at ~150 km. This would imply that the anomaly is purely lithospheric. All experiments agree, however, that the anomaly does not extend through the mantle transition zone and into the lower mantle (Christiansen *et al.* 2002).

How does the plate hypothesis fare at Yellowstone? Volcanism started up over the entire region at ~17Ma, when the whole region that is now the ~1,000km wide Basin & Range intraplate extensional province began to stretch. The newly forming Yellowstone system was mirrored by a similar and coeval zone of northwestward migrating volcanism, the "Newberry trend", which is also called the "High Lava Plains". As the two zones formed, the Basin & Range province to the south widened by ~ 250km. In contrast, the region to the north widened by only a few tens of kilometres, reducing to zero a short distance further north. The eastern Snake River Plain marks a major change both in extensional behaviour and lithospheric structure. The thin, hot, extending lithosphere of the Basin & Range province to the south meets the much thicker, cold lithosphere of the North American craton to the north. Migration of the silicic volcanism that is presently represented by the active Yellowstone volcano thus likely has its origins in the abrupt change in lithosphere structure that imposed a northern limit on the region that underwent the remarkable Basin & Range style of continental extension.

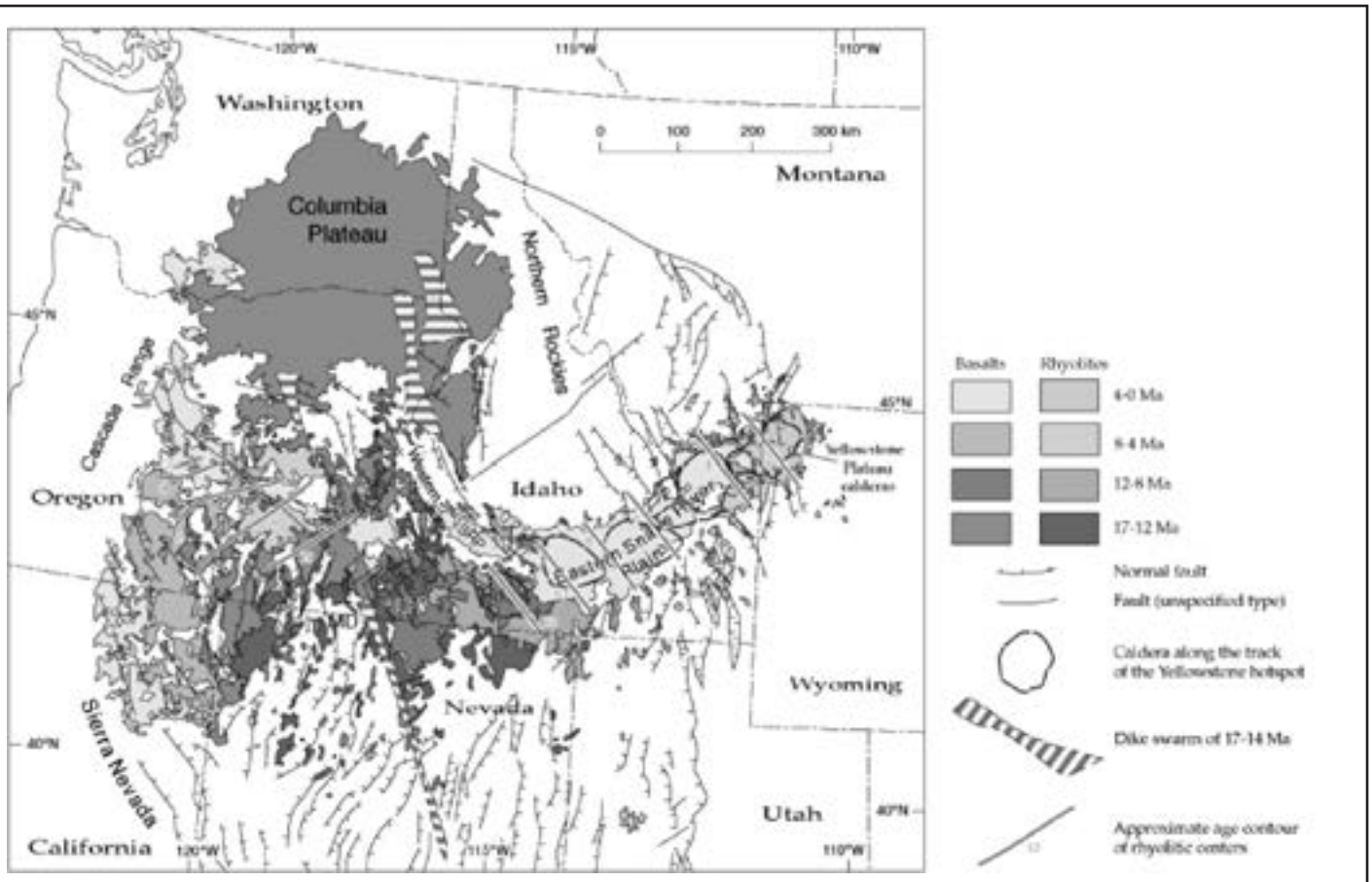

Figure 8. Regional context of the Yellowstone melting anomaly (from Christiansen *et al.* 2002).

Looking backward and forward

A huge amount of work has been done to study melting anomalies during recent decades, including many highly ambitious experiments using equipment of ever-increasing technological sophistication. Vast bodies of information have been assembled through painstaking efforts that have occupied whole careers. Some of these careers have been devoted almost entirely to gathering observational evidence, and others have been dedicated to theoretical modelling, particularly of plumes.

Serious and fundamental discrepancies between observation and the predictions of the plume hypothesis have been brought into a focus so sharp that no reasonable scientist can dismiss the problems out of hand. Why, then, is there still great resistance to questioning a theory that many have come to suspect has become a sacred cow? Why is it so difficult to test, and how is it that our grand technology can put men on the moon but not solve the problem of whether plumes exist or not? Most importantly, what is the way forward?

Some of the answers may lie not in science but in the way that we do science. Scientific theories should make predictions which are capable of being tested and which, if they come up negative, should result in rejection of the theory. Unfortunately, this is not the way things work in the case of plumes. The contemporary form of the plume hypothesis has become so flexible that none of its basic predictions are thought necessary to fulfill. Plumes have even been proposed to explain volcanism at places where not one of the five predictions listed above are successful, e.g., the Eifel volcanic field, Germany. In the contemporary plume hypothesis, plumes may be headless, the requirement for precursory uplift may be waived, and the lack of time progression can be explained away by invoking lateral flow that disrupts the expected pattern. The lack of petrological evidence for high temperature may be explained away as the expected petrologies being hidden from sight by thick overlying lava flows and the lack of a seismically imaged "plume tail" may be dismissed by the argument that the expected tail is narrower than the resolution of the seismic experiment that was conducted. Seemingly endless searches for data supporting the plume hypothesis persistently turn up negative far more frequently than would be seemingly expected by chance.

Weighing in alongside this, in the minds of Earth scientists of a critical inclination, are the many apparent coincidences – the many melting anomalies that form on spreading ridges or in rift valleys and the almost ubiquitous geochemical signature of fertile, recycled slabs in the erupted lavas. The majority of melting anomalies are clearly intimately related to surface tectonic events or structures or both. Is this a result of pre-existing lithospheric conditions influencing the eruption of plume magmas, or do the lithospheric conditions themselves cause the magmatism? The question may ultimately reduce to whether we are satisfied with a theory that has been adapted to fit the observations, or whether we need one that can successfully predict what we find at new localities.

References

Anderson, D. L. (2005), Scoring hotspots: The plume and plate paradigms. *In:* G. R. Foulger, J.H. Natland, D.C. Presnall and D.L. Anderson (ed.) *Plates, Plumes, and Paradigms*. Geological Society of America, 31-54.

Christiansen, R. L., G. R. Foulger & J. R. Evans (2002) Upper mantle origin of the Yellowstone hotspot. *Bull. Geol. Soc. Am.* **114**, 1245-1256.

Clague, D. A., W. S. Weber & J. E. Dixon (1991) Picritic glasses from Hawaii. *Nature* **353**, 553-556.

Courtillot, V., A. Davaillie, J. Besse *et al.* (2003) Three distinct types of hotspots in the Earth's mantle. *Earth planet. Sci. Lett*. **205**, 295-308.

Eldholm, O. & K. Grue (1994) North Atlantic volcanic margins: Dimensions and production rates. *J. geophys. Res.* **99**, 2955–2968.

Fitton, J. G., A. D. Saunders, M. J. Norry et al. (1997) Thermal and chemical structure of the Iceland plume. *Earth planet. Sci. Lett*. **153,** 197-208.

Foulger, G. R., M. J. Pritchard, B. R. Julian *et al.* (2000) The seismic anomaly beneath Iceland extends down to the mantle transition zone and no deeper. *Geophys. J. Int.* **142,** F1-F5.

Foulger, G. R. (2002) Plumes, or plate tectonic processes? *Astron. Geophys.* **43,** 6.19-16.23.

Foulger, G. R., J. H. Natland & D. L. Anderson (2005) A source for Icelandic magmas in remelted Iapetus crust. *J. Volc. Geotherm. Res.* **141,** 23-44.

Foulger, G. R. (2007), The "Plate" model for the genesis of melting anomalies. *In:* G. R. Foulger and D. M. Jurdy (eds.) *Plates, Plumes, and Planetary Processes.* Geological Society of America, Boulder, Colorado, 1-28.

Hales, T. C., D. L. Abt, E. D. Humphreys et al. (2005) Lithospheric instability origin for Columbia River flood basalts and Wallowa Mountains uplift in northeast Oregon. *Nature* **438**, 842-845.

Herzberg, C., P. D. Asimow, N. T. Arndt *et al*. (2007) Temperatures in ambient mantle and plumes: Constraints from basalts, picrites, and komatiites. *Geochem. Geophys. Geosys.* **8**.

Hooper, P. R., V. E. Camp, S. P. Reidel *et al.* (2007), The Columbia River Basalts and their relationship to the Yellowstone hotspot and Basin and Range extension. *In:* G. R. Foulger and J. M. Jurdy (eds.) *Plumes, Plates, and Planetary Processes.* Geological Society of America, Boulder, Colorado, 635-668.

Morgan, W. J. (1971) Convection plumes in the lower mantle. *Nature* **230,** 42-43.

Ritsema, J., H. J. van Heijst & J. H. Woodhouse (1999) Complex shear wave velocity structure imaged beneath Africa and Iceland. *Science* **286**, 1925-1928.

Smith, W. H. F. & D. T. Sandwell (1997) Global sea floor topography from satellite altimetry and ship depth soundings. *Science* **277,** 1957–1962.

Sobolev, A. V., A. W. Hofmann, D. V. Kuzmin et al. (2007) The amount of recycled crust in sources of mantle-derived melts. *Science* **316**, 412-417.

Wilson, J. T. (1963) A possible origin of the Hawaiian Islands. *Can. J. Phys*. **41,** 863-870

Does Acid Rain Reduce Methane Emission?

Nancy Dise[1] and Vincent Gauci[2]

[1] Department of Environmental and Geographical Sciences, Manchester Metropolitan University, Manchester M1 5GD

[2] Department of Earth and Environmental Sciences, The Open University, Walton Hall, Milton Keynes, MK76AA

Abstract

Microbial populations in wetlands can be strongly influenced by their chemical environment, which is partly determined by the composition of atmospheric deposition. Human activity originating hundreds or thousands of kilometres away can modify this atmospheric deposition. For example, sulphur emitted to the atmosphere from burning fossil fuels eventually falls back to Earth as acid rain. This reactive sulphur can confer competitive advantages to particular groups of microbes, shifting the composition of whole microbial communities. This in turn can lead to ecosystem-scale and sometimes biosphere-scale changes in the emission of greenhouse gases.

Depending on their activity as toxins, nutrients or energy sources, compounds in deposition can have different and sometimes contradictory effects on biota, making the net response difficult to predict. Untangling the web of biotic interactions and feedbacks that emerge as humans have profoundly changed the composition of global atmospheric deposition is similar in complexity to unravelling the influence of increasing atmospheric CO_2, and requires a similar cross-disciplinary approach.

Microbes, Humans, and The Earth System

In the exceptionally brief time industrial humans have been on the Earth, we have become a global force. That life can have a profound influence on the planet is, however, nothing new. Our current oxygen-rich atmosphere, for instance, is the product of billions of years of oxygenic photosynthesis. This did not come about so that you or I could exist – rather, it emerged through the cumulative effect of immense numbers of microbes going about their business of gaining energy, metabolising, growing, producing waste, interacting and competing. The impact of humans on the Earth is similarly a by-product of the exploitation of energy and resources by a large (albeit not *as* large) number of highly successful organisms.

A clear way in which human activity has global repercussions is in the burning and release to the atmosphere of fossil fuels. The sulphur and nitrogen oxides produced become chemically transformed in the atmosphere to produce sulphuric acid and nitric acid, and are ultimately deposited as rain or snow onto ecosystems like forests, soils, streams or wetlands. There, these compounds can acidify soils and surface waters, release toxic metals such as aluminium, kill or disrupt sensitive species, and cause forest and vegetation decline. Although acid deposition has declined in North America and most of Europe, it is increasing in other parts of the world, particularly Asia, so that overall, the emission and deposition of acids due to human activity will continue to be high into the foreseeable future.

The deleterious effects of acid deposition on sensitive surface waters, forests and other natural communities have been well documented for several decades. But we are interested in another, more subtle aspect. Can the enrichment of rain and snow with sulphate from the industrial activity of humans change the composition of microbial communities?

Microbe Wars

For most of the Earth's existence the atmosphere contained very little oxygen – and the Earth supported abundant life. Thus, oxygen is far from the only compound that can be used for respiration: nitrate, carbohydrates, iron, sulphate and even carbon dioxide can all be used by different groups of organisms (Table 1). But there is a catch: as one goes down the hierarchy of reactions shown in Table 1, the energy yield becomes less and less. Added to that, some of the products of these respiration reactions (right-hand side of arrows in Table 1) are powerful greenhouse gases (shown in Table 1 in italics). Since oxygen diffuses about 10 000 times slower in water than in air, productive wetlands such as peat bogs, swamps, and marshes are good places to find thriving communities of anaerobic organisms today.

Table 1. Energy hierarchy of major respiration reactions, and main groups of organisms using the reactions. Respiration products in italics are greenhouse gases.

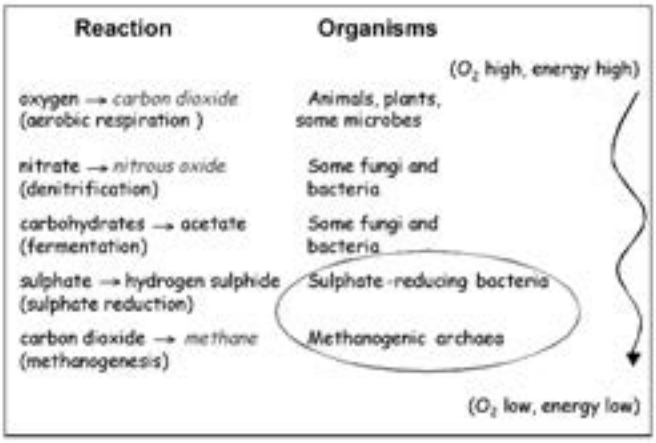

Way down the competitive hierarchy are the sulphate-reducing bacteria and the methanogenic archaea (circled in Table 1). Sulphate-reducing bacteria use energy from the reduction of sulphate to hydrogen sulphide, and methanogenic archaea (which used to be considered bacteria but have since been assigned to their own kingdom based on their significant differences with other life forms) reduce carbon dioxide to methane or ferment simple carbohydrates such as acetate to carbon dioxide and methane. Although neither process is very efficient in relation to, say, aerobic respiration, sulphate reduction has a slight upper hand. So when there is enough sulphate around, sulphate reducers can out-compete methanogens for resources. Thus salt marshes and mangrove swamps, where there are high levels of sulphate from the sea, have sulphate reduction predominating over methanogenesis.

But, although the energy difference between the two reactions is not great, there is a big difference in the global effects of their products. Methane is the second-most important human-influenced greenhouse gas, after carbon dioxide. Reduced sulphur gases may be a little smelly, but they are not greenhouse gases, and in fact contribute toward global cooling through cloud formation. So by

suppressing methane emission, sulphate reduction can reduce the net emission of a powerful greenhouse gas.

Enter Humans

The interplay between these microbial communities leads to a possibility: can sulphate from acid rain change the balance of competition between sulphate-reducing bacteria and methanogenic archaea? Or, outlined as a hypothesis:

- Acid rain contains sulphate
- Sulphate energises sulphate-reducing bacteria
- Sulphate-reducing bacteria out-compete methane-producing archaea; therefore
- Sulphate from acid rain should reduce methane emission in wetlands

Does it?

The Experiments

To test this hypothesis we designed a field experiment in a peatland called Moidach More, in Scotland east of Inverness. This part of the UK receives very low levels of sulphate in deposition, and methanogenesis predominates over sulphate reduction. We added sulphate to experimental plots in three levels: 25, 50 and 100 kilograms of sulphur per hectare and year (kg S ha^{-1} y^{-1}), equivalent to (a) 2.5, (b) 5 and (c) 10 grams of S added per square meter per year. These levels are about the same, respectively, as (a) the highest level of acid rain currently found in the UK and North America, (b) levels in the 1970s in Europe and North America, and currently in some areas in Asia, and (c) levels in the 1970s in parts of eastern Europe and other very polluted regions, or close to point sources such as power plants. Sulphate was dissolved in water and applied by spray can on the plots every week or two to mimic actual rainfall patterns.

The sulphate treatments caused a significant suppression of methane emission by about 30% in all plots (Gauci *et al*. 2002). The amount of sulphur added did not make a difference – there was no evidence of increased suppression with increased treatment. Subsequently, the effect was tested in different ways – in peat cores in the laboratory (Figure 1), in greenhouses, and, crucially, in tests run by colleagues in other countries – and results were broadly similar. When we compiled these results we found that there was a broad relationship unfolding. We were able to represent this relationship in a simple mathematical model that links the amount of methane suppression with the amount of sulphate deposition. The consensus is that, under conditions that favour both sulphate reduction and methanogenesis, the addition of sulphate of more than 15 kg S ha^{-1} y^{-1} leads to a fairly consistent suppression of methanogenesis by 30-40%, and below that level there is diminishing suppression.

Scaling Up

Armed with clear evidence of a consistent effect of sulphate deposition on methane emission, we decided to 'scale up' the results – that is, to see if this effect could potentially be important as a mechanism for reducing global methane emission from wetlands.

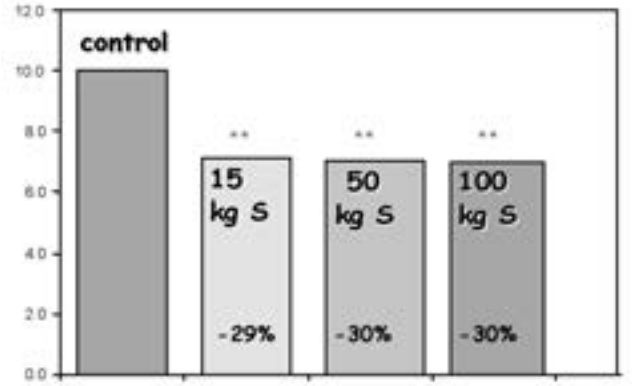

Figure 1. Suppression of methane emission by sulphate added to intact peat cores, adapted from Gauci et al. 2004a. Asterisks show level of probability that treatment differs from control; ** = p< 0.01.

First, we took a model of global sulphate deposition estimated for the past, present and into the future, using estimates of industrial growth and pollution abatement, developed by colleagues from the NASA Goddard Institute. We used a similar-scale model of global methane emission. We then used our simple evidence-based model of suppression of CH_4 emission with sulphate deposition to link these two global models, so that the effect of acid rain on wetland methane emission could be quantified on a planetary scale.

The results were remarkable. The calculations suggested that, despite global warming (which should increase methane emission) current levels of methane emission from natural wetlands are today lower than they were in pre-industrial times, due to suppression from acid rain (Gauci *et al.* 2004b). They also indicated that this suppression to pre-industrial levels will not 'wear off' until the mid-21st century, when levels of pollution are expected to decline and wetland methane emission continues to increase due to the warming of the planet. Of course, there are many assumptions and simplifications put into the model - it should be viewed only as a rough guide. Also, because there are many other contributors to the greenhouse effect, it is unlikely that the suppression of methane emission by acid rain translates into a major reduction of global warming. What it does say, however, is that our activities can impact the atmosphere, then reverberate through the biosphere and back into the atmosphere, in very complicated, sometimes unexpected ways. Our existence may well be a by-product of life at the microbial level, but it looks like we may be getting our own back on the microbes.

References

Gauci, V., Dise, N.B. and Fowler, D., 2002. Controls on suppression of methane flux from a peat bog subjected to simulated acid rain sulfate deposition. *Global Biogeochemical Cycles,* **16 (1)**: Art. No. 1004.

Gauci, V., Fowler, D., Chapman, S. and Dise, N.B., 2004a. Sulfate deposition and temperature controls on methane emission and sulfur forms in peat. *Biogeochemistry*, **71(2)**, 141-162.

Gauci, V., Matthews, E., Dise, N., Walter, B., Koch, D., Granberg, G., Vile, M., 2004b. Sulfate suppression of the wetland methane source in the 20th and 21st centuries. *Proceedings of the National Academy of Sciences USA*, **101,** 12583-12587.

Volcanoes in the Laboratory

Stephen J. Lane and Steven B. Corder,
Lancaster Environment Centre, Lancaster University, Lancaster, LA1 4YQ, UK.

Abstract
The laboratory modelling of flows that have similar characteristics to those occurring in volcanic conduits can give insight into essentially unobservable processes. The linking of experimental results with numerical models and field observation increases confidence that the insights are well founded.

Introduction
The magnitude of volcanic eruptions may be classified using the Volcanic Explosivity Index (VEI) (Newhall & Self 1982; Pyle 2000). The lowest VEI of zero covers non-explosive activity (such as the production of lava flows) and is generally associated with low magma effusion rates or low viscosity magmas, like carbonate-based carbonatites (Woolley & Church 2005). For silicate-based magmas, which are generally more viscous than carbonatites, the boundary between effusive and explosive volcanism is commonly marked by Hawaiian fire-fountaining activity (Parfitt 2004). Magmas with a high silica content, or a lower temperature (and thus higher viscosity) can erupt either explosively, or non-explosively as lava flows or dome-building eruptions (Yokoyama 2005). Some eruptions switch between effusive and explosive behaviour dependent on prevailing physicochemical conditions (e.g., Jaupart & Allegre 1991, Ida 2007), with magmas tending to become more explosive at higher effusion rates. High VEI eruptions are, therefore, associated with high flow rates, large erupted volumes and substantial eruption plumes.

Such explosive activity comprises a wide range of phenomena, which result from complex non-linear interactions and feedback mechanisms. Processes that initiate in the subsurface plumbing or conduit system determine the nature of following events and control eruption styles. On emerging from the vent, volcanic material enters the atmosphere and the ensuing interactions are key in determining the consequent transport of volcanic debris that defines the impact on the environment and on human lives and infrastructure. On Earth, our capability to mitigate such volcanic hazard relies in large part on forecasting explosive events, a process which requires a high degree of understanding about the physicochemical factors operating during explosive volcanism.

In common with many science disciplines, the approaches taken to gain an understanding of explosive volcanism have relied on a combination of: field observations of events, their products and consequences, mathematical and numerical models of processes, and laboratory experimental modelling of materials and mechanisms. Field observations form the 'ground truth' for numerical and experimental modelling (and provide vital historical data), but are often very difficult to unambiguously interpret due to their scarcity in both space and time. Numerical modelling complements field observations by providing much greater information density and, hence, the potential to examine processes in great detail. However, the accuracy of the results depends on correctly including all relevant materials properties and system processes in the model and the results can be difficult to verify against often-unobservable field phenomena. Laboratory investigation of the properties of volcanic materials, their modes of interaction and the behaviours of analogous systems provides the third complementary approach and is the area we focus on in this contribution.

In the context of explosive volcanic activity, laboratory experiments cover a wide range of investigations. Here, we concern ourselves with analogue experimentation, i.e., using non-volcanic fluids at small scale to 'mimic' into volcanic behaviour. This involves the concept of scaling (Barenblatt 2003, Burgisser *et al*. 2005), which links the applicability of experimental results using small samples of analogue material to large volumes at natural scales that are often several orders of magnitude larger. For experiments that replace natural volcanic products with analogue materials (for example, in order to relax the experimental pressure and temperature requirements), scaling arguments are crucial. A scaling approach permits adjustment of experimental durations and sizes, whilst maintaining similitude with much larger and longer events. Consequently, analogue experimentation has allowed investigation of explosive phenomena in the broader context of fluid-dynamic behaviour, and is a powerful means of giving 'insight' into volcanic processes.

Explosive volcanism is also a difficult phenomenon to observe in action, and there are three reasons for this. Firstly, explosions do not happen very often, and the larger the explosion the more infrequent it is, with, for example, repeat timescales of order 10^3 years for VEI 6 events like the Krakatau, 1883 eruption. This makes detailed syn-event measurements of large explosive episodes infrequent on the timescale of contemporary volcanology. Secondly, high VEI events tend to destroy near-field observation equipment, making measurements very difficult to obtain even when an event does occur. Thirdly, processes that comprise an explosive event can be difficult to access directly; perhaps a prime example of this is how to obtain data about the nature of flow in the volcanic conduit system during explosive activity. Direct measurements are not possible and our main source of information is the deformation of the conduit wall created by unsteady flow, which is calculated from the interpretation of ground motion signals detected by seismometers (Chouet *et al.* 2003).

These considerations mean that there are many field observations, numerical and experimental models that await comparison with their companion approaches, however, the detailed study of volcanoes with low VEIs is one area where combined tactics are possible. We review the contribution that experimental modelling has made to the understanding of fluid flow in the conduit feeding VEI 1-2 explosions at Stromboli Volcano, Italy. Here it has been possible to measure signals from many 1000s of events, over the period of a few years, with a network of seismometers and other instruments, as well as detailed sampling of eruption products. This field data is key to testing both numerical and experimental models of explosive volcanic activity wherever it occurs.

Strombolian Eruptions
Low VEI eruptions commonly occur at volcanoes where magma viscosity is low and degassing water is able to separate from the magma; indeed, this separation is required for low VEI events. Analogue experiments of separating flows may, therefore, be compared

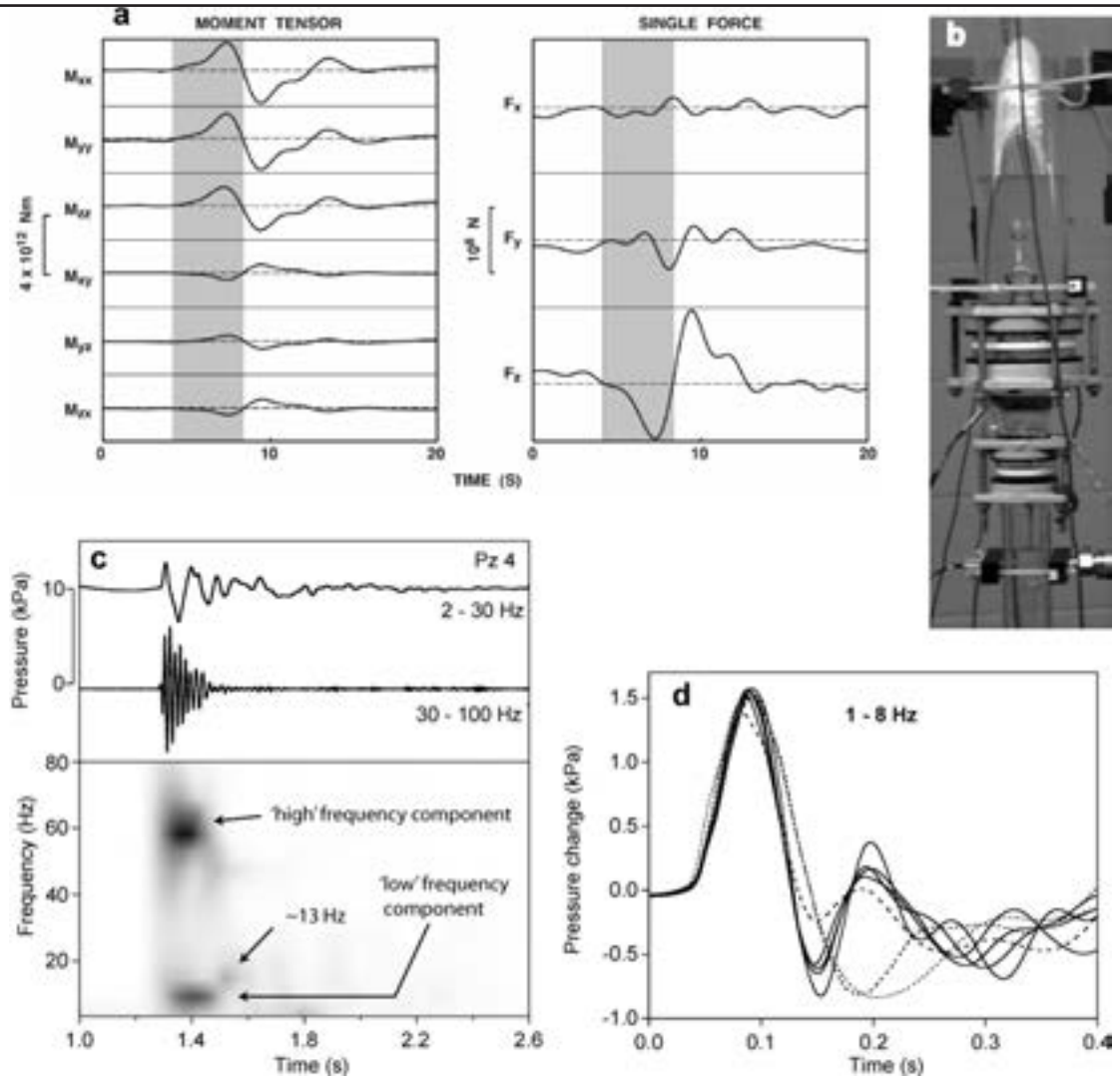

Figure 1 The geometry of experimental tubes has been observed to change flow behaviour in a number of instances. James *et al*. (2006) investigated the dynamics of a gas slug ascending through a tube widening. Inversion of seismic data measured at Stromboli volcano (a, Chouet *et al*. 2003) indicated an initial downward force of about 10^8 N, accompanied by pressure increase expanding the conduit. This was followed by upward force and conduit contraction with a period of about 10 s. The experimental ascent of a gas slug through a tube widening (b) caused breakup of the slug and production of a transient gas jet. Spectral analysis of pressure (c) showed three resonant components. The low frequency component (d, about 6 Hz) showed one to two cycles of pressure increase followed by decrease, qualitatively consistent with pressure change in the conduit at Stromboli during explosive eruption. Measurement of apparatus displacement indicated a peak downward force of 30 N, which when naïvely scaled by 100^3 for physical dimension and 2.5 for density difference gives a force of 7.5×10^7 N, encouragingly close to that estimated from seismic inversion.

with relatively well-studied natural processes in ways that high-VEI events cannot. Experimental conditions are also simplified in relation to those applied to high-VEI processes, with the assumptions that liquid rheology and temperature remain constant being easier to justify. Low-VEI processes may also be studied without shock tube or high-pressure apparatus, making observation and measurement more straightforward.

Strombolian eruptions are characterised by short-lived explosive events that have a mass fraction of water significantly higher than that dissolved in magma (Chouet *et al.* 1974; Blackburn *et al*. 1976) separated by longer periods of relative quiescence. Such behaviour suggests the presence of slug flow in the conduit, where gas-rich regions rise up the conduit separated by regions of relatively gas-poor magma. However, evidence from extensive research on water-gas systems indicates that for such a flow pattern to be stable in the conduit the overall gas volume fraction would probably need to exceed about 0.25 (Clift *et al.* 1978), and the time intervals between explosions would be similar to, or less than explosion duration. It is also very questionable that slug flow would form from numerous small bubbles in a relatively high-viscosity liquid like basalt magma. This suggests that other mechanisms operate to promote formation of gas slugs.

Experimental Approach

Jaupart & Vergniolle (1988; 1989) recognised that volcanic conduits are not straight vertical tubes, but exhibit significant geometrical heterogeneity that may play a major role in eruptive behaviour. Experiments were carried out to examine the effect of a flat roof in trapping the numerous small bubbles rising through

basaltic magma. Small air bubbles were injected at variable rate into the base of a tank of water-based liquid of variable viscosity. The bubbles rise to the roof of the tank, which has a vertical small diameter outlet tube. Three modes of system behaviour were observed. At lower liquid viscosity, a raft of bubbles forms at the roof. At some critical thickness the bubble raft collapses on the scale of the tank roof and flows up the outlet tube as a large gas bubble. This behaviour was considered analogous to Hawaiian eruptions. At higher liquid viscosities, the bubble raft collapses on a scale smaller than the tank roof and a series of bubbles that are much larger than those injected, but smaller than the low-viscosity case, emerge up the outlet pipe. This gives insight into strombolian eruptive activity. The final mode of behaviour was the development of a relatively stable bubble raft and the escape of small bubbles up the outlet pipe to give bubbly flow at the surface.

The ascent of large gas bubbles, or slugs, up a tube can be controlled by surface tension, liquid viscosity or liquid inertia. In basaltic systems surface tension has no control, and inertia dominates with some component of viscous influence (Seyfried & Freundt 2000). Conveniently, this allows the use of water and air at laboratory scale to give inertia-controlled slug flow. Seyfried & Freundt (2000) carried out experiments applying the flow patterns that develop with increasing air flux through a column of water to basaltic volcanism. Single gas slug ascent was found to only occur through sudden incidents of limited volume gas release, with one mechanism being that of foam collapse from a trap (Jaupart & Vergniolle 1988; 1989). It was observed that slug burst in the tube was a gentle process, but that if the liquid level was in the reservoir atop the tube (akin to a lava lake) then burst was more vigorous, nee strombolian; another example of the impact of conduit geometry on flow. Experiments with gas traps in the water column found that the coalescence of trapped gas pockets resulted in significant pressure oscillations that were a potential source mechanism for volcanic tremor; linking volcano-seismic signals to fluid flow could be a powerful method of experimental scaling inaccessible in high VEI events.

Fluid Flow and Seismicity

Seismic signals may result from the collapse of a foam layer trapped at a roof. Measurements made within apparatus similar to that of Jaupart & Vergniolle (1988; 1989) reveal pressure fluctuations both within the fluid and in the air above the fluid surface in the outlet tube (Ripepe *et al*. 2001). These could be linked to seismic and acoustic signals measured at Stromboli volcano and give insight into the role of fluid-flow on the generation of seismo-acoustic waves during explosive volcanism. During the build up of the foam layer, no pressure changes were detected. Collapse of the foam layer and motion of the gas slug up the outlet pipe produced pressure changes in the liquid tank of a few-hundred Pa, and of a few-tenths Pa in the air above the liquid level. Collapse of the foam layer produces downward motion of the dense liquid phase in the outlet pipe, reducing pressure. Oscillation of liquid on the gas spring of the slug produces pressure oscillations within and above the liquid. Slug burst results in a sudden increase in oscillation frequency above the liquid, and a small pressure pulse in the liquid due to decay of liquid flow around the slug nose (James *et al*. 2004). Ripepe *et al*. (2001) postulate that seismic signals measured

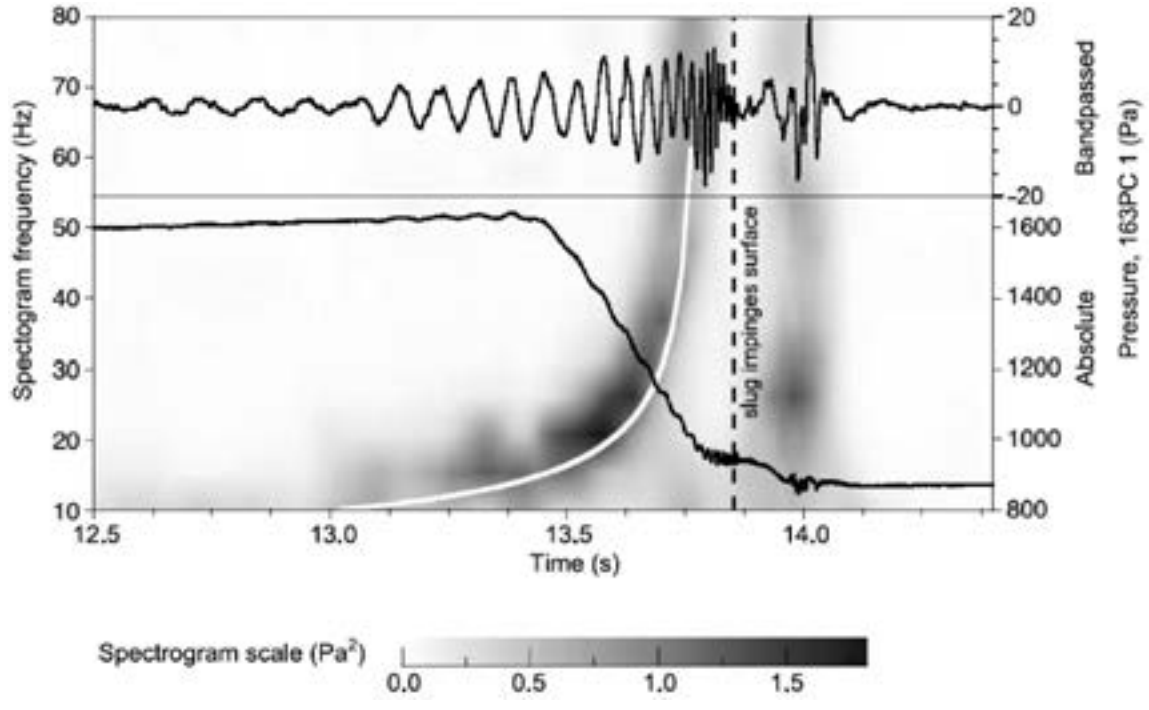

Figure 2 Strombolian eruptions are short-lived, periodic and have high volatile content. For these reasons they are associated with the formation, ascent and bursting of large bubbles of water vapour (often known as slugs), rather than the expansion of a vesicular magma. The ascent of air slugs in water during small-scale experiments caused pressure oscillations (James *et al*. 2004, reprinted with permission from Elsevier.). A spectrogram (grey shading) of band-passed (upper trace) pressure data (lower trace) was found to match well with calculations of the oscillation frequency (white trace) of the water above the gas slug bouncing resonantly on the gas slug. This oscillatory mechanism did not account for the seismic signals used to image the conduit at Stromboli (Chouet *et al*. 2003).

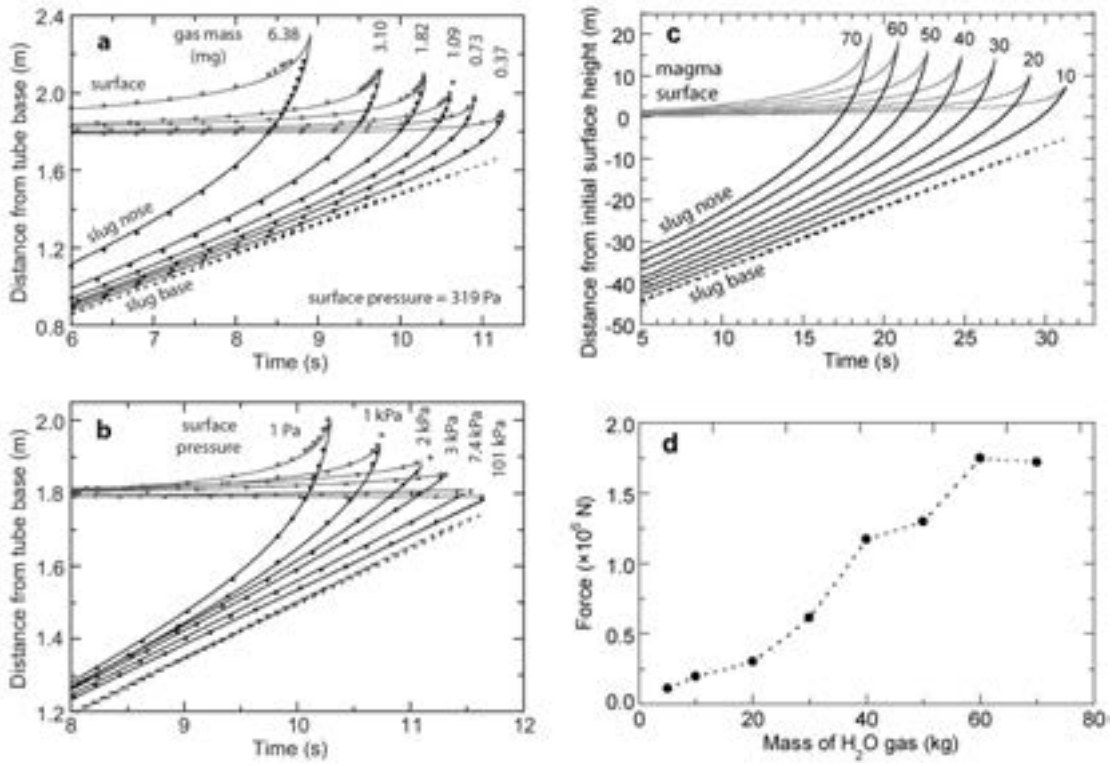

Figure 3 Experiments on slug flow are numerous in the engineering literature, but volcanic flows operate under conditions not investigated for anthropogenic purposes. One of these conditions is the large pressure change a gas bubble will experience in rising from some depth. James *et al*. (2008) investigated the dynamics of rapid gas slug expansion as a result of this decompression using an air bubble and vacuum pump oil as analogue fluids. Using surface pressures below atmospheric allows the air bubble to undergo considerable decompression under laboratory conditions. The degree of slug expansion, and hence explosivity on burst, was found to depend on (a) the mass of gas in the slug as well as (b) the applied surface pressure. Computational fluid dynamic modelling was used to apply the experimental findings at volcanic scale (c). The process of slug expansion generated significant pressure change and vertical force (d), but these did not account for the seismic signals used to image the conduit at Stromboli (Chouet *et al*. 2003; 2006; 2008).

at Stromboli are generated during rapid gas expansion during foam collapse, and estimate that the slug be about 4.5m long and induce a pressure drop of 0.1 MPa in the magma.

Inversion of highly repeatable seismic waveforms measured at Stromboli Volcano, Italy (Chouet *et al*. 2003; 2006; 2008) have enabled imaging of the conduit as well as revealing the forces and pressures being created by magma flow during strombolian eruptions. In summary, Stromboli's plumbing system appears to comprise a dyke dipping about 72° that runs from the vent system to an intersection with a dyke dipping about 45° and 900m below the vent system. Stable and repeatable seismic sources are inferred at a depth of about 220m below the vent system, and have the characteristics of a dyke segment intersecting the main conduit. Another, weaker, seismic source is located at the intersection of the two main dykes about 900m below the vents. The dominant seismic source at 220m below vent generates a downward vertical force of about 10^8N followed by an upward force of similar magnitude (Figure 1). The source volume increases during the downward force and decreases with the upward force. These measurements provided a means of testing laboratory models of strombolian eruptions.

James *et al*. (2004) studied pressure oscillations resulting from the ascent of single gas slugs in a vertical tube. The oscillations observed at the top of the liquid column (Figure 2) showed an increasing amplitude and decreasing period as the slug ascended, with oscillations ceasing as the slug reached the surface. Burst of the meniscus produced further pressure fluctuation. Modelling of the oscillations revealed the source mechanism as bouncing of the liquid mass above the slug on the spring of gas within the slug. The observed pressure oscillations were not similar to the change in volume of the seismic source at Stromboli, nor were oscillation amplitudes sufficient to account for forces of 10^8N at volcanic scale. Bubble bursting was also quiescent rather than explosive.

Experiments on strombolian processes have not been scaled for expansion of the gas slug as it rises from depth, which gas chemistry suggests could be between 900m and 2700m (Burton *et al*. 2007). A slug ascending from 1000m in magma will expand about 200 times to reach atmospheric pressure. Experimentally, expansions were in the region of 1.2. James *et al*. (2008) used low vapour-pressure vacuum pump oil as an analogue liquid and varied the ambient pressure above the liquid surface between 10^5 and 10Pa. The reduction in ambient pressure provided a proxy for slug ascent from depth and allowed potential gas expansions of factors up to 10^4. The positions of the slug base, slug nose and liquid surface for various slug masses and ambient pressures are shown in Figure 3. Regardless of ambient pressure and slug mass, the ascent velocity of the slug base remained nearly constant. However, the slug nose accelerated rapidly on approach to the surface when ambient pressure was low, and burst with a pressure higher than ambient. Gas slugs that underwent little expansion burst at ambient pressure.

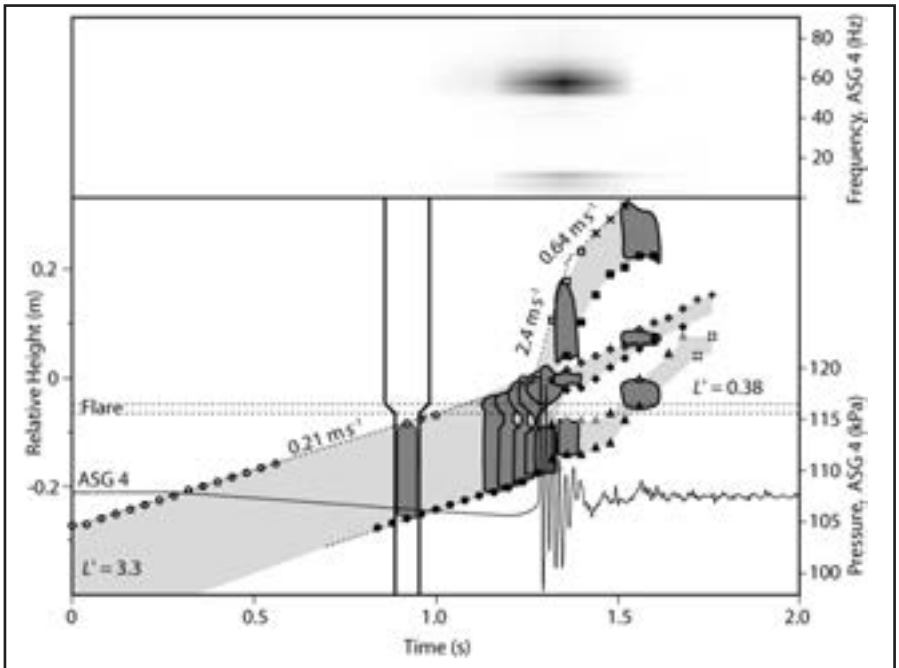

Figure 4 The source mechanism suggested by laboratory experiment (Figure 1) for seismic signals measured by Chouet *et al*. (2003) at Stromboli Volcano, Italy is the rapid deceleration of a downward-moving liquid piston formed as a gas slug breaks up in a conduit widening (James *et al*. 2006). The liquid piston 'bounces' on the lower portion of the slug for a cycle or two before being consumed by the ascending remains of the original slug. The cartoon above correlates the position of gas bubbles with pressure measurement and spectral analysis of pressure fluctuations. The dramatic velocity increase of the slug nose does not appear to play an obvious role as a source mechanism and may be associated with the highly unstable bubble in the tube widening.

Scaling to the volcanic case was undertaken using experimentally verified CFD modelling. This showed that slug burst pressure is a function of conduit radius and slug mass, with large slugs in narrow conduits producing gas overpressures in the region of 1 MPa at burst. This overpressure will fragment the upward-moving (10s m/s) meniscus of liquid existing just prior to burst. The effect of such decompression on the vesiculated basalt magma flowing down the conduit walls and slug base could be explosive fragmentation (Namiki & Manga 2006). This would eject pyroclasts, adding greatly to the pyroclast volume from the meniscus and explaining how explosive slug burst results in the ejection of significant masses of pyroclasts. There is also the possibility that the gas slug is not a single bubble, but more accurately described as a foam raft, although such a structure may not survive the degrees of expansion undergone in ascent from 1000 m depth with its bubble walls intact. The rapid 1MPa decompression of a foam raft would also produce pyroclasts as the foam fragments.

Rapid slug expansion, which generates the explosivity of strombolian eruptions, is a process operating within about 10 m of the top of the magma column. This, and the fact that the forces generated are of order 10^6N upward, means that slug expansion is not the fluid dynamic source process responsible for the seismic signals inverted by Chouet *et al*. (2003). Slug expansion plays no role in this particular seismic signal, because at a depth of 200m the slug is not expanding at any appreciable rate. The stable position of the seismic source suggests geometric control of a flow process, a phenomenon we have seen a number of times before. James *et al*. (2006) measured pressure and force as a gas slug ascended from a narrow tube through a flare into a wider tube. The gas slug segmented on passing through the flare and liquid flow during this process generated pressure oscillations (Figure 4). Analysis of these oscillations (Figure 1) revealed three components centred on 60, 13 and 6Hz. The low frequency component showed increasing pressure followed by a decrease, and resembled the expansion-contraction waveform from inversion of seismic data (Figure 1a, Chouet *et al*. 2003). The vertical force generated during the pressure increase was 30 N downward. Applying a simplistic scaling based on density and volume differences between laboratory and volcano gives a force in the region of 10^8N, of similar magnitude to that emerging from inversion of seismic data. It was, therefore, suggested that the source mechanism for seismic signals measured at Stromboli by Chouet *et al*. (2003) was the ascent of slugs sourced at depth (Burton *et al*. 2007) through a geometric widening of the feeder dyke inclined at 72°. The upward widening disrupts the downward flow of liquid around the ascending slug, allowing significant thickening of the falling film. As this thickening falls through the downward narrowing, it pinches closed and segments the slug. The resulting liquid piston continues to descend because of its inertia, and increases pressure below it. The piston then oscillates for a cycle or two before being disrupted by the buoyancy of the gas beneath. Experimental insight suggests that the source mechanism for the seismic signal is the deceleration of the liquid piston.

References

Barenblatt GI (2003) *Scaling.* Cambridge University Press, ISBN 0-521-53394-5

Blackburn EA, Wilson L, Sparks RSJ (1976) Mechanisms and dynamics of strombolian activity. *J Geol Soc Lond* **132**; 429-440

Burgisser A, Bergantz GW, Breidenthal RE (2005) Addressing complexity in laboratory experiments: the scaling of dilute multiphase flows in magmatic systems, *Journal of Volcanology and Geothermal Research* **141**; 245– 265

Burton M, Allard P, Muré F, La Spina A (2007) Magmatic gas composition reveals the source depth of slug-driven Strombolian explosive activity. *Science,* **317**; 227-230

Chouet B, Dawson P (2006) Shallow-conduit dynamics at Stromboli volcano, Italy, imaged from waveform inversions. The Physics of Fluid Oscillations in Volcanic Systems: Workshop, Lancaster University. http://www.es.lancs.ac.uk/seismicflow/downloads/ChouetDawson.zip

Chouet B, Dawson P, Martini M (2008) Shallow-conduit dynamics at Stromboli Volcano, Italy, imaged from waveform inversions. In Lane SJ, Gilbert JS (eds) *Fluid Motion in Volcanic Conduits: A Source of Seismic and Acoustic Signals*. Geological Society, London, Special Publications

Chouet B, Dawson P, Ohminato T, Martini M, Saccorotti G, Giudicepietro F, De Luca G, Milana G, Scarpa R (2003) Source mechanisms of explosions at Stromboli Volcano, Italy, determined from moment-tensor inversions of very-long-period data. *J Geophys Res* **108(B1)**; 2019, doi:10.1029/2002JB001919

Chouet BA, Hamisevicz B, McGetchin TR (1974) Photoballistics of volcanic jet activity at Stromboli, Italy. *J Geophys Res* **79**; 4961-4976

Clift R, Grace JR, Weber ME (1978) *Bubbles, Drops and Particles*. Academic Press 380 pp. ISBN 012176950X

James MR, Lane SJ, Chouet B, Gilbert JS (2004) Pressure changes associated with the ascent and bursting of gas slugs in liquid-filled vertical and inclined conduits. *Journal of Volcanology and Geothermal Research* **129(1-3)**; 61-82

James MR, Lane SJ, Chouet BA (2006) Gas slug ascent through changes in conduit diameter: Laboratory insights into a volcano-seismic source process in low-viscosity magmas, *J. Geophys. Res*., **111**, B05201, doi:10.1029/2005JB003718

James MR, Lane SJ, Corder SB (2008) Modelling the rapid near-surface expansion of gas slugs in low-viscosity magmas. In Lane SJ, Gilbert JS (eds) *Fluid Motion in Volcanic Conduits: A Source of Seismic and Acoustic Signals*. Geological Society, London, Special Publications

Jaupart C, Allegre CJ (1991) Gas content, eruption rate and instabilities of eruption regime in silicic volcanoes. *Earth and Planetary Science Letters* **102;** 413-429

Jaupart C, Vergniolle S (1988) Laboratory models of Hawaiian and Strombolian eruptions. *Nature* **331**(6151); 58-60

Jaupart C, Vergniolle S (1989) The generation and collapse of a foam layer at the roof of a basaltic magma chamber. *Journal of Fluid Mechanics* **203**; 347-380

Namiki A, M Manga (2006) Influence of decompression rate on the expansion velocity and expansion style of bubbly fluids. *J. Geophys. Res.* **111**; B11208

Newhall CG, Self S (1982) The explosivity index (VEI) - an estimate of explosive magnitude for historical volcanism. *J Geophys Res* **87**(NC2): 1231-1238

Parfitt EA (2004) A discussion of the mechanisms of explosive basaltic eruptions. *Journal of Volcanology and Geothermal Research* **134;** 77-107

Pyle DM (2000) Sizes of volcanic eruptions. In Sigurdsson H, Houghton B, McNutt SR, Rymer H, Stix J (Eds) (2000) *Encyclopaedia of Volcanoes,* Academic Press, ISBN 0-12-643140-X, pp 263-269

Ripepe M, Ciliberto S, Della Schiava M (2001) Time constraints for modeling source dynamics of volcanic explosions at Stromboli. *Journal of Geophysical Research-Solid Earth* **106**(B5); 8713-8727

Seyfried R, Freundt A, (2000) Experiments on conduit flow and eruption behavior of basaltic volcanic eruptions. *Journal of Geophysical Research-Solid Earth,* **105**, 23727-23740

Woolley AR, Church AA (2005) Extrusive carbonatites: A brief review. *Lithos* **85** (1-4): 1-14

Yokoyama I (2005) Growth rates of lava domes with respect to viscosity of magmas. *Annals of Geophysics* **48(6)**; 957-971

Introduction to Geomicrobiology by Kurt O Konhauser (University of Alberta, Edmonton, Canada), 2007, Blackwell Science Ltd. 425pp, £34.99 (paperback) ISBN 13: 9780632054-54-1

The book is written to provide a single comprehensive book describing "current knowledge of how microbial communities have influenced biochemical and mineralogical processes through time."

Designed by a Canadian lecturer as a core text for upper undergraduate and graduate students, it is process-oriented, the pervasive theme being "geological consequences of microbial activity". The seven comprehensive chapters can stand alone, but are linked through a natural progression, each ending with a summary. It is hoped that the book will be a useful resource for researchers from various backgrounds.

There are impressive colour and mono photos and micrograms and very helpful diagrams and info-boxes. The many references are aimed at providing a starting point for further study; together with in-text references there is a 55-page list of full references and a 29-page index. My slight quibble is irritation with some of the American spellings – molded, favor, sulfate, behavior are a few!

Chapter 1 – Microbial properties and diversity – covers classification of life, physical properties of micro-organisms, requirements for growth, diversity, life in extreme environments including deep sea, extra-terrestrial and "Panspermia".

Chapter 2 – Microbial metabolism – covers biogenetics, photosynthesis, catabolic processes, respiration, reduction and oxidisation

Chapter 3 – Cell surface reactivity and metal sorption – covering cell structure, microbial surface charge, passive, active and bacterial metal adsorption and sorption, role in contaminant mobility and industrial applications. Surface charge properties of micro-organisms can facilitate attachment to submerged surfaces allowing their manipulation for industrial processes including bio-recovery and bio-remediation, helping "clean up" toxic areas contaminated with various metals.

Chapter 4 – Biomineralisation – covering both biologically induced and controlled mineralisation and fossilisation, Bio-mineralisation either involves mineral precipitation in open environments with no apparent cellular control over mineral product, or can be completely regulated allowing organisms to precipitate minerals serving some physiological purpose. Ferric and manganese minerals including nodules, silica and carbonates are important bio-minerals, with $CaCO_2$ contributing to microbialite growth (including Stromatolites and Thrombolites)

Chapter 5 – Microbial weathering – covers mineral dissolution, sulphide oxidation and microbial corrosion, including fungi.

Chapter 6 – Microbial zonation – covers microbial mats and marine sediments.

Mats have been the most successful ecological systems on earth for much its existence.

Marine sedimentary diagenisis depends largely on materials being deposited, reactivity of organic matter and mineralogy of inorganic detritus.

Chapter 7 – Early microbial life – includes prebiotic Earth, first cellular life forms, evolution of photosynthesis, metabolic diversification and the Earth's oxygenation

I found the content fascinating, but because of the comprehensive chapters, I concentrated on just 3.

The book would be of interest to Oceanography, Geology, Chemistry and Biology students as well as to general readers looking for this type of information. I wish I had seen it earlier!

M.Rosemary Darby
BA(Open), BSC(Hons)Open, Certs Ed.(UK + NZ)

Dynamic Planets Elsewhere

David A. Rothery, Dept of Earth Sciences, The Open University

The geology of the Earth is fashionably seen in terms of cycles, such as the rock cycle, the hydrologic cycle, the carbon cycle, and so on. Although it is true that the Earth is a particularly dynamic planet, it is not unique in this respect. The operation of analogous cycles can be recognised in several other planetary bodies in our Solar System, notably Mars, Venus, Io, Europa, Enceladus and Titan.

I do not propose to discuss all these in detail here. If you want to know more, you should study S196 (Planets: an introduction) or S283 (Planetary Science and the Search for Life), though even those leave much unsaid. What I will try to do here is to just draw attention to some aspects of our modern insights into how planetary bodies function. I say 'planetary bodies' rather than 'planets', because so far as their geology goes, many satellites (moons, if you prefer) function in the same way as planets.

Furthermore, when I came to turn what I had prepared as a picture-rich, and indeed picture-led, talk into a conventional paper, I found that it could not easily be done. Therefore I present you here with some of the copyright-free illustrations from my talk, accompanied by extended captions. The pictures – all of them images sent back by visiting spacecraft – are the backbone of the tale, and are all from NASA except where credited differently. They are among the best that I am aware of for illustrating the ways in which other planetary bodies can be 'dynamic'. I defy anybody, having looked at the images I have chosen for Mars, to deny that it lacks a long and complex hydrologic cycle (still active today) accompanied by erosion and depositional aspects of the rock cycle.

Figure 1. A cliff-promontory dubbed 'Cape St Vincent' jutting into Victoria crater on Mars, imaged by NASA's Opportunity rover in May 2007. The solid cliff is about 20m high. The pale stratum marks the base of the ejecta layer, thrown out when the crater was excavated. Below this, in the undisturbed bedrock, can be seen classic high-angle aeolian dune cross-bedding.

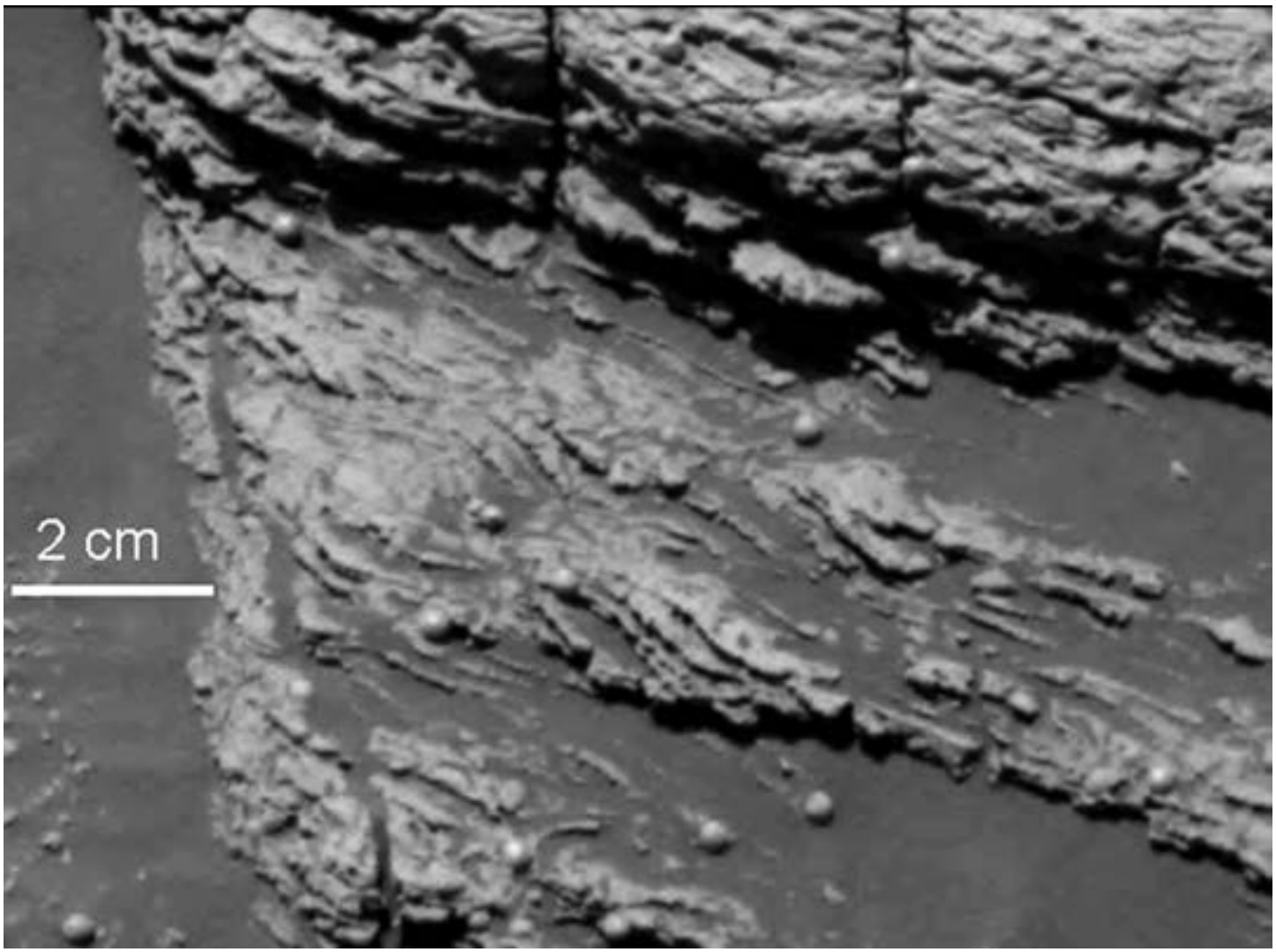

Figure 2. Ripple cross-bedding seen close up by NASA's Opportunity rover in a rock dubbed 'Last Chance'. The ripples appear to be fluvial, and embedded in the rock are some spherical 'blueberries', which are hematite concretions that grew during diagenesis requiring wet conditions.

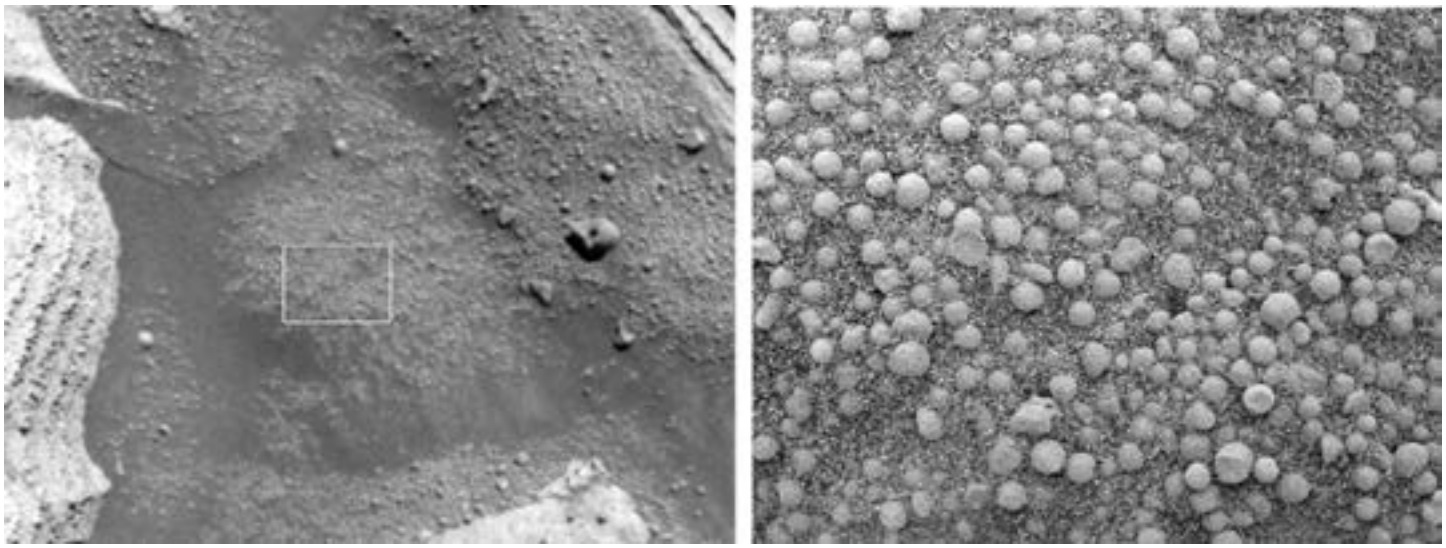

Figure 3. Left: 20cm wide view from NASA's Opportunity rover at a site named Alamogordo Creek. Laminated outcrop surrounds an area where weathered-out 'blueberries' have become concentrated. Right: 3cm wide close-up of the box on the left showing the 'blueberries' clearly.

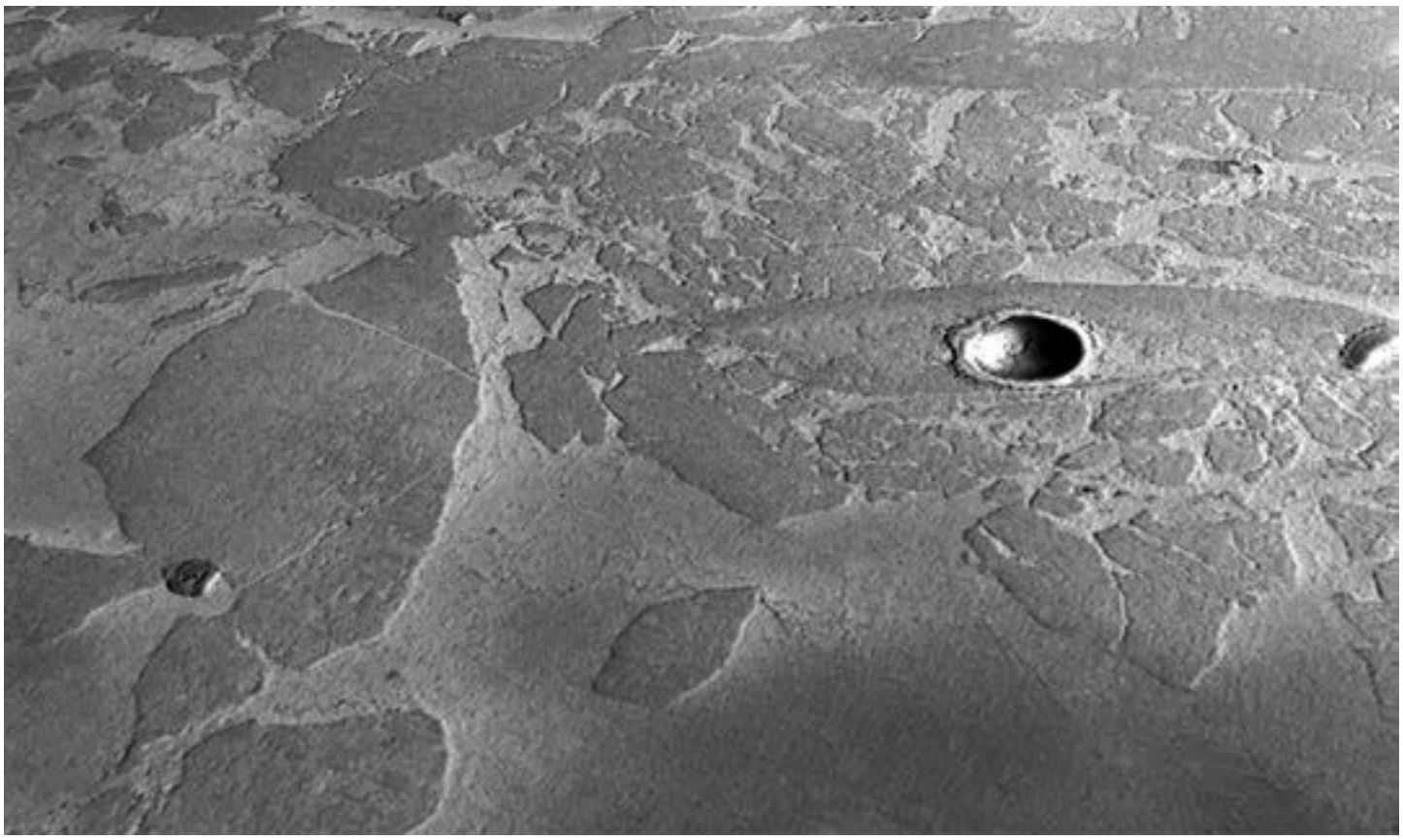

Figure 4. 60km wide view of Mars from ESA's Mars Express, showing an area interpreted to be preserved rifted ice floes on a now fully frozen and dust-covered sea. Dating is uncertain, but the sea is unlikely to be more than 50 million or less than 5 million years old. (Image courtesy of ESA/DLR/FU Berlin)

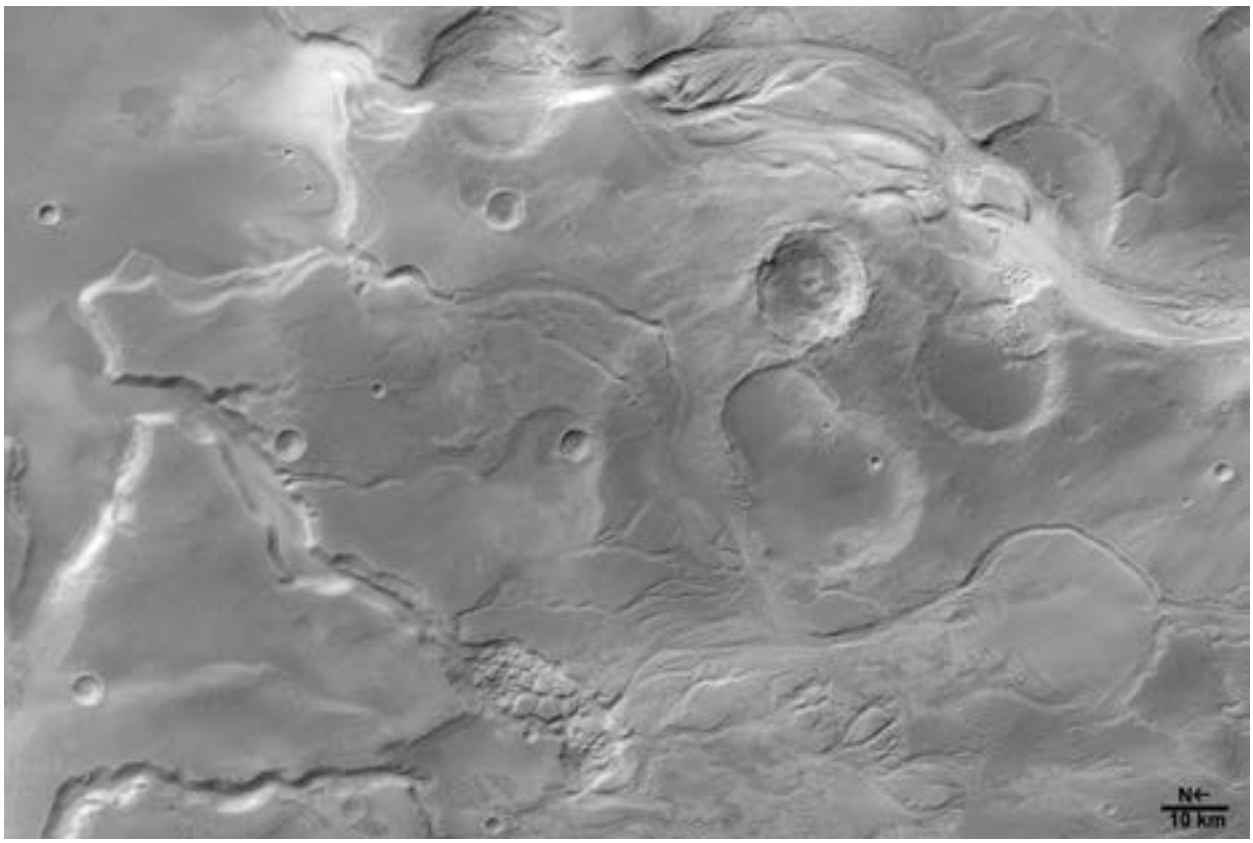

Figure 5. 200km wide view showing ancient valley networks draining from the martian southern highlands (on the right) into the northern lowlands (on the left). If you, look carefully, you can see abundant signs of multiple episodes of valley formation. Flow at times appears to have been catastrophic, such as formed post-glacial 'channelled scablands' on Earth. (Image courtesy of ESA/DLR/FU Berlin)

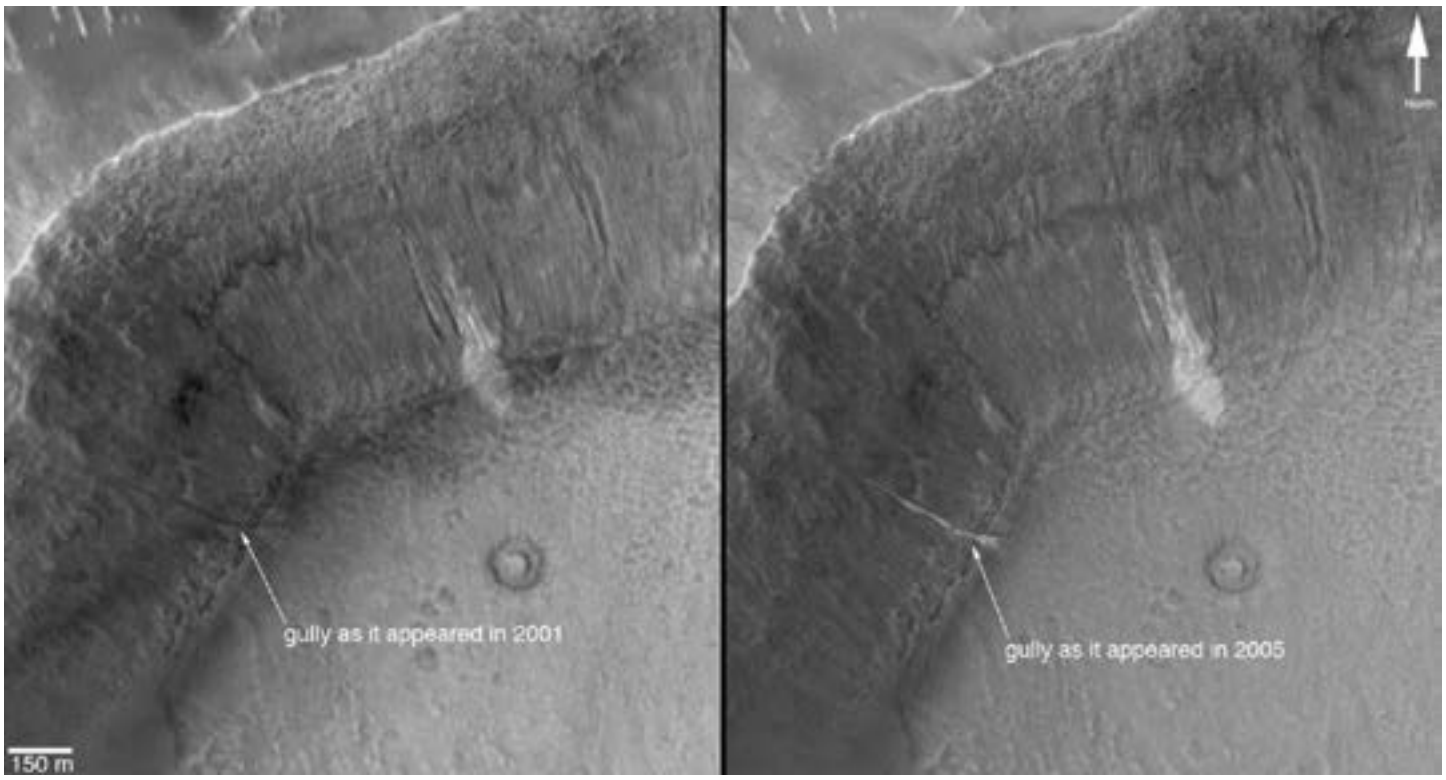

Figure 6. Large drainage channels on Mars have been well-known for decades, but these tiny gullies, some of them active in the past few years, were not discovered until the 1990s. These two images from the Mars Observer Camera highlight a gully on the inner wall of a crater where something, most likely water, flowed between 2001 and 2005.

For Mars, I have left out dust storms, dust devils, seasonal changes in the polar caps and glacial and volcanic landforms. Beyond Mars the choice is mind-boggling, and I have too little space available to do justice to anything. What follows is very much 'edited highlights'. For reasons of space I have left out Europa, the satellite of Jupiter with an ocean below only a few km of ice which may support chemosynthetic life at 'black smoker' hydrothermal vents on the ocean floor or even photosynthetic life in tidal cracks within the ice.

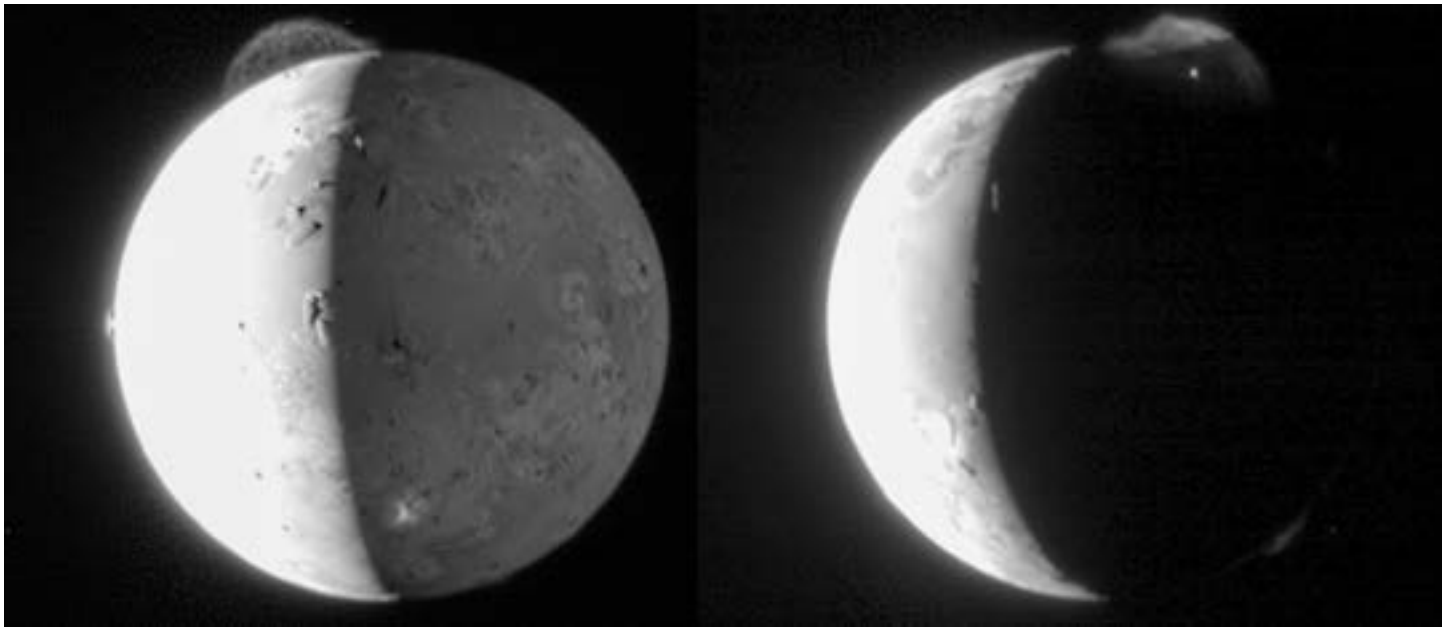

Figure 7. Two views of Io, the most volcanically active body in the Solar System, seen by NASA's Pluto-bound New Horizons probe when it flew past the Jupiter system in February 2007. The largest eruption plume in each view rises 330 km above the caldera known as Tvashtar, which was also active during the Galileo mission in the 1990s. The view on the left reveals, for the first time, structure within the eruption plume, whereas the view on the right, recorded after the vent had passed into night, reveals the incandescent glow of a fire-fountain or lava flow. Other, smaller, eruption plumes are visible in both images, some from volcanoes not previously known to be active. If you think of Europa as a less-active, ice-covered version of Io, you can appreciate the energy and nutrients available for life on its ocean floor.

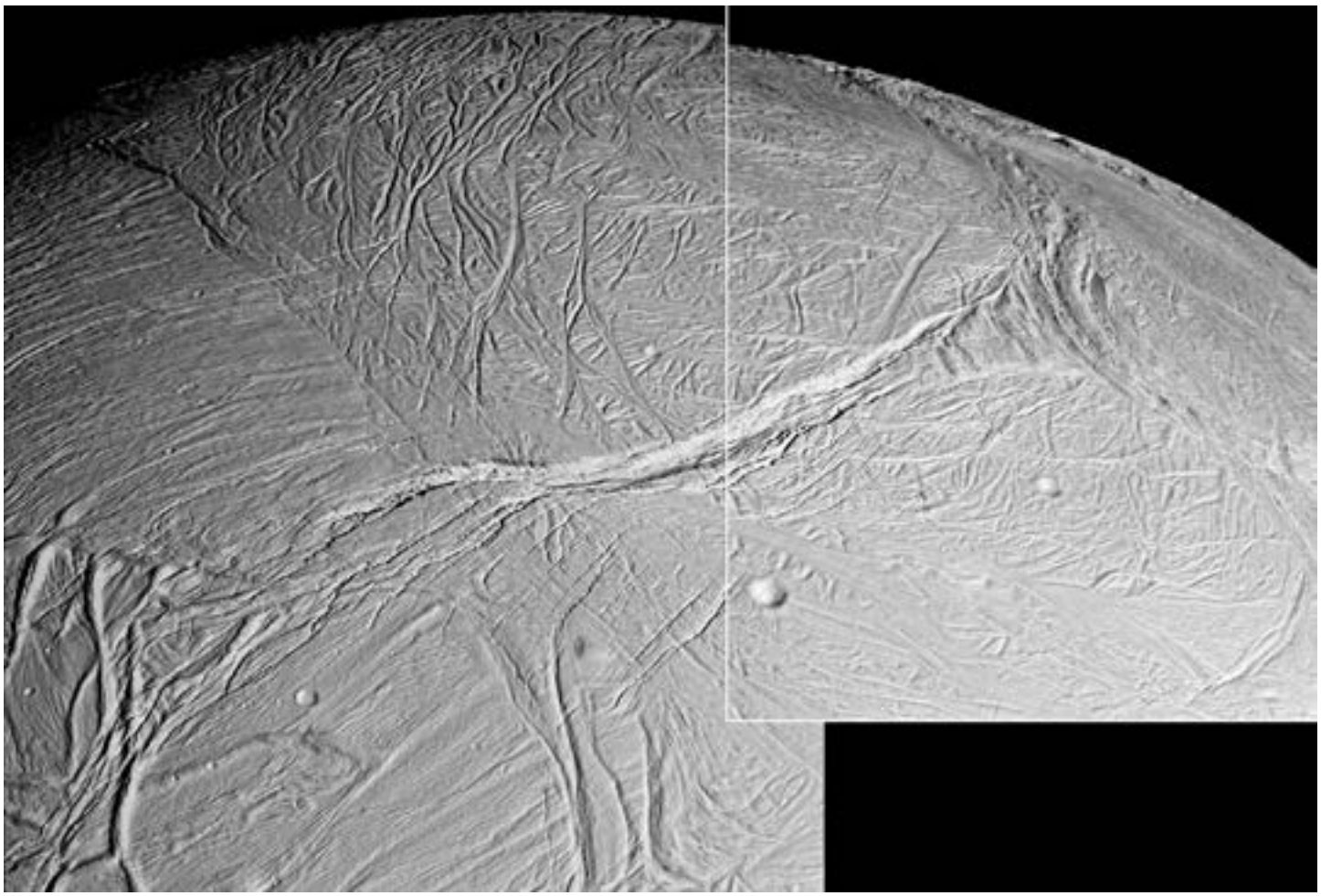

Figure 8. A mosaic of two Cassini images of Enceladus, a 249 km radius icy satellite of Saturn. Sunlight is coming from the right. This part of the surface has suffered multiple episodes of tectonism. Most of the linear features are fissures, but those in the lower left are ridges and may be extrusions of viscous icy magma. Impact craters are few, showing that this is a relatively young surface.

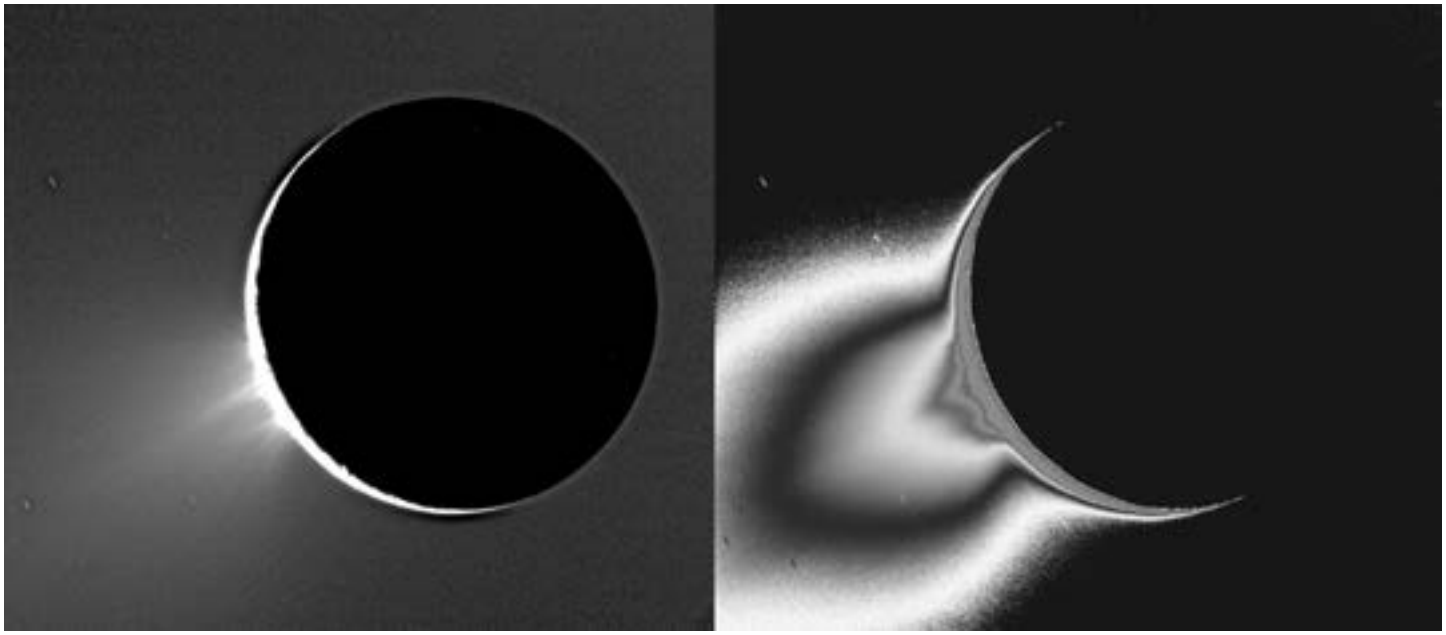

Figure 9. The crescent Enceladus, seen by Cassini looking towards the Sun in November 2005. Jets of ice crystals are expelled to space from geysers in young fissures low in the southern hemisphere. Left: normal view, Right: contoured view to show the extent of the plume.

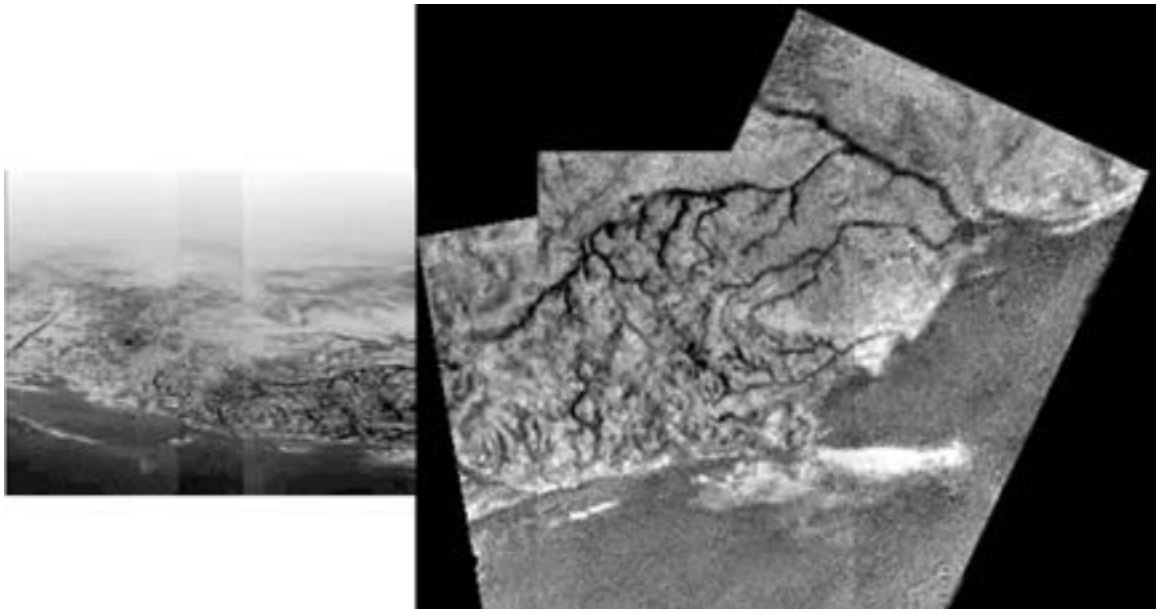

Figure 10. Part of the surface of Titan seen from a height of 8 km by the Huygens probe during its parachute descent. Left: oblique. Right: vertical, about 7 km across (covering the lower-right portion of the oblique view). Titan has an atmosphere of nitrogen, methane and more complex hydrocarbons that make an optically opaque haze. The pale areas are high ground where ice 'bedrock' is exposed, washed clean by methane rainfall. Lower areas where tarry tholins (dirt from the atmosphere) accumulate are darker. Valley bottoms are darkest of all, revealing complex dendritic drainage, almost certainly fed by precipitation. (ESA/NASA).

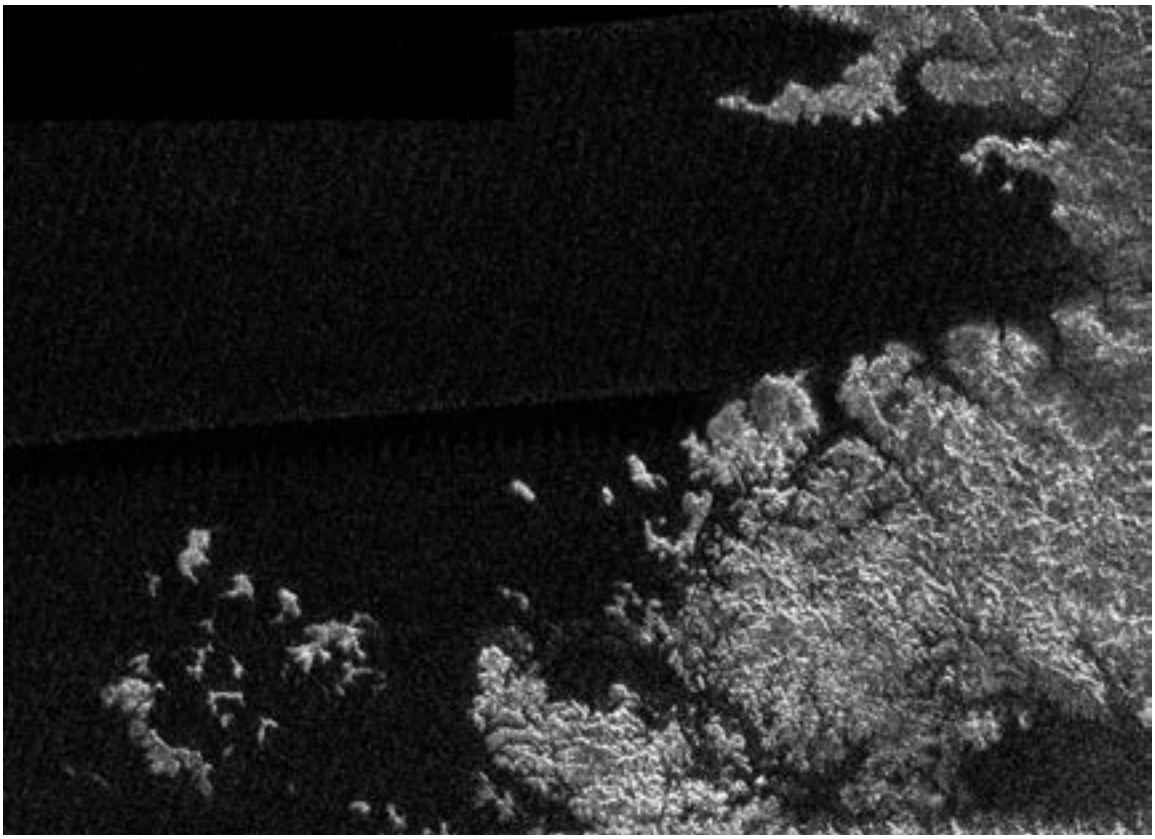

Figure 11. The low ground in the Huygens landing area was dry, but there are seas (larger than North America's Great Lakes) aplenty at high northern latitudes. Here is the shoreline of one, in a 270 km wide radar image from the Cassini orbiter. The radar-dark area is liquid (almost certainly mostly methane) and the radar-bright area is exposed icy terrain. The image reveals a classic drowned shoreline, with flooded valleys making broad estuaries like the 'rias' on the south coasts of Cornwall and Devon. The extent to which Titan's surface processes respond to seasonal or longer-term climate change is unknown, but there is clearly an active 'methanologic' cycle directly analogous to the Earth's hydrologic cycle. Moreover, there must be a rock cycle too, with ice playing the part of rock that is eroded, transported and deposited. There is growing evidence for cryovolcanism, which would be the 'igneous' part of Titan's rock cycle. There must be tectonic uplift too, otherwise erosion ought to have planed everywhere flat.

Such is the pace at which new images arrive that by the time this appears in print some of my choices may have become second-best. If you want to play the game of finding better examples, or just want to keep up to date in general, websites that I particularly recommend are:

http://saturn.jpl.nasa.gov/multimedia/images/index.cfm Saturn's satellites (and Saturn as well) from the Cassini mission.

http://marsrovers.jpl.nasa.gov/home/index.html To watch the continuing adventures of NASA's Mars Exploration Rovers (Spirit and Opportunity)

http://mars.jpl.nasa.gov/mro/gallery/images.html Images of parts of Mars from orbit, showing details as small as tens of cm in size.

http://photojournal.jpl.nasa.gov/index.html for NASA's general public archive

---

Exploring the landscape of Charnwood Forest and Mountsorrel: A Walkers' guide to the rocks and landscape of Charnwood Forest and Mountsorrel by Keith Ambrose, John Carney, Graham Lott, Gill Weightman and Annette McGrath, 2007, British Geological Survey, 52pp, £12.00 (paperback) ISBN 9780852725702

This attractive booklet is in the Earthwise series and comes in a plastic wallet complete with a map.

The first page includes a brief description of the area and a paragraph about the walks. There are then nine pages about the geology, including a basic explanation of plate tectonics and an overview of the geological timescale and events from Precambrian to the Quaternary.

Eleven walks are described, the first six giving the geological setting, the ascent, distance and difficulty and a grid reference for the start point. The other five which are to quarries, a reservoir and a disused railway cutting just give the starting grid reference. The numbered localities mentioned in the walk details are also shown on the accompanying map and on the illustrations in the book. Hard hats are recommended for some of the locations and although most of the walks are described as fairly easy there is the occasional warning about some steep scrambles and descents and for Walk 3 it is advisable to take a compass or GPS.

The main map is a simplified geological map taken from the 1:50,000 sheets for Loughborough, Coalville and Leicester enlarged to 1:25,000 scale; there are inset maps for walks 1 to 5, eight photographs of some of the rocks, a key to the map plus a cross-section and a cartoon showing a typical Charnwood volcano.

Following the pages devoted to the walks there are some interesting facts about the minerals of Charnwood, quarrying and building stone, together with some excellent photographs. The last few pages contain a geological glossary, some Tourist information, a further reading list and two pages about The National Forest.

The wallet containing the booklet and map is a convenient size for a rucksack or large pocket and as the blurb on the back cover states "There is something here for everyone, from the Sunday stroller to the keen walker, as well as both amateur and professional geologists."

Elizabeth Maddocks BA (Open)

Geology of the Salisbury district: a brief explanation of the geological map Sheet 298 Salisbury. Sheet explanation of the British Geological Survey 1:50 000 Sheet 298 Salisbury (England and Wales)/Sheet 298 Salisbury (Bedrock and Superficial Deposits) by P M Hopson, A R Farrant, A J Newell, R J Marks, K A Booth, L B Bateson, M A Woods, I P Wilkinson, J Brayson and D J Evans, 2007, British Geological Survey, £18 (paperback) including map, 38pp. (NB No ISBN provided by the publisher)

This concise and informative guide accompanies the newly resurveyed sheet of the Salisbury district, which stretches from Stonehenge in the north to Broad Chalke in the south. Based on resurvey work completed in 2003, the guide outlines the geological setting of the district and provides a detailed account of its geology and applied geology.

The Chalk outcrop dominates the district, with Jurassic sediments (Kimmeridge Clay Formation and younger) exposed in the incised valley of the River Nadder. Marine deposition in the Late Triassic to Kimmeridgian and the Cretaceous were followed by erosion, 'Alpine' compression, uplift and further erosion. Palaeogene sediments overly Mesozoic strata in the south-west and Quaternary deposits constitute the district's superficial deposits. Evidence of the underlying geology, down to the Permo-Triassic, is provided from four deep boreholes.

Detailed descriptions of the Jurassic and Cretaceous strata are accompanied by tables showing the nomenclature used by other authors, invaluable for anyone intending to utilise the reference list. Readers with an interest in Quaternary deposits will appreciate the comprehensive coverage, including palaeoenvironmental interpretation, provided in the guide.

The applied geology section covers hydrogeology, karstic solution features in the Chalk and building stones. Portland Group building stones have been quarried extensively in the Vale of Wardour (River Nadder), yielding freestones used in the Chapter House of Westminster Abbey, Romsey Abbey and Balliol College, Oxford, and the Chilmark stone, an oolitic freestone used in Salisbury Cathedral's west front. Gault, Palaeogene and some Quaternary clays have been used locally for brick-making.

Numerous tables and figures plus colour plates, for example, showing hardgrounds within the Chalk and Quaternary solifluction features, supplement the text. Marginal sketches on Sheet 298 show the district's major structural features, cross sections of major streams and their associated Quaternary deposits and the inferred underlying Pre-Permian geology.

Together, the map and sheet explanation provide a compact, but comprehensive and accessible guide to the district, recommended for the enthusiastic student as well as the professional user.

Caroline Peters BSc (Hons) Geoscience (Open)

The Geology of the Canary Islands: a Review

Duncan Woodcock

Introduction

The Canary Islands comprise a group of seven major islands together with a number of smaller islands (Figure 1). The islands are blessed with sunny weather for most of the year and the surrounding Atlantic Ocean moderates any extremes of temperature. The climate is particularly attractive during the winter, when conditions are usually ideal for geological fieldwork (Woodcock, 2000). The islands display a wide variety of volcanic and magmatic features; these are generally well exposed, particularly along the coasts and in the walls of "barrancos" - deep erosional valleys cut by infrequent but intense rainstorms. In recent years the islands have benefited from an EC-funded programme of road modernisation: as well as improving access generally, other benefits (for geologists) include the availability of clean roadcut exposures and abandoned loops of old road that often provide excellent traverses away from the traffic.

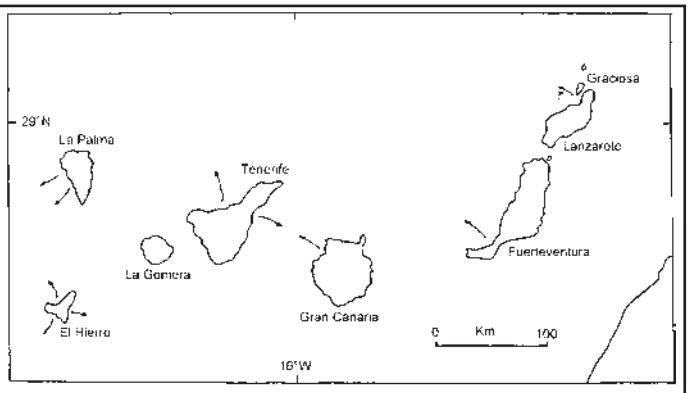

Figure 1. Outline map of the Canary Islands. Arrows indicate location and direction of giant lateral collapses (based on Carracedo *et al.* 1999).

Interest in the geology of the Canary Islands goes back to the 19th century, when the German geologist Leopold von Buch made an extended visit in 1815, followed by Charles Lyell in 1854. These two visits spawned the first of many controversies in Canary Islands geology: the origin of the large calderas on La Palma and Tenerife (Wilson 1998). In the 1950s, Hans Hausen began a series of visits to the Canary Islands: his somewhat idiosyncratic output, published in an obscure journal, provided the first comprehensive coverage of the geology of the islands (Hausen 1956, 1973). Hausen's monographs were complemented by the publication in 1968 of Spanish monographs on the four eastern islands (Fuster 1968). Over the last twenty years or so there has been an explosion in the geological literature on the Canary Islands; much of it addressing topics such as the growth and collapse of volcanic islands, the origin of Canary Island magmatism, historical eruptions and the ignimbrite deposits on Gran Canaria and Tenerife.

There are now excellent reviews on Canarian geology (Carracedo *et al.* 2002) together with an excellent field guide (Carracedo & Day 2002). In parallel there has been a recent revision of the large scale Cartografia Militar de Espana topographic maps. A recent development is the availability of the high resolution satellite imagery from Grafcan by Google Earth: this coverage is of such high resolution that mapping directly onto a print of the image has become my preferred method of field mapping.

A comprehensive review of Canary Island geology would easily fill a complete edition of the Journal! Hence this paper concentrates on a number of topics that are under active consideration: they include the origin of ocean island magmatism, the growth and evolution of ocean islands, giant lateral collapses, felsic magmatism, sea-level and climate change and geoconservation.

Overview of Canary Islands Geology

One of the fascinations of the Canary Islands is that each island has its own "geological character". In general, the islands become younger, and the geology less complicated, in going from east to west along the archipelago. Unfortunately this was the reverse order in which the islands were studied in detail (Carracedo *et al.* 2001)

At the simplest level, the geological history of the older islands can be summarised as follows:

i. Submarine growth of a seamount on pre-existing ocean crust, to produce a "Basal Complex"

ii. Intense and prolonged subaerial basaltic volcanism, producing thick sequences of sub-horizontal lava flows: the "shield-building" stage

iii. A period of volcanic quiescence and intense erosion

iv. "Post-erosional" volcanism, comprising infrequent eruptions of varying intensity.

Table 1 (based on Carracedo & Day 2002) shows the ages of the "shield-building" and "post-erosional" periods of volcanism for the main islands. Note the overall age progression from east to west. There is recent (Holocene) activity on all islands except La Gomera, with historic eruptions on Lanzarote, Tenerife and La Palma.

Canary Islands: Origin and Evolution

The origin of Canary Islands has been controversial since systematic studies of the islands began. In his series of monographs, Hausen considered that the islands were the remnants of a Canarian

Table 1. Ages (Ma) of main periods of volcanism in the Canary Islands.

	Fuerteventura	Lanzarote	Gran Canaria	Tenerife	La Gomera	La Palma	El Hierro
Shield-building	22 - 12	16 - 5	15 - 8	12 - 4	11 - 4	2 - 0	1.2 - 0
Post-erosional	5 - 0	4 - 0	6 - 0	3 - 0	Inactive		

A more detailed overview of Canary Islands geology (with dates from Carracedo & Day, 2002) is presented in Table 2

Table 2. Overview of Canary Islands geology.

	"Basal Complex"	"Shield-building" phase	"Post-erosional" phase
Fuerteventura	Pre-existing basaltic ocean crust overlain by Early Jurassic- early Cretaceous pelagic limestones and siliciclastic sediments. Seamount stage comprises submarine pillow lavas and hyaloclastites intruded by a dyke swarm, major mafic –ultramafic plutons (48-22Ma) and minor carbonatitic bodies. (Figure 2) Outstanding exposure in W of island.	Extensive alkali basalt lava flows with subordinate explosive activity.	Minor alkali basalt lava flows and scoria cones. No historic activity.
Lanzarote	Not exposed	Extensive alkali basalt lava flows with subordinate explosive activity (Figure 3).	Infrequent and ongoing. Recent volcanism includes: • 70-50 ka: Volcan Corona • 1730-36 :Timanfaya (Figure 4) • Minor activity in 1820
Gran Canaria	Not exposed	Initial basaltic phase (15-14 Ma) followed by development of a shallow fractionating magma chamber producing rhyolitic magmas and extensive ignimbrite eruptions (Figure 5).	Particularly vigorous, including: • Roque Nublo stratovolcano (5.5-3 Ma) with later collapse and low T ignimbrites • Plio-Pleistocene alkali volcanics
Tenerife	Not exposed	Extensive alkali basalt lava flows, developing three overlapping shield volcanoes (Teno, Anaga, Roque del Conde) to produce the "Old Basaltic Series".	Particularly vigorous, including: • Las Canadas series, with the development of felsic magmas and extensive ignimbrite eruptions • Historic eruptions including Montana Negra (1706) , Narices del Teide (1798) & Chinyero (1909).
La Gomera	Submarine extrusive volcanics, associated plutonics and dense dyke swarms exposed in N of island.	At least two phases of basaltic volcanism separated by a period of quiescence and erosion. Intrusion of trachytic and phonolitic domes and dykes (Figure 6).	Volcanically quiescent. Erosion ongoing to produce a radial pattern of ravines.
La Palma	"Seamount" phase well exposed in the erosional inlier in Barranco de las Angustias: pillow lavas (Figure 7) and volcaniclastics together with a dyke swarm and subvolcanic intrusions.	Cycles of effusive eruption and lateral collapse in centre and N of island but now dormant. Activity now focussed on southern Cumbre Vieja with seven eruptions since 16th century.	
El Hierro	Not exposed	Cycles of effusive eruption (Figure 8) and lateral collapse ongoing. Currently dormant.	

Figure 2. Mesozoic turbidites intruded by a basaltic dyke. Basal Complex, Barranco de Ajuy, Fuerteventura.

Figure 3. Subparallel lava flows of the shield-building phase: Punta Fariones, Lanzarote.

Figure 4. Crevasse in the surface of the extensive lava flows from the 1730-36 eruption on Lanzarote – an example of post-erosional volcanism.

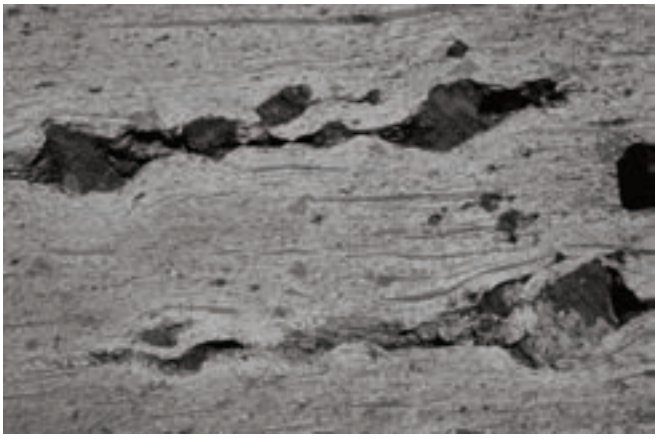

Figure 5. Extreme eutaxitic foliation in a peralkaline welded ignimbrite, Barranco de los Frailes, Gran Canaria. Hammer handle (middle RHS) is c.30mm across.

Figure 6. The 200 m high phonolitic dome dominates the skyline of the Vallehermoso area, La Gomera.

Figure 7. Pillow lavas of the "seamount series", Barranco de las Angustias, La Palma.

Table 3. Comparison of the development of the Canary Islands with the Hawaiian Islands (Carracedo 1999).

	Hawaiian Islands	Canary Islands
Seamount stage	Bathymetric uplift precedes volcanism	Uplift as consequence of magmatism
Shield-building stage	Predominantly tholeiitic basalts with later minor alkali basalts ("alkali cap")	Alkali basalts with differentiation to produce felsic magmas: phonolitic, trachytic and rhyolitic intrusive and extrusive magmatism
Volcanic quiescence and erosion	Typically 1Ma	Much longer: up to 7Ma on Fuerteventura
Post-erosional stage	Silica-undersaturated magmatism: strong contrast to shield-building stage	Wide compositional variation, even within a single eruptive episode
Subsidence	Major post-shield stage subsidence	Subsidence absent: exposures of Basal Complexes right along the chain: Fuerteventura (east) , La Gomera (central) and La Palma (west).

microcontinent underlain by sialic crust that had become broken up by faulting and then partially subsided, leaving the islands as unfoundered blocks (Rothe & Schmincke 1968). Subsequent seismic investigations established early on that the five westernmost islands were underlain by oceanic crust (Schmincke 1982). The two easterly islands of Lanzarote and Fuerteventura have a very different morphology to the other islands and were originally thought to be underlain by continental crust; however more recent investigations, including detailed mapping of the Basal Complex on Fuerteventura, have established that these two islands are also underlain by oceanic crust.

There are essentially two hypotheses for the origin of the Canary Islands in play at present:

- The "propagating fracture" hypothesis, which emphasises the role of regional fractures in the development of magmatism
- The "hotspot" hypothesis, which proposes that magmatism is due to a thermal anomaly in the underlying mantle.

The current paradigm for the origin and evolution of ocean island chains worldwide appears to be the hotspot hypothesis. The classic example is the Hawaiian island chain, where magmatism is considered to be a consequence of the interaction of a mantle plume tail with a fast-moving plate to produce a clear age progression along the chain. There has been a tendency to attempt to "force fit" this standard Hawaiian model to other volcanic island chains. In the case of the Canary Islands there are significant differences from the standard model. Table 3 attempts to summarise the key differences

The differences between the Canary Islands and the Hawaiian Islands may be due to the different geodynamic settings. The Hawaiian Islands are in the middle of the Pacific plate that is moving rapidly at around 10 cm/yr with respect to the putative hot spot. In contrast, the Canary Islands have developed on old oceanic crust adjacent to the African continental margin on a plate moving at one cm/yr or less. The slower plate movement may account for the extended time scales and rather irregular age progression of volcanism along the chain.

The role of mantle plumes in the formation of ocean islands has been challenged recently (Foulger 2007, Foulger & Natland 2003) and a new "Plate" hypothesis asserts that magmatism is a consequence of the adiabatic decompression of fertile mantle in a tensional environment. This may stimulate a resurgence of the "propagating crack" hypothesis in a modified form. In its original form it proposed a "leaky megashear" that connected the Canary Islands and the Altas mountains via an oceanwards extension of the S. Atlas Fault (Anguita & Hernan 1975). However subsequent geophysical surveys have shown no evidence for the offshore propagation of the fault into the mechanically stronger ocean lithosphere. (Carracedo *et al.* 1998).

Giant Lateral Collapses

In recent years there has been an increasing recognition of the role of giant lateral collapses in the development of volcanic ocean islands. Collapse is caused by a combination of gravitational failure as a consequence of piling up the products of eruptions onto steep slopes and the wedging apart of the volcanic edifice by repeated dyke intrusion (Carracedo *et al.* 1999).

In the Canary Islands, evidence is particularly clear on the youngest island of El Hierro, where three large collapse scars have been traced offshore to giant submarine debris avalanche deposits (Gee *et al.*. 2001). On La Palma, there is evidence of repeated growth and collapse in the centre of the island until around 0.5Ma. Shield-building activity on La Palma has now shifted to the southern Cumbre Vieja, where there have been seven eruptions in historic (since late 15th Century) times. During the 1949 eruption, part of the west side of the Cumbre Vieja was downfaulted by around three metres. There is ongoing concern that a catastrophic collapse of the Cumbre Vieja could precipitate a mega-tsunami with potential to devastate the eastern seaboard of the United States (Day *et al.* 1999).

Evidence of giant lateral collapses in the form of collapse scars and corresponding offshore debris avalanche deposits has now been found for most of the Canary Islands (Figure 1). Sedimentary deposits from mega-tsumamis relating to giant lateral collapses have been described on Gran Canaria (Perez-Torrado *et al.* 2006).

Felsic magmatism

Although the Canary Islands are predominantly basaltic, the products of felsic magmatism are encountered on most islands. The source of the felsic magmas is probably fractional crystallisation of basaltic magmas in shallow magma chambers (Schmincke 1982). In most cases the felsic magmas were intruded to produce features such as the "salic domes" that characterise the eroded landscape of La Gomera (Figure 6). On Gran Canaria and Tenerife, felsic magmas developed to the point that large scale explosive eruptions

Figure 8. Recent pahoehoe flow field near Restinga, El Hierro: part of the current shield-building stage on the youngest Canarian island.

Figure 9. Pliocene lava flow, pillowed on seaward side, overlying shallow marine sediments. Caleta Negra, Fuerteventura.

occurred that deposited large ignimbrite flows. The ignimbrites on Tenerife are generally welded proximal to the eruptive centre but unwelded distally. In contrast, on Gran Canaria many ignimbrite flows are welded at some distance from the eruptive centre. Many of these flows are peralkaline in composition and show rheomorphic features (Woodcock 2005); they attracted attention early in the geological study of the islands (Schmincke & Swanson 1967).

Sea-level & Climate Change

In contrast to the Hawaiian Islands, the Canary Islands have been remarkably stable with little or no post-erosional tectonic subsidence. Evidence for this long term stability includes (Carracedo *et al.* 1998) the position relative to present day sea level of features such as wave-cut platforms, beach deposits and coastal volcanic features such as littoral cones. At Caleta Negra, on Fuerteventura, cliff exposures around 20 m above present sea level show a section through Pliocene marine sediments deposited on the wave-cut top of the Basal Complex. The sediments are overlain by a lava flow that has become pillowed seawards as it entered the sea (Figure 9).

Evidence of more recent Plio-Quaternary glacio-eustatic sea level change includes the areas of carbonate sand on Fuerteventura. During marine highstands an extensive shallow marine carbonate sand body developed between Lanzarote and Fuerteventura. This body was exposed during subsequent lowstands and the sands were blown south west onto Fuerteventura. Some of this material has been dissolved by rainfall and then re-precipitated as a white caliche layer as groundwater has been drawn upwards by surface evaporation.

The present climate of the Canary Islands is relatively dry, although subject to the occasional torrential rainstorm in winter. The climate has previously been much wetter as evidenced by the steeply incised "barrancos" on most islands and the presence of abundant fossil bee nests on Lanzarote and Fuerteventura (Alonso-Zarza & Silva 2002); evidently these now rather arid islands had much more vegetation, perhaps with an abundance of wild flowers.

As global warming continues, the Canary Islands may experience an increasingly humid climate: this will help alleviate the water shortages that are experienced on the more arid islands, but will be looked upon less favourably by the sun-seeking tourist or the geologist trying to keep map and field notes dry!

Geoconservation

Around 40% of the Canary Islands has at least some level of protection. The highest level of protection is afforded to the Parques Nacionales, such as Timanfaya on Lanzarote, Las Canadas on Tenerife, Garajonay on La Gomera and Caldera de Taburiente on La Palma. A lesser degree of protection is afforded to the Parques Naturales, such as the Roque Nublo area on Gran Canaria.

In Timanfaya, visitors are restricted to certain roads within the park and walking tours are restricted to those accompanied by the park guides. This policy has been very successful in maintaining a pristine volcanic landscape, which could easily be ruined by tracks from walkers or off-road vehicular traffic. Paradoxically, and perhaps fortunately, many areas of outstanding geological interest are currently outside of the Timanfaya Parque Nacional.

In many areas, unrestricted development, together with the dumping of waste in barrancos, poses a threat to many outstanding sites, particularly the coastal exposures of ignimbrites on the more populated islands of Tenerife and Gran Canaria. The problem is particularly acute on the SW coast of Gran Canaria, where several exposures described in the early papers on ignimbrites have now vanished.

Acknowledgements

I'd like to acknowledge three people in particular who have helped and encouraged me in my studies of Canary Islands geology. Alan Diggles of the OUGS NW branch was my earliest inspiration; his photographs, samples and descriptions of the Fuerteventura Basal Complex stimulated my first geological visit to the islands. Andy Harris, formerly at the OU and now at HIGP/SOEST, University of Hawaii, was a great teacher of things volcanological during OUGS trips to the Aeolian islands and to Hawaii. Last but not least, Jane Clarke, who has edited my contributions to the OUGS Journal on various aspects of Canary Islands geology over the years.

References

Alonso-Zarza, A.M. & Silva, P.G. (2002). Quaternary laminar calcretes with bee nests; evidences of small-scale climatic fluctuations, eastern Canary Islands, Spain. *Palaeogeography, Palaeoclimatology, Palaeoecology*, **178,** 119-135.

Anguita F & Hernan F, 1975. A propagating fracture model versus a hotspot origin for the Canary Islands. *Earth & Planetary Science Letters,* **27**, 11-19.

Carracedo J C, 1999. Growth, structure, instability and collapse of Canarian volcanoes and comparisons with Hawaiian volcanoes. *Journal of Volcanology and Geothermal Research,* **94,** 1-19.

Carracedo J C, Day S, Guillou H, Rodrigues Badiola E, Canas J A & Perez Torrado F J, 1998. Hotspot volcanism close to a passive continental margin: the Canary Islands. *Geological Magazine*, **135,** 591-604.

Carracedo J C, Day S J, Guillou H & Perez Torrado FJ, 1999. Giant Quaternary landslides in the evolution of La Palma and El Hierro, Canary Islands. *Journal of Volcanology and Geothermal Research,* **94,** 169-190.

Carracedo J C & Day S, 2002. *Canary Islands* . Terra Publishing, Harpenden. 294pp.

Carracedo J C, Badiola ER, Guillou H, de la Nuez J & Perez Torrado FJ, 2001. Geology and Volcanology of La Palma and El Hierro, Western Canaries. *Estudios Geologicos,* **57,** 175-273.

Carracedo J C, Perez Torrado F J, Ancochea E, Meco J, Hernan F, Cubas C R, Casillas R, Rodrigues Badiola E & Ahijado A, 2002. Cenozoic volcanism II: the Canary Islands. *In:* Gibbons W & Moreno T (eds), *The Geology of Spain.* The Geological Society, Bath. 649pp.

Day S J, Carracedo J C, Guillou H & Gravestock P, 1999. Recent structural evolution of the Cumbre Vieja volcano, La Palma, Canary Islands: volcanic rift zone reconfiguration as a precursor to volcano flank instability? *Journal of Volcanology and Geothermal Research,* **94**, 135-167.

Foulger G R, 2007. The Great Plume Debate, OUGS Journal, **28(2)**, 16-21.

Foulger G R & Natland J H, 2003. Is "hotspot" volcanism a consequence of plate tectonics? *Science,* **300,** 921-922.

Fuster J H, 1968. Geologica y Volcanologica de las Islas Canarias (in four parts). Instituto Lucas Mallada (CSIC), Madrid.

Gee M J R, Watts A B, Masson D G & Mitchell N C, 2001. Landslides and the evolution of El Hierro in the Canary Islands. *Marine Geology,* **177**, 271-293.

Hausen H, 1956. Contributions to the geology of Tenerife (Canary Islands). *Societas Scientiarum Fennica, Commentationes Physico-Mathematicae* **18.**

Hausen H, 1973. Outlines of the geology of Hierro (Canary Islands). *Societas Scientiarum Fennica, Commentationes Physico- Mathematicae* **43**, 65-146.

Perez-Torrado FJ, Paris R, Cabrera M, Schneider J-L, Wassmer P, Carracedo JC, Rodriguez-Santana A & Santana F, 2006. Tsunami deposits related to flank collapse in oceanic volcanoes : The Agaete Valley evidence, Gran Canaria, Canary Islands. *Marine Geology,* **227**, 135-149.

Rothe P & Schmincke H U, 1968. Contrasting Origins of the Eastern and Western Islands of the Canarian Archipelago. *Nature,* **218,** 1152-1154.

Schmincke H U, 1982. Volcanic and chemical evolution of the Canary Islands. *In:* Von Rad U, Hinz K, Sarnthein M & Siebold E (eds), *Geology of the Northwest African Margin,* 273-306.

Schmincke H U & Swanson D A, 1967. Laminar viscous flowage structures in ash-flow tuffs from Gran Canaria, Canary Islands. J*ournal of Geology,* **75**, 641-663.

Wilson LG, 1998 "Lyell: the man and his times". In Blundell D J & Scott A C (eds). *Lyell: the Past is the Key to the Present*. Geological Society Special Publication No.143.

Woodcock D C, 2000. Stripped bare in Fuerteventura: an introduction to the geology and guide to selected field locations. *OUGS Journal*, **21(1)**, 17-25.

Woodcock D C, 2005. Welded ignimbrites on Gran Canaria: an introduction and field guide to selected locations. *OUGS Journal*, **26(1),** 15-22.

Author

Duncan Woodcock MA, CEng, MIChemE, BSc Hons (Open), FGS is a senior process engineer with ABB Ltd.

Geological observations in the Precambrian and Cambrian rocks of the St. David's Peninsula

John Downes

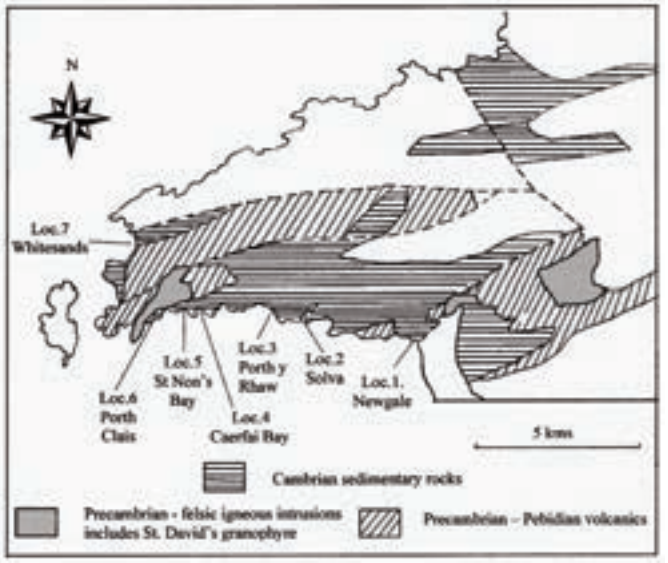

Figure 1. Precambrian and Cambrian outcrops in the St. David's peninsula

The oldest rocks in the St. David's peninsula are the Pebidian volcanics of late Precambrian age [570–590 Ma]. Although generally described as tuffs, they are composed of bedded volcanic debris that has been eroded from a land surface and later deposited in shallow water. These tuffaceous sediments have been subsequently intruded by a suite of felsic igneous rocks including the St.David's granophyre [Figure 1]. Finally the region underwent uplift and erosion before the deposition of the Cambrian strata in the shelf seas on the southern margin of the Iapetus Ocean.

The basal Cambrian conglomerates rest unconformably on the eroded Precambrian rocks [Figure 2] that form two fault bounded anticlines in the St David's and Hayscastle areas. These major folds have an ENE – WSW trend and on their southern flank the Cambrian rocks dip steeply south whilst to the north and west the dip is generally to the north west. These folds and faults have been produced by the Caledonian earth movements or orogeny that occurred at the end of Silurian times. However, the inland scenery of the St David's peninsula is dominated by the Pliocene marine platform which has a mean height of 60 metres O.D. There are several residual hills [monadnocks] formed by igneous intrusions such as Carn Llidi that rise above the general level. The field localities described below extend from Newgale in the east to Whitesands Bay on the far western side of the peninsula.

Locality 1

Newgale [SM847224] is a small village on the A487 at the northern end of St Bride's Bay where the northern boundary of the Pembrokeshire coalfield is faulted against the Cambrian strata of the St David's peninsula. Cars can be parked in Newgale village opposite the café but during the tourist season it is probably better to use the car park on Pinch Hill [SM851216] and walk over the shingle storm beach to examine the cliffs at the northern end of Newgale Sands. The storm beach blocks the entrance of Brandy Brook and the water percolates through the pebbles emerging on the beach

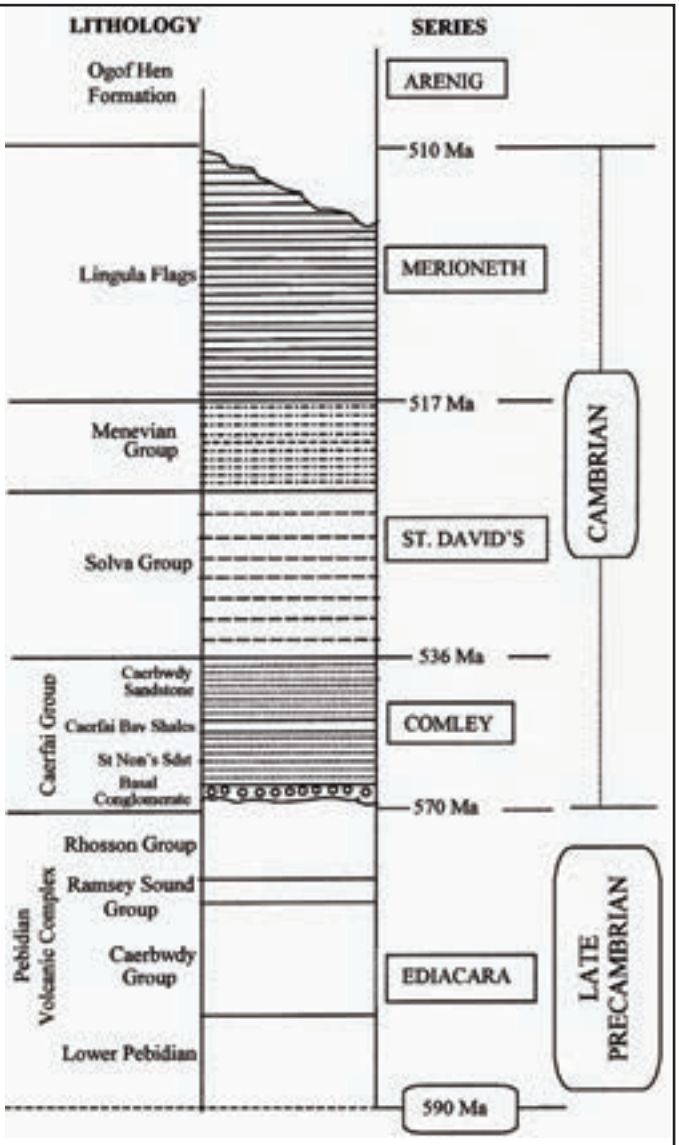

Figure 2. Stratigraphical column for the Precambrian and Cambrian of the St. David's peninsula.

as a series of gushing springs. On the cliff face the sandstones and conglomerates of the Middle Solva Group [Figure 2] can be seen to dip at 45°S. Marine erosion has removed some of the outer sandstone layers particularly where intersecting joints are exposed. On the north side of the first headland the bedding is distorted in the direction of dip by a monoclinal fold, much brecciated in the hinge area. The strata are well exposed in several small sea caves where the sandstones display sedimentary structures such as graded bedding, ripple lamination and load casting. Some of the conglomerates contain clasts of igneous material possibly derived from the underlying Precambrian.

About 200m to the north is Pwll March where Middle Solva grey sandstones are downthrown in the centre of a graben structure against adjacent pebbly sandstones of the Lower Solva Group [Figure 3]. A small cave on the south side of Pwll March is cut into these beds which display parallel folds [Figure 4]. The competent

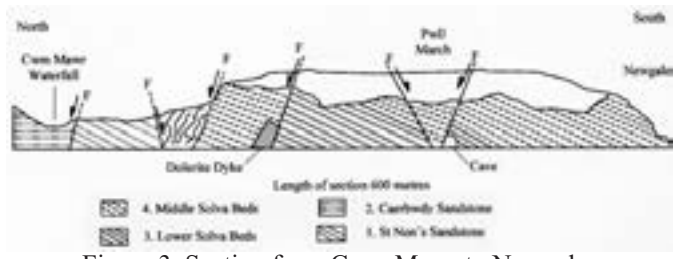

Figure 3. Section from Cwm Mawr to Newgale.

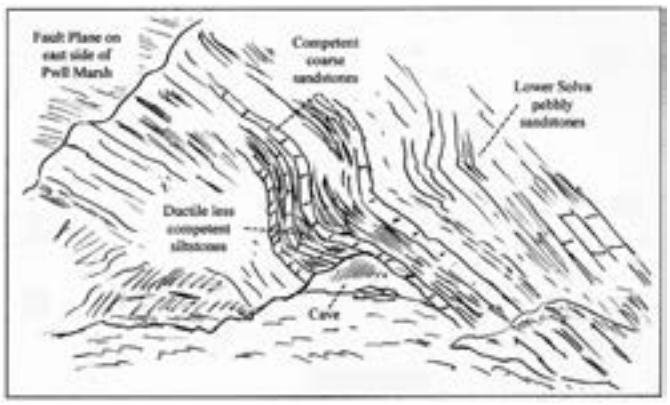
Fault Plane on east side of Pwll Marsh
Competent coarse sandstones
Lower Solva pebbly sandstones
Ductile less competent siltstones
Cave
Figure 4. Pwll March cave.

sandstone layers maintain a constant thickness around the folds but the less competent siltstone layers show evidence of ductile deformation, thickening in the open hinge areas. Note also that the layers are cut by numerous tension joints particularly around the fold hinges. This section illustrates the process of crustal shortening produced by the Caledonian earth movements as the Iapetus Ocean began to close during Ordovician times.

Continue north towards Cwm Mawr (Figure 3) stopping to examine the dolerite dyke that cuts through the Lower Solva Group where the cliff line is indented by a major fault downthrowing to the NW. Beyond the dyke is a brecciated fault zone which separates the Middle Solva Group from the older St Non's Sandstone dipping at about 40°S. There is a faulted junction near the Cwm Mawr waterfall that separates the St Non's Sandstone from the purple Caerbwdy Sandstone that extends north towards Cwm Bach.

Locality 2

Solva is located about 6kms west of Newgale on the A487. There is a car park [SM806243] in the centre of the village adjacent to The Harbour Inn. The deep water inlet that forms Solva harbour was produced by the Solfa river cutting down to a lower sea level during the late Devensian glaciation [10,000-120,000 BP]. A subsequent eustatic rise in sea level has created the present day Solva ria or drowned valley. Note that the upper harbour is orientated NE-SW along a fault zone whilst the outer harbour has a N-S trend.

Walk to the old quarry at SM805244 alongside the main road where the pebbly sandstones of the Lower Solva Group are exposed [Figure 5]. These coarse grained feldspathic sandstones are massively bedded dipping at 25°S. Return to the car park and cross the bridge adjacent to the pub. Follow the track up to the Gribin [SM806241] where the purple sandstones and shales of the Middle Solva Group form a craggy outcrop. Then walk SW along the ridge crossing exposures of both felsite and dolerite; the former can be examined in more detail at the lifeboat station.

Continue along the path to the headland where the Lingula Flags outcrop at the summit [SM801238]. These thin bedded medium

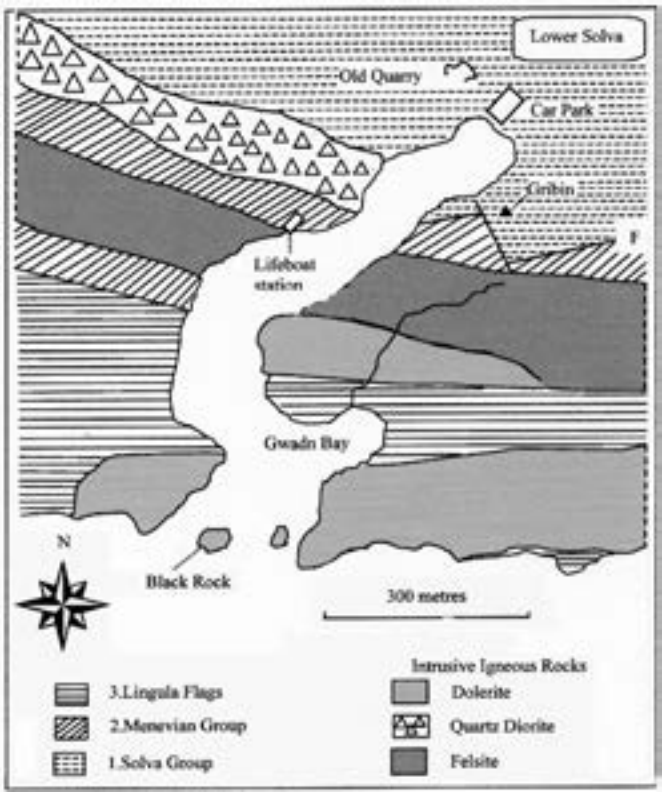

Figure 5.The geology around Solva Harbour.

grained sandstones and interbedded shales are dipping at 75°S. They represent a distal turbidite sequence showing examples of graded bedding, ripple lamination, flute marks and load casts. The flagstones strike E-W and can be seen outcropping on the east side of the adjacent Gwadn Bay The latter has a shingle bar which almost completely blocks the drainage from the marshy Gwadn valley. The outer headlands guarding Solva harbour are formed of resistant dolerite which is also intruded along the northern margin of the *Lingula* Flags.

Return to the car park by taking the path down to the old lime kilns. These were supplied with coal and limestone by small sailing vessels in the 19th century. The limestone was then burnt to produce lime, mainly for agricultural use.

Next follow the track along the west side of the harbour until you reach the quay and yacht club. Here there is an intrusion of quartz diorite exposed for 100m alongside the track. This rock is coarse grained with prominent crystals of dark green amphibole and whitish plagioclase feldspar. Cleaved Menevian mudstones can be seen behind the boathouse. They belong to the zonal horizon that has yielded large trilobites such as *Paradoxides davidis* [See Locality 3]. Walk around to the front of the old lifeboat station to a felsite intrusion that is considered to be of Ordovician age [Figure 6]. The felsite is porphyritic and has a distinct flow texture with plagioclase laths arranged parallel to the contact zone. The mudstones have been baked by contact metamorphism where they are adjacent to the intrusion. Here a chilled margin develops along the boundary of the hot igneous intrusion as it is cooled by the relatively cold mudstone.

Locality 3

Porth y Rhaw [SM786242] is a small inlet about 2kms west of Solva. It can be accessed from Nine Wells on the A487. There is a

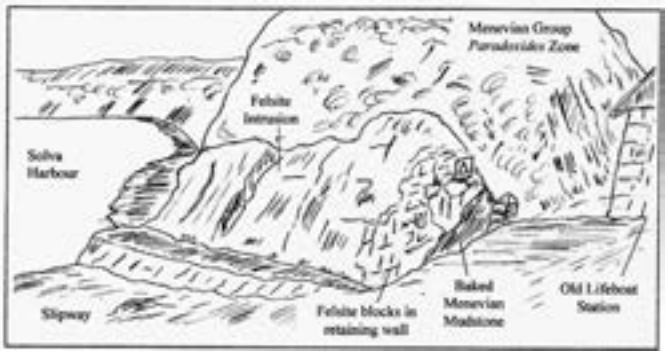

Figure 6. Solva old lifeboat station outcrop.

small car park adjacent to Ty'r Pwmp cottage. Follow the track down to the coast stopping at the old quarry at SM788246 where a sill of quartz dolerite is in contact with the Lingula Flags dipping at about 50°S. The latter are downfaulted against the Solva Group about 100m to the south. Near the bridge carrying the coast path over the stream [SM787243], the Solva beds pass conformably into Menevian strata which are well exposed around the inlet of Porth y Rhaw where the beds are dipping at 80°S. At low tide it is possible to examine the dark cleaved mudstones in the eastern cliff that belong to the *Paradoxides davidis* zone. It was in these rocks that in 1862 John W Salter, a palaeontologist with the Geological Survey, first discovered a rich trilobite fauna containing fragments of a specimen of *Paradoxides davidis* that was almost 60cm long. One can see a complete specimen of this distinctive trilobite in the National Museum of Wales in Cardiff. The Menevian sediments must have been laid down in calm relatively shallow water under reducing conditions since the beds contain much disseminated pyrite and phosphatic material. However, towards the end of Menevian times, coarse sandstones were deposited as a result of turbidite flows and these rocks, which contain the brachiopod *Orthis hicksii*, can be seen on the eastern headland of Porth y Rhaw

Locality 4

Caerfai Bay [SM760244] is accessed from the A487 on the eastern outskirts of St David's. Follow the signposted minor road that leaves the main road near to the 'park and ride' bus stop; then drive southwards to the car park that overlooks Caerfai Bay. Walk down the cliff path which is cut through the St Non's Sandstone near the base of the Cambrian succession. [The basal conglomerate is best seen in St Non's Bay] The sandstone beds weather to a greenish colour due to the presence of interstitial chlorite and epidote. Major bedding planes can be seen to dip at around 50°S. Note the major fault zone running ENE – SSW through the bay that produces the crushed rocks immediately to the west of the beach steps. The fault breccia lies between two parallel strike slip faults that are clearly seen at beach level. At low tide walk along the eastern side of the bay. The green sandstones change to a red-purple colour as the first recess is approached. Here the relatively soft red cleaved mudstones known as the Caerfai Bay Shales have been deeply eroded by the sea [Figure 7]. The original bedding is marked by a sequence of volcanic tuffs, each less than 10cm thick. The light coloured tuffs are generally coarse grained and display sharp erosional bases with load casting. Sedimentary structures such as graded bedding and cross lamination within the bands indicate that the volcanic ash was deposited under water. The tuffs, which can be traced along the coast to Newgale, are the only evidence of vulcanicity during Cambrian times in Pembrokeshire.

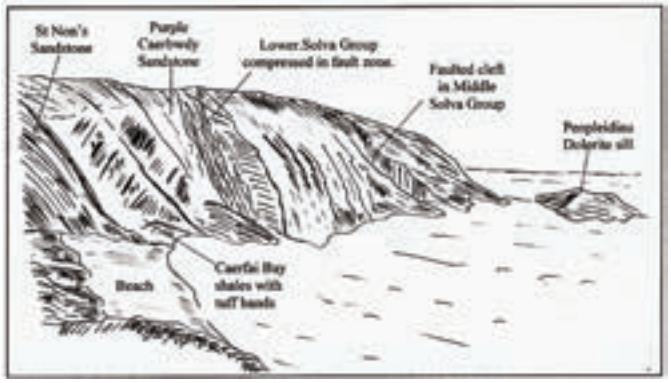
St Non's Sandstone
Purple Caerbwdy Sandstone
Lower Solva Group compressed in fault zone.
Faulted cleft in Middle Solva Group
Penpleidiau Dolerite sill
Beach
Caerfai Bay shales with tuff bands

Figure 7.Caerfai Bay: East side.

The purple coloured Caerbwdy Sandstone outcrops for 150m to the south of the red cleaved mudstones. The sandstone is medium grained, micaceous, felspathic and massively bedded. There is a cave at SM761242 where the Caerbwdy sandstone passes conformably into the vertical Lower Solva Group. The latter appear to be considerably compressed alongside a steep reverse fault complex.

In order to explore the higher Cambrian beds of the headland it is necessary to retrace ones steps to the head of Caerfai Bay and then follow the cliff path southwards. The purple sandstones of Middle Solva age are exposed in the deep faulted cleft at SM762240 where a major bedding plane dips steeply down to the sea on the north side. The headland itself and the small islands of Penpleidiau are formed of a well jointed dolerte sill which is rests on a narrow outcrop of Menevian mudstones. From the vantage point of the headland look across Caerbwdy Bay to the spectacular folds in the Caerbwdy Sandstone and Lower Solva Group.

Follow the coast path to the head of Caerbwdy Bay where there are several disused quarries that worked the Caerbwdy Sandstone. These quarries were the source of much of the building stone for the nearby St. David's Cathedral, the construction of which began in 1180. Recent restoration work on the cathedral in 1972 and 1998 resulted in the temporary reopening of one the quarries.

Locality 5

St Non's Bay [SM753243] can either be approached from the car park at Caerfai Bay following the coastal path around Pen y Cyfrwy or from Goat Street in St David's taking the narrow lane past the Warpool Court Hotel to St Non's Retreat. From here walk about 150m westwards along the coast track to where a steep path leads down into a narrow faulted cleft [SM751242] that gives access to the foreshore. The cleft is occupied by the stream flowing from St Non's Well and great care should be taken when descending the rocky path particularly when it is wet and slippery. At the base of the cleft there are thick Pebidian rhyolites adjacent to vertical bands of silicified ash [formerly referred to as halleflinta] each band being 10-20cms wide [Figure 8]. An E-W ridge of Cambrian basal conglomerate runs along the seaward edge of the foreshore and at high tide this forms a line of sea stacks extending into the bay. This conglomerate is overturned [ie/ rotated through about 100° from its original horizontal position] which means that it now dips steeply north and so the oldest layers are exposed on top of the bed on the landward side. On the foreshore you will see that the conglomerate makes unconformable contact with the underlying Pebidian tuffs. The tuffs near the contact are purple in colour that

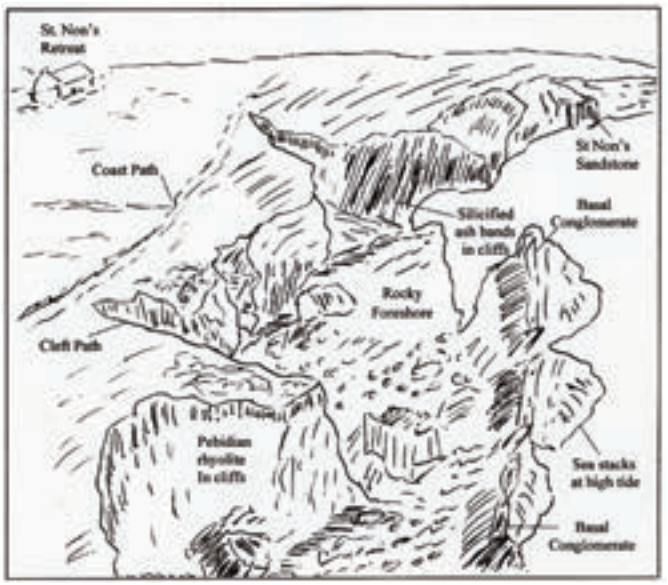

Figure 8. View eastwards across St. Non's Bay.

may represent an original weathered surface. The basal conglomerate can be examined in some detail at low tide. The pebbles are composed of vein quartz, dark red quartzite, silicified tuff and granophyre set in a sandy matrix. These clasts have been derived from underlying Precambrian rocks and show a preferred orientation resulting from tectonic forces. The conglomerate can be described as being clast supported since most pebbles are in contact with each other.

Locality 6

Porth Clais [SM741242] can be reached from St David's via Goat Street continuing for about 1.5kms SW along the lane through Lower Moor and thence to the car park near the ford at the head of the Porth Clais inlet. The Precambrian St David's granophyre is exposed in a small quarry behind a bungalow about 100m north of the ford but this rock can be better examined in its coastal outcrops. Walk along the west side of the inlet towards the headland; from the track one can see the faulted junction between the Caerbwdy Sandstone and the St Non's Sandstone near the north end of the quay [SM 743240] on the eastern side of the inlet. [This site can be visited by descending the steps down to the breakwater from the eastern headland] Beyond the breakwater one can also observe the prominent bedding planes of the Caerbwdy Sandstone dipping at about 80°S. This sandstone is relatively fine grained and so has developed widely spaced cleavage at a high angle to the bedding; the result of uplift and compression during the Caledonian orogeny.

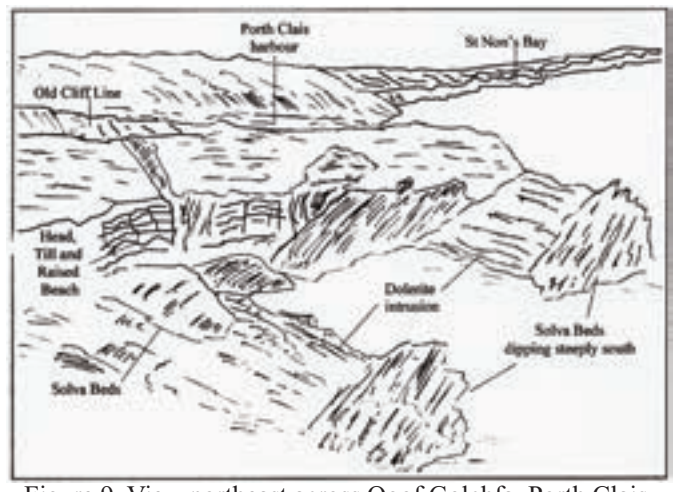

Figure 9. View northeast across Ogof Golchfa, Porth Clais

Follow the coast path to Ogof Golchfa [SM741237] which is a fault gully where there is a magnificent exposure of a dolerite intrusion that runs E-W parallel to the coast. It is possible to clamber down to the foreshore to examine the contact zone between the 6m wide dyke and the surrounding steeply dipping Solva beds [Figure 9].

Standing on the wave cut platform it is possible to examine several metres of a Quaternary sequence overlying the erosion surface of the upturned Solva beds. Firstly, there is a raised beach deposit, considered to have been formed during the Ipswichian interglacial period [130-120,000 BP] when marine transgression raised the sea level by up to 10m above the present day level. Secondly, overlying the beach deposit is a boulder clay [glacial till] laid down by Irish Sea ice during the late Devensian period [120-10,000 BP]. At this time Irish Sea ice moved eastwards across Pembrokeshire and a variety of local pebbles and rock fragments are found within the till. These include quartz porphyry pebbles from Ramsey Island but there is also material from farther afield; on the headland to the west, there was a large erratic boulder of Scottish picrite that has now unfortunately disappeared over the cliff. At the top of the sequence lies a deposit of head; poorly sorted rock debris that was laid down by surface water under periglacial conditions. Note also the break of slope beyond the coastal path that marks the position of old cliff line, now much degraded.

Continue westwards along the coast path that crosses the headland of Carreg Fran. This is at the most southerly tip of the St David's granophyre intrusion. It is a highly siliceous, coarse grained igneous rock composed of quartz, orthoclase, oligoclase feldspar and chlorite. The western side of the granophyre intrusion is faulted against the Ramsay Sound Group of the Pebidian Volcanic Series. The latter are formed of sheared chlorite tuffs and ashes that are relatively less resistant to erosion than the granophyre. Hence the deep inlet known as Porthlysgi Bay is excavated in the softer volcanic material. The contact between the resistant granophyre intrusion and the Ramsey Sound Group can be examined in the eastern corner of the bay.

Locality 7

Whitesand Bay is a popular surfing location on the western end of the St David's peninsula. Take the Fishguard road out of St David's then turn left on to the B4583 that terminates in a large car park at SN734272. From here walk NW along the coast towards Trwynhwrddyn [Ram's Nose]; this headland is formed of the *Lingula* Flags of Upper Cambrian age (Figure 10). Here the strata are riddled with quartz veins in a fault shatter zone and these veins have strengthened the resistance of the headland to erosion. The beds include sandstones and shales that appear to represent a turbidite sequence. The sediments show graded bedding, flute casts, ripple lamination and deformation structures. From the evidence of graded bedding in the sandstone, one should be able to work out the direction of younging in these steeply dipping beds. On some of the shale bedding planes there are small dark shelled brachiopods known as *Lingulella davisii*; these are one of the first brachiopods to appear in the geological record. Remarkably, these organisms have changed little over the last 500Ma and can still be found today as *Lingula* in the Sea of Japan.

Return to the car park and walk southwards along the beach. Note the vertical beds of the Menevian Group are planed off and overlain

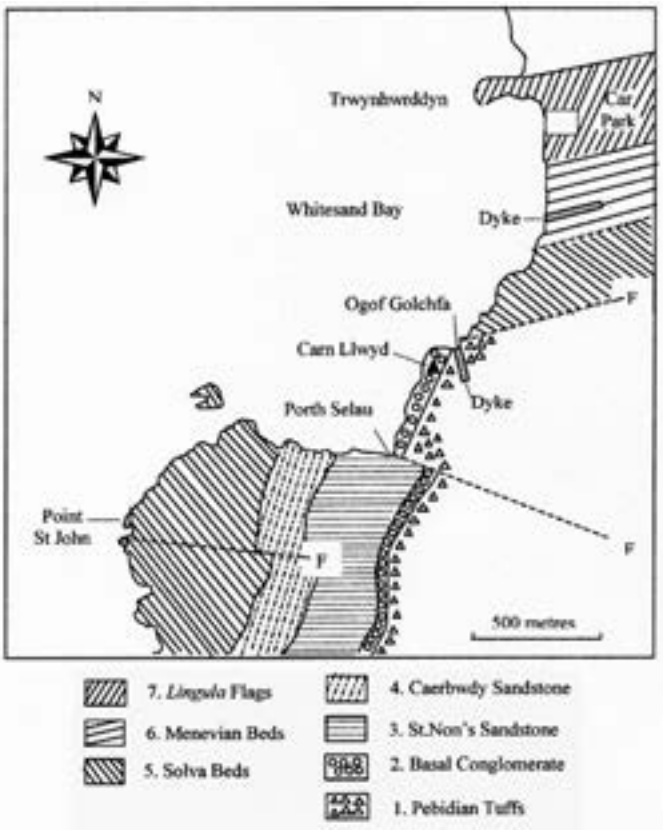

Figure 10. The geology of Whitesand Bay.

by about 2m of a raised beach deposit containing well rounded pebbles and cobbles and capped by blown sand [dunes]. Immediately north of the steps [SM733269] the Menevian beds are cut by a dolerite dyke about 10m wide. Continue walking southwards to where the Solva beds are exposed dipping at about 60°NW. The sequence consists of fine grained sandstones and siltstones in which the cleavage is almost parallel to the bedding resulting in sharp jagged rock outcrops rising from the beach. The Solva beds are cut off by an E-W normal fault downthrowing to the N in the deep inlet adjacent to Ogof Golchfa ("washing place cave") [SM730264]. On the south side of the fault, grey Pebidian cleaved tuffs are intruded by a dolerite dyke 20m thick that extends into the cave [Figure 11] where the unconformable contact between the tuffs and the basal Cambrian conglomerate appears to be dipping at about 50°NW. The well rounded pebbles and cobbles are set in a sandstone matrix and exhibit imbrication in some beds. However, this conglomerate is more easily examined in the crags of Carn Llwyd [SM729263] alongside the coast path about 100m to the south. Unfortunately it is necessary to return to the steps in order to reach the cliff top path and then walk southwards. Some of the clasts in the crags near to the cliff top bungalow near Porth Selau are up to 20cm across composed of Pebidian tuffs, vein quartz and dark red quartzite.

Another E-W fault downthrowing to the south, reaches the coast at Porth Selau and offsets the basal conglomerate 200m to the east.

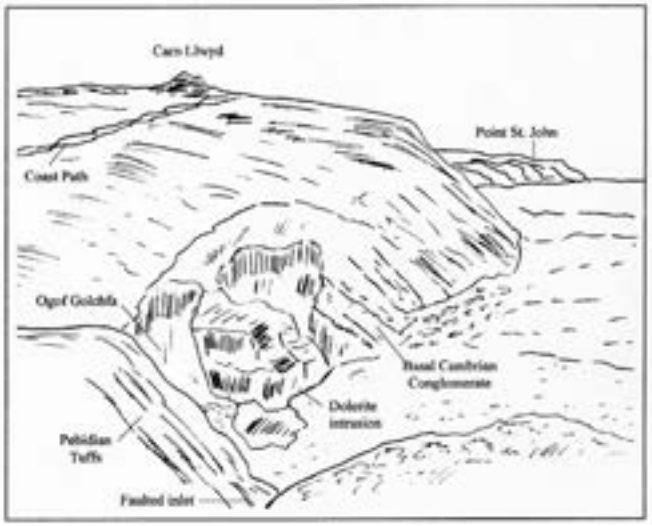

Figure 11. View southwest over Ogof Golchfa, Whitesand Bay.

The view SW across the bay shows a succession of Cambrian strata including the St Non's Sandstone, the Caerbwdy Sandstone and the Solva beds; all dipping NW at approximately 50°. Continue along the path to the headland of Point St. John [SM719258] where a thick dolerite sill with columnar jointing can be seen resting on the steeply inclined sandstones and siltstones of the Solva beds. From this excellent view point one can look across to Ramsey Island and identify the two main peaks of Carn Ysgubor in the north and Carn Llundain in the south, formed of Ordovician dioritic gabbro and rhyolitic tuffs respectively.

Bibliography

Baker J W, 1982, *The Precambrian of South West Dyfed,* Geological Excursions in Dyfed, South West Wales, National Museum of Wales, pp15-25.

Brenchley P T & Rawson (eds), 2006, *The Geology of England and Wales,* The Geological Society, pp16-19, 37-39.

Owen T R, 1973, *Geology Explained in South Wales*, David & Charles, pp23-32.

Williams B P J & Stead T G, *The Cambrian Rocks of the Newgale - St David's Area*, pp27-49.

Maps

Geological Survey
1:50,000 Sheet 209 St David's
1:25,000 Sheet SM72/62/73 St David's

Ordnance Survey
1:25,000 Outdoor Leisure Sheet 36 North Pembrokeshire

Author

John Downes BSc (Hons). M Phil. Dip Ed. is a retired college lecturer now living in Pembrokeshire. He has worked for the Open University as an Associate Lecturer since 1976. A copy of this article can be found at www.jdgeology.co.uk

At last, the Ruapehu Crater Lake Lahar

Philip Clark

I wrote in the Symposium Edition 2005 (Volume 26(2)) about the certainty that there would soon be a significant lahar from the breaching of the tephra dam which had been in place above the crater lake on Mt. Ruapehu, North Island, New Zealand, since the eruptions of 1995-6. The lahar was already then somewhat overdue: the authors of the April 1999 Environmental & Risk Assessment (ERA) report for the Department of Conservation (DOC) wrote: "The range of years from 2000 to 2006 would be likely to cover the extreme possibilities". In fact, because the lake filled slower than expected, the lahar did not finally occur until 18 March 2007. About $1.3x10^6m^3$ of water poured from the lake, significantly less than the $1.8x10^6m^3$ which caused the "Tangiwai disaster" of 1953 when a railway bridge and train were swept away 42km downstream, with the loss of 151 lives. Fortunately the dam collapsed when the water had risen to 1.1-1.2m below the crest; had the lake been full to the top the volume discharged would of course have been more. Also, the hard rim of lava underlying the dam did not erode during the break, so the amount released fell well short of the maximum impoundable volume, in current conditions, of $1.6x10^6m^3$.

The March lahar raised the water level at Tangiwai about 7.1m, considerably higher than in 1975 when a lahar with even greater water volume occurred from phreatomagmatic causes; in 1953 the rise at Tangiwai had been about 5.1-6.5m. The average height of the lahar was about 4m. The tephra dam had been 80 metres long before the collapse; the breach in it was 50-60 metres wide at the top and 40m at the hard rock (Figure 1). It collapsed in a series of bursts, mostly over about 45 minutes, and lasting in total 2.5 hours. The peak flow rate (discharge), which had previously been identified as the key factor in the destructiveness of Ruapehu lahars, must have averaged around $600m^3s^{-1}$, rather less than in 1953, 1975, and 1995 within the National Park (that is, on the mountain), but greater at Tangiwai than any of these (as predicted in ERA) and probably than in the poorly documented 1895 and 1861 eruptions.

There had been a further DOC report in 2003 by the Scientific and Technical Advisory Panel (STAP) on the likely mode of dam failure, its timing, and how the dam breach might develop; all happened very much as then predicted. Dr. Harry Keys writes that "it appears that the dam failed mainly due to increased pressure and flow of seepage of lake water through the dam inducing toe sloughing and retrogressive slumping on the downstream face".

Figure 1. The 40m breach in the tephra dam allows the water to flow into the Whangaehu valley once again. Photograph Dave Wakelin, reproduced by permission of New Zealand Department of Conservation.

The lahar's fastest measured speed was 36km/hour about 500m height and 3km distance below the breach, opposite the Tukino Skifield. It reached Tangiwai after 2 hours, at an average speed of about 20km/hr, and lower down the Whangaehu River speeded up, reaching the coast earlier and with higher flow depths than expected.

The sensors recommended in ERA and placed on the lake rim worked as hoped; adequate notice was given to all interested parties and the lahar passed down the Whangaehu river with minimal disruption. Damage was less than expected. Even the Round the Mountain track footbridge was only damaged and not destroyed as predicted. The water got within a few metres of the bund constructed at the head of the alluvial fan as the river gradient changes at the foot of the mountain worked, so that although probably no lake water would have entered the Waikato stream and the environmentally sensitive Tongariro river the building of this barrier was vindicated (Figure 2).

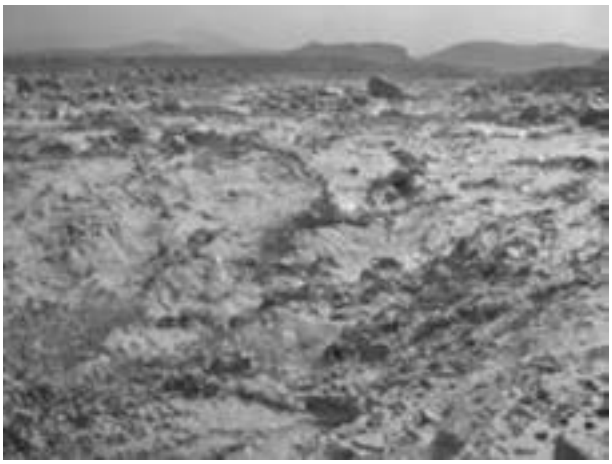

Figure 2. The March Lahar at the site of the bund to prevent overspill northwards. Photo by Dr Harry Keys, reproduced by permission of New Zealand Department of Conservation.

Further downstream, a concrete ford was severely eroded, and a concrete toilet block washed away at the Tangiwai memorial. Further down again, Strachan's bridge was overtopped but suffered only minor damage; this was probably because the lahar was "more watery than expected". It carried a major bed load - a boulder of 20 tonnes was among the debris – but probably did not bulk up with as much sediment as expected. However, as well as the dam material eroded, geomorphic effects on the mountain were large, including removal of glacier ice and widening of the river channel (Figure 3).

Since the lahar, there has been an increase in the number of small volcanic earthquakes. These are thought to indicate changes in the volcano's hydrothermal system as it adjusts to rapid lowering of the lake by 6m.

Figure 3. The Whangaehu Gorge reamed out by the lahar. Photo by Dr Harry Keys, reproduced by permission of New Zealand Dept of Conservation.

The DOC believe that the smooth working of the systems put in place has vindicated their decision to undertake no major works at the crater, which is a double World Heritage Site (cultural and environmental). This did not stop an opposition politician claiming that engineering works would have been cheaper and created less risk. The current minister gave this short shrift: "Certainly not. All of the technical advice stated that slicing a trench through the wall of the crater lake would have been extremely dangerous for the staff involved, was not a long-term solution, and risked creating a more serious lahar in the future. I remind members of the House that the member who raised this question was once Minister of Conservation, had the chance to do that, did not, and now is politically grandstanding."

For general hazard considerations, the DOC's comments are relevant: "In the last few years there has been strong commitment by local authorities and the Police to quality emergency management planning in a co-ordinated fashion. The plans have been tested via regular training exercises and have been refined where necessary. The outcome is a victory for quality science, good planning, commitment to principles and cohesive emergency management. The timing of the lahar, its size, speed and impact were all in accordance with predictions. The warning system and emergency management were implemented as described. It has been a credit to Harry [Keys] and other staff who have shown commitment to the Crater Lake Lahar issue. We can now see the proof that this process has strengthened Tongariro National Park World Heritage Area's management systems; local and national public infrastructure; as well as community and public safety."

Perhaps the most interesting question is why the lake took so long to fill up to the lava sill and then to the height against the tephra barrier, 6.5m, which as predicted caused it to collapse. The graph of "lake volume as percentage of fullness" shows a fairly steady rise, with no marked drop since 1999 but a significant levelling off in the (austral) winters since 2003.

The answer is mainly, it seems, because of the weather. A DOC staff member, Colin Lawrence, commented to me that "excluding the 2006 autumn/early winter, the last few years during mid summer to early winter has been reasonably dry. This corresponds to the time we observe greatest net inflow into the lake". In the past much of the inflow has been meltwater but with global warming there is now less snow and ice on the mountain top. "With more detailed monitoring we now have a greater understanding of the influence of evaporation and the complexity of the influence of the hydrothermal system beneath the lake". The "plumbing" of crater lakes is even now not well known, and water seeps back into the hydrothermal system more than once thought.

This article is compiled from various sources accessed on-line, principally from an article by Dr. Harry Keys accessed at:

http://www.taupomuseum.co.nz/Presentation/Presentation1.aspx?ID=537 on 4 June 2007.

In my original article I should have thanked my SXG390 tutor, Andrew Bell, for keeping me to the work when I found the demands of the course hard going; I'm glad to do so now, albeit belatedly.

Author

Philip Clark added BSc (hons) Geosciences from the Open University to long ago Oxford degrees in Modern History and in Theology. His previous paper *The crater lake lahar hazard on Mount Ruapehu* (2005) was from a study for SXG390.

Siberian Winter

Frozen meandering river, around 800km north of Novosibirsk, NW Siberia. The picture shows good examples of scroll bars on the point bars inside meander loops together with meander loop cutoffs of varying ages. Taken from cruising altitude during a Lufthansa flight from Nagoya to Frankfurt on 18 May 2007 (one of the few pleasures of this year's business travel!). © Duncan Woodcock